Supporting information

A Unimolecular Near-Infrared Fluorescent Probe for In Vivo Imaging of Enzymes with Minimized False-Negative Signals

Jinliang Han,[a] Mingwang Yang*[a], Chengyuan Lv,[a] Kang Li,[a] Jiangli Fan*[ab] and Xiaojun Peng[a]

[1] State Key Laboratory of Fine Chemicals, Dalian University of Technology, Dalian116024 China.
[2] Liaoning Binhai Laboratory, Dalian, 116023, China.

1. Experimental Section

1.1 Instruments and Raw Materials

All solvents were analytical grade and purchased from commercial suppliers. Unless otherwise stated, no further purification was required. Column chromatography used silica gel (200-300 mesh), with dichloromethane/methanol or petroleum ether/ethyl acetate as the mobile phase. All ultrapure water used in experiments was prepared from a Milli-Q system. The nuclear magnetic resonance hydrogen spectra (^{1}H NMR) and nuclear magnetic resonance carbon spectra (^{13}C NMR) of each compound were measured by a Bruker Avance II 400 MHz nuclear magnetic resonance spectrometer, with tetramethylsilane (TMS) as the chemical shift reference during testing, and samples dissolved in $CDCl_3$ or DMSO-d_6. High-resolution mass spectrometry (HRMS) was determined by LTQ Orbitrap XLMS liquid chromatography-mass spectrometry system from Thermo Scientific, USA. UV-visible absorption spectra were measured on a UV-visible spectrophotometer (Agilent Technologies CARY 60), and fluorescence spectra were measured on a fluorescence spectrophotometer (Varian CARY Eclipse). Excitation and emission slit widths were optimized to obtain appropriate fluorescence intensity measurement values. Cell imaging experiments were performed on a confocal laser scanning microscope (Olympus FV3000, Olympus, Japan)，objective lens specifications (40× oil-immersion objective), microscope model (Olympus FV3000 confocal laser scanning microscope), laser wavelengths for excitation (640 nm for red channel, 405 nm for blue channel), emission filter settings (670-750 nm, 440-480 nm), and image acquisition parameters. High-performance liquid chromatography (HPLC) analysis used appropriate chromatographic systems for product confirmation. Animal in vivo fluorescence imaging used NightOWL II LB983 small animal in vivo imaging system, equipped with 660 nm excitation light source and 700-750 nm emission filters for near-infrared fluorescence detection. Flow cytometry analysis used corresponding flow cytometers for single-cell resolution fluorescence intensity quantitative analysis. Microplate reader (Thermo Fisher Scientific) was used for MTT cell viability detection, measuring absorbance values at 570 nm and 630 nm wavelengths. Molecular docking simulation used the Flexible Docking module of Discovery Studio software.

1.2 Determination of Photophysical Properties of Probe Molecules

All optical experiments were performed in PBS buffer (10.0 mM, pH 7.4, containing 20% DMSO). **Cy-GGT-β-gal**, **Cy-GGT**, and **Cy-β-gal** were respectively dissolved in DMSO at 5 mM concentration as stock solutions and stored at -20°C for future use. For titration experiments, a certain amount of GGT or β-gal was added to a 2.0 mL total volume solution. The resulting solutions were fully shaken, then incubated at 25°C for 60 minutes before spectral measurements.

1.3 Verification of Molecular Responsiveness to GGT and β-gal

Time-dependent studies: Cy-GGT-β-gal (5 μM) solutions were respectively mixed with GGT (100 U/L) or β-gal (1.2 U/L, containing 500 μM NADH) in PBS buffer and incubated at 37°C. Samples were taken at different time points (0, 10, 20, 30, 40, 50, 60, 90, 120 minutes) for fluorescence measurements, excitation wavelength 660 nm, emission wavelength 720 nm.
Concentration-dependent studies: Different concentrations of GGT (0-100 U/L) and β-gal (0-1.2 U/L) solutions were prepared, respectively incubated with **Cy-GGT-β-gal** (5 μM) in PBS buffer for 2 hours, fluorescence intensity changes were measured to establish concentration-fluorescence intensity relationship curves.

1.4 Selectivity Testing of Molecules for GGT and β-gal

Cy-GGT-β-gal (5 μM) was respectively incubated with various biologically relevant substances, including NADH, NTR, APN, ALP, BSA, GSH, H_2O_2, Hcy, and Cys (each 10 μg/mL or corresponding concentrations). After incubation at 25°C for 90 minutes, fluorescence intensity was measured using excitation wavelength 670 nm and emission wavelength 720 nm.

1.5 HPLC Analysis for Verification of Activation Mechanism

High-performance liquid chromatography (HPLC) was used to analyze reaction products. Samples included: pure **Cy-GGT-β-gal**, **CyI-OH** standard, reaction mixture of **Cy-GGT-β-gal** with GGT, reaction mixture of **Cy-GGT-β-gal** with β-gal. The reaction mixtures consisted of acetonitrile/water (60:40) and $NaHCO_3$ (5 equivalents), analyzed after hour incubation period. Detection wavelength was 670 nm.

1.6 Molecular Docking Analysis

Molecular docking studies were performed using the Flexible Docking module in Discovery Studio 2019 software package. Protein structure data came from the Protein Data Bank (PDB), crystal structures of GGT (PDB ID: 4GDX) and β-gal (PDB ID: 1JZ8) were preprocessed, including removing water molecules, adding hydrogen atoms, optimizing side chain conformations, and other steps. The three-dimensional structure of ligand molecule **Cy-GGT-β-gal** was constructed through ChemDraw 3D and optimized through energy minimization.
The docking process used the CDOCKER algorithm, with active site radius set to 15 Å. Docking parameters were set as: number of random conformations generated was 10, molecular dynamics steps was 1000 steps, final energy minimization steps was 500 steps. Binding energy calculation used CHARMm force field, protein-ligand interaction analysis used LigPlot+ program to generate two-dimensional interaction diagrams.

1.7 Cell Culture and Treatment

Ovarian cancer cell lines (IOSE80, OVCAR3, SKOV3, SHIN3, A2780, and OVCAR5) were purchased from the Institute of Basic Medical Sciences (IBMS) of the Chinese Academy of Medical Sciences. Cells were cultured in DMEM medium supplemented with 10% fetal bovine serum, 1% penicillin, and 1% streptomycin, placed at 37°C in a humidified atmosphere containing 5% CO_2 and 95% air. Before imaging experiments, cells were cultured in 18 mm glass dishes.

1.8 Live Cell Fluorescence Imaging Experiments

IOSE80, OVCAR3, SKOV3, SHIN3, A2780, and OVCAR5 cells were seeded in confocal culture dishes at approximately 2×10^4 cells/mL concentration. Then cells were incubated with 5 μM **Cy-GGT-β-gal**, **Cy-GGT**, and **Cy-β-gal** at 37°C for 60 minutes, washed 3 times with PBS, and then scanned under confocal microscope. Excitation wavelength: 640 nm, emission wavelength: 670-750 nm.

1.9 Cytotoxicity Evaluation

Cell viability was assessed using the MTT method, which measures the reduction of 3-(4,5-dimethylthiazol-yl)-2,5-diphenyltetrazolium bromide to formazan crystals by mitochondrial dehydrogenases. SHIN3, SKOV3, OVCAR3, OVCAR5, A2780, and IOSE80 cells were seeded in 96-well plates at 1×10^5 cells/mL density in 100 μL DMEM supplemented with 10% FBS. After 24-hour attachment in cell culture incubator, cells were exposed to different concentrations of **Cy-GGT-β-gal** in 100 μL medium for 60 minutes. Untreated cells served as controls, with six replicates per experimental condition established to ensure statistical reliability.

After 12 hours of incubation, the medium was replaced with 100 μL MTT solution (5 mg/mL in DMEM) and incubated for an additional 4 hours at 37°C. Subsequently, the MTT solution was carefully aspirated, and the resulting formazan crystals were dissolved in 100 μL DMSO. After gentle agitation for 10 minutes, absorbance measurements were recorded at 570 nm and 630 nm using a Thermo Fisher Scientific microplate reader.

1.10 Co-culture Cell Imaging Experiments

Three co-culture models were established: OVCAR3/IOSE80, OVCAR5/IOSE80, and SHIN3/IOSE80. Cancer cells were first seeded and incubated at 37°C for 24 hours, labeled with Hoechst nuclear dye. Cells were washed seven times with DMEM to remove excess nuclear dye. Subsequently, IOSE80 cells were carefully introduced into the same culture vessel and incubated for an additional 24 hours to create mixed populations. Each co-culture system was then treated with **Cy-GGT**, **Cy-β-gal**, or **Cy-GGT-β-gal** for comparative imaging analysis.

1.11 Three-Dimensional Tumor Sphere Model Construction and Imaging

In vitro 3D tumor sphere models were cultured according to reported methods. OVCAR3, SHIN3, and OVCAR5 cells were seeded at 10^4 density per well in low-adhesion 96-well plates. Cells were cultured in normoxic atmosphere at 37°C for 3-5 days, with medium changed every 2 days. After macroscopic tumor spheroids (approximately 300-500 μm in diameter) were formed, intact spheroids were carefully transferred to confocal dishes and replaced with fresh medium. Subsequently, the medium was changed to fresh medium containing compounds **Cy-GGT-β-gal**, **Cy-GGT**, and **Cy-β-gal** (5 μM), and tumor spheres were incubated for an additional 2 hours. Finally, tumor spheres were placed under CLSM for 3D depth scanning.

1.12 Animal Model Establishment

Five-week-old female BALB/c mice were purchased from the SPF (Specific Pathogen Free) Experimental Animal Center of Dalian Medical University. All animal experiments were conducted in compliance with the Guide for the Care and Use of Laboratory Animals published by the National Institutes of Health. The experimental protocol was approved by the Animal Ethics Committee of Dalian University of Technology (approval number: 2018-043). Female Balb/c mice (4-5 weeks old) received subcutaneous injections of 4T1 cells (5×10^6) in the axillary region. When tumors reached approximately 200 mm^3, mice were randomly assigned to four experimental groups. Tumor dimensions were monitored using vernier calipers, with volume (V) calculated according to the formula: $V = 1/2 \times a \times b^2$, where a represents the maximum tumor diameter and b denotes the perpendicular diameter.

1.13 In Vivo Fluorescence Imaging Experiments

Anesthetized mice were administered 50 μM **Cy-GGT-β-gal** and evaluated using a NightOWL II LB983 small animal imaging system equipped with 660 nm excitation and 700±20 nm emission filters.

1.14 In Vivo Probe-Guided Tumor Resection Experiments

SHIN3 xenograft tumor models were established, and when tumors reached appropriate size, **Cy-GGT-β-gal** was directly sprayed onto exposed tumor surfaces. Under fluorescence imaging system guidance, tumor tissue was precisely excised along fluorescence boundaries. After resection, the probe was reapplied to the resection site to verify resection completeness.

1.15 Lung Metastasis Model Imaging Experiments

Lung metastatic tumor models were established in BALB/c mice through tail vein injection of SHIN3 tumor cells (1×10^6). Ten days after administration, imaging analysis was performed through tail vein injection of **Cy-GGT-β-gal**. Temporal changes in lung fluorescence signals were

monitored using in vivo imaging systems. Mice were euthanized 24 hours later for ex vivo imaging analysis and histopathological examination.

1.16 Histopathological Analysis

Tissue samples were fixed in 4% paraformaldehyde, paraffin-embedded, and sectioned at 5 μm thickness. Histopathological analysis was performed using hematoxylin and eosin (H&E) staining. Tissue morphological changes were observed using optical microscopy.

1.17 Data Analysis

Quantitative data are presented as mean ± standard deviation (SD). Each experiment was repeated at least three times. Data analysis and graphing were completed using Origin 2017. Statistical analysis between groups was conducted using t-tests (and nonparametric tests). Statistical significance was defined as $p < 0.05$, with significance levels indicated by asterisks as follows: *$p < 0.05$, **$p < 0.01$, ***$p < 0.001$.

2. Synthesis

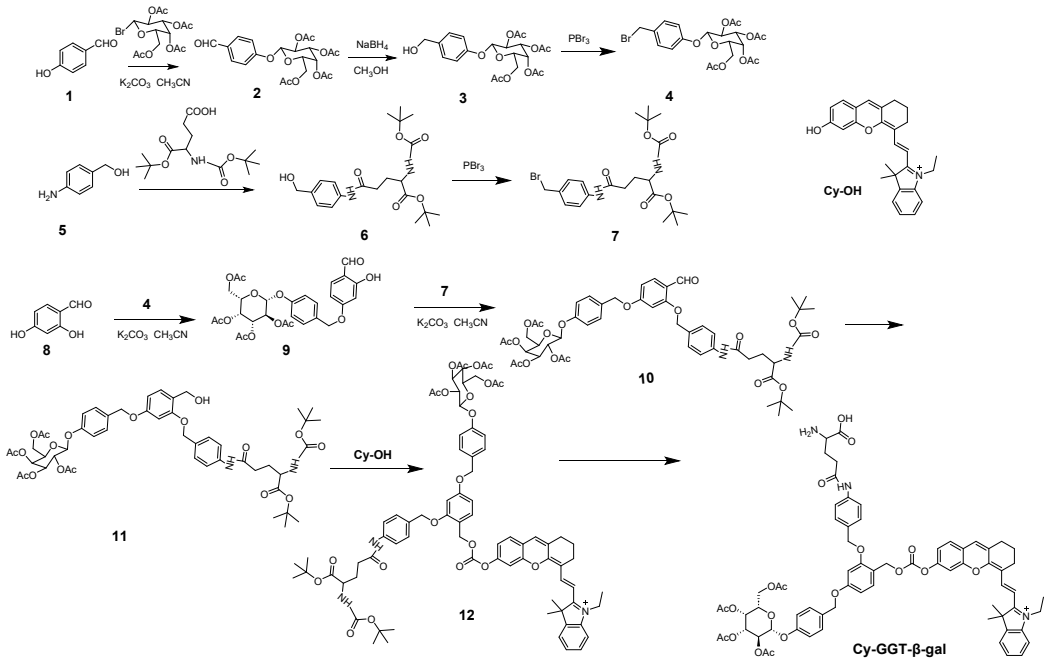

Scheme S1. Chemical structures and synthetic approaches to **Cy-GGT-β-gal.**

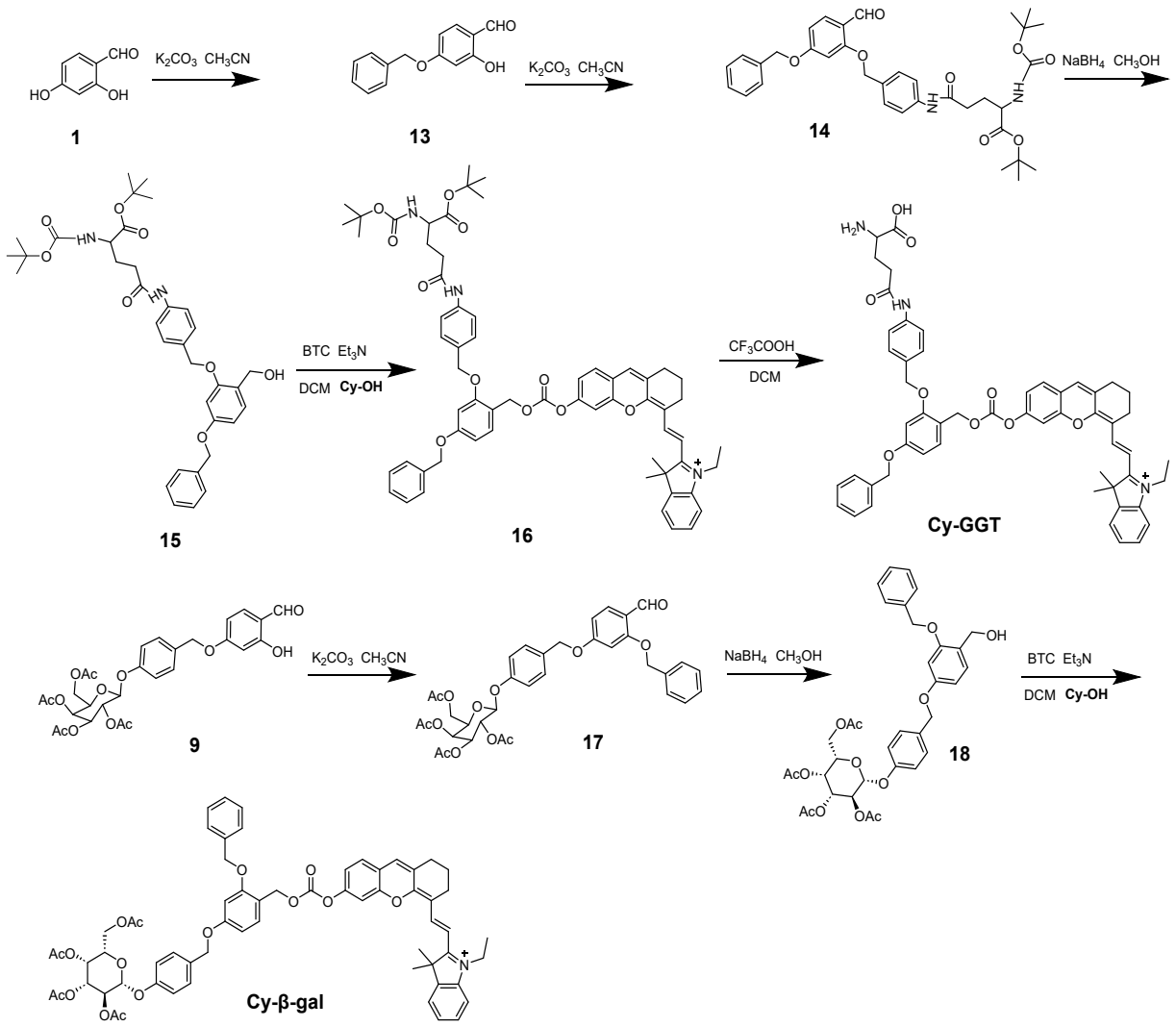

Scheme S2. Chemical structures and synthetic approaches to **Cy-β-gal** and **Cy-GGT**.

(1) Synthesis of Compound 2

To dichloromethane (200 mL) were sequentially added 4-hydroxybenzaldehyde (2.0 g, 16.4 mmol), 2-(acetoxymethyl)-6-bromotetrahydro-2H-pyran-3,4,5-triyl triacetate (13.5 g, 32.7 mmol), and tetrabutylammonium bromide (5.3 g, 16.4 mmol) to prepare the reaction solution. Subsequently, 5% aqueous NaOH solution (1.83 g NaOH dissolved in 36.6 mL water, 45.7 mmol) was added, and the mixture was stirred at room temperature for 4 hours. After completion of the reaction, the reaction mixture was transferred to a separatory funnel and the aqueous phase was extracted with dichloromethane (3×100 mL). The combined organic phases were dried over anhydrous sodium sulfate and concentrated under reduced pressure to remove the solvent. The crude product was purified by silica gel column chromatography (eluent: petroleum ether/ethyl acetate = 2:1) to give white solid product **2** (6.06 g, 81.8% yield). ^{1}H NMR (500 MHz, DMSO) δ 9.93 (s, 1H), 7.93 (d, J = 8.3 Hz, 2H), 7.20 (d, J = 8.3 Hz, 2H), 5.69 (d, J = 7.5 Hz, 1H), 5.39 (d, J = 3.0 Hz, 1H), 5.34 – 5.26 (m, 2H), 4.52 (t, J = 6.2 Hz, 1H), 4.14 (t, J = 8.6 Hz, 2H), 2.16 (s, 3H), 2.05 (s, 3H), 2.03 (s, 3H), 1.97 (s, 3H).

^{13}C NMR (500 MHz, DMSO) δ 191.41, 169.90, 169.78, 169.48, 169.16, 160.83, 131.68, 131.32, 116.45, 96.90, 70.62, 70.06, 68.20, 67.17, 61.26, 20.39, 20.32, 20.29, 20.25, 14.00. $C_{21}H_{24}O_{10}$: MS(ESI, m/z): $[M+Na]^+$ calcd for target, 475.12; found 475.14.

(2) Synthesis of Compound 3

At 0°C, sodium borohydride (250.8 mg, 6.6 mmol) was carefully added in portions to a methanol solution (150 mL) of compound **2** (3.0 g, 6.6 mmol). After stirring at room temperature for 4 hours, tetrahydrofuran was removed under reduced pressure. A mixture of saturated ammonium chloride solution (200 mL) and dichloromethane (250 mL) was added, the two phases were separated, and the aqueous phase was extracted with dichloromethane (3 × 50 mL). The combined organic phases were dried over anhydrous sodium sulfate and concentrated under reduced pressure. The crude product was purified by silica gel column chromatography (eluent: petroleum ether/ethyl acetate = 1:1) to give white solid product **3** (2.46 g, 82.3% yield). ^{1}H NMR (500 MHz, DMSO) δ 7.27 (d, J = 8.3 Hz, 2H), 6.95 (d, J = 8.4 Hz, 2H), 5.42 (d, J = 7.8 Hz, 1H), 5.35 (d, J = 3.2 Hz, 1H), 5.29 (dd, J = 10.3, 3.4 Hz, 1H), 5.21 (dd, J = 10.2, 8.0 Hz, 1H), 5.09 (t, J = 5.7 Hz, 1H), 4.44 (d, J = 5.7 Hz, 2H), 4.41 (d, J = 6.3 Hz, 1H), 4.14 – 4.05 (m, 2H), 2.15 (s, 3H), 2.03 (d, J = 8.3 Hz, 3H), 2.01 (s, 3H), 1.95 (s, 3H). ^{13}C NMR (500 MHz, DMSO) δ 169.92, 169.78, 169.48, 169.16, 155.40, 137.07, 127.82, 116.15, 98.06, 70.30, 70.16, 68.45, 67.25, 62.37, 61.28, 20.41, 20.37, 20.32, 20.27, 14.02. $C_{21}H_{26}O_{10}$: MS(ESI, m/z): $[M+Na]^+$ calcd for target, 477.13; found 477.14.

(3) Synthesis of Compound 4

At 0°C, phosphorus tribromide (714.9 mg, 2.6 mmol) was carefully added to a dichloromethane solution (200 mL) of compound **3** (2.4 g, 5.3 mmol), and the mixture was stirred at room temperature for 2 hours. Saturated sodium bicarbonate solution (20 mL) was added dropwise, followed by further dilution with water (200 mL). The two phases were separated, and the aqueous phase was extracted with dichloromethane (3 × 50 mL). The combined organic phases were dried over anhydrous sodium sulfate and concentrated under reduced pressure. The crude product was purified by silica gel column chromatography (eluent: petroleum ether/ethyl acetate = 5:1) to give white solid product (2.05 g, 75.2% yield). ^{1}H NMR (500 MHz, $CDCl_3$) δ 7.33 (d, J = 8.5 Hz, 2H), 6.98 (t, J = 9.1 Hz, 2H), 5.51 – 5.44 (m, 2H), 5.11 (dd, J = 10.4, 3.3 Hz, 1H), 5.05 (d, J = 7.9 Hz, 1H), 4.52 (d, J = 39.9 Hz, 2H), 4.27 – 4.19 (m, 1H), 4.16 (dd, J = 11.3, 6.2 Hz, 1H), 4.07 (t, J = 6.6 Hz, 1H), 2.17 (d, J = 7.0 Hz, 3H), 2.05 (d, J = 7.8 Hz, 6H), 2.00 (d, J = 9.0 Hz, 3H). ^{13}C NMR (500 MHz, $CDCl_3$) δ 170.28, 170.17, 170.04, 169.30, 156.86, 132.78, 130.44, 130.04, 117.16, 99.55, 99.48, 71.12, 70.80, 68.62, 66.88, 61.36, 33.06, 20.68, 20.61, 20.53. $C_{21}H_{25}BrO_{10}$: MS(ESI, m/z): $[M+Na]^+$ calcd for target, 539.05; found 539.10.

(4) Synthesis of Compound 6

To anhydrous dichloromethane were sequentially added Boc-L-glutamic acid-1-tert-butyl ester (1 g, 3.3 mmol) and EDCI (631.9 mg, 3.3 mmol). After stirring for 30 minutes, 4-aminophenol (397.9 mg, 3.23 mmol) was added. The reaction was then conducted in an ice bath for 1.5 hours. After completion of the reaction, extraction

separation was performed and the solvent was removed by rotary evaporation. The crude product was purified by column chromatography (eluent: petroleum ether/ethyl acetate = 1:1) to give yellow solid product (996.8 mg, 75.6% yield). ^{1}H NMR (500 MHz, DMSO) δ 9.83 (s, 1H), 7.52 (d, J = 8.2 Hz, 2H), 7.22 (d, J = 8.2 Hz, 2H), 7.07 (dd, J = 45.6, 19.6 Hz, 1H), 5.06 (t, J = 5.6 Hz, 1H), 4.43 (d, J = 5.5 Hz, 2H), 4.03 (q, J = 7.1 Hz, 1H), 2.39 (t, J = 7.4 Hz, 2H), 2.00 (d, J = 11.5 Hz, 2H), 1.38 (t, J = 14.0 Hz, 18H). ^{13}C NMR (500 MHz, DMSO) δ 171.55, 170.13, 155.49, 137.83, 137.07, 126.82, 118.77, 80.27, 78.02, 62.62, 59.68, 53.90, 32.61, 28.15, 27.62, 26.25, 20.68, 14.02. $C_{21}H_{32}N_2O_6$: MS(ESI, m/z): $[M+Na]^+$ calcd for target, 431.21; found 431.19.

(5) Synthesis of Compound 7

First, compound **6** (1 g, 2.45 mmol) was dissolved in anhydrous dichloromethane, then triphenylphosphine (963.14 mg, 3.67 mmol) and N-bromosuccinimide (NBS, 653.56 mg, 3.67 mmol) were sequentially added under nitrogen protection. The reaction solution was stirred at room temperature for 4 hours. After completion of the reaction, extraction separation was performed using ethyl acetate and saturated brine. The crude product was purified by silica gel column chromatography (eluent: petroleum ether/ethyl acetate = 5:1) to give white solid compound for use in the next step. ^{1}H NMR (500 MHz, DMSO) δ 9.78 (s, 1H), 7.53 (d, J = 8.1 Hz, 2H), 7.25 (d, J = 8.1 Hz, 2H), 7.08 (dd, J = 46.6, 19.5 Hz, 1H), 4.42 (d, J = 5.5 Hz, 2H), 4.05 (q, J = 7.2 Hz, 1H), 2.37 (t, J = 7.4 Hz, 2H), 2.01 (d, J = 11.6 Hz, 2H), 1.39 (t, J = 14.1 Hz, 18H). ^{13}C NMR (500 MHz, DMSO) δ 172.91, 170.45, 156.75, 138.08, 137.15, 130.26, 129.73, 80.88, 78.72, 62.89, 59.38, 53.76, 31.75, 28.92, 27.53, 26.07, 20.44, 14.60. $C_{21}H_{31}BrN_2O_5$: MS(ESI, m/z): $[M+Na]^+$ calcd for target, 471.14; found 471.05.

(6) Synthesis of Compound 9

2,4-Dihydroxybenzaldehyde (1.38 g, 10 mmol, 1.0 equiv), **4** (5.16 g, 10 mmol, 1.0 equiv), anhydrous K_2CO_3 (2.76 g, 20 mmol, 2.0 equiv), and catalytic amount of KI (166 mg, 1 mmol, 0.1 equiv) were dissolved in anhydrous acetonitrile solution. The reaction mixture was refluxed at 85°C for 8 hours. The reaction mixture was then cooled to room temperature, the solvent was dried using a rotary evaporator, and petroleum ether:ethyl acetate = 3:1 (v/v) mixed solvent was used as the developing agent. Purification by silica gel column chromatography gave a yellow oily liquid (3.73 g, 65.2% yield). ^{1}H NMR (500 MHz, $CDCl_3$) δ 11.46 (s, 1H), 9.72 (s, 1H), 7.44 (d, J = 8.7 Hz, 1H), 7.36 (d, J = 8.5 Hz, 2H), 7.03 (d, J = 8.5 Hz, 2H), 6.59 (dd, J = 8.7, 2.2 Hz, 1H), 6.49 (d, J = 2.1 Hz, 1H), 5.52 – 5.36 (m, 2H), 5.12 (dt, J = 10.0, 5.0 Hz, 1H), 5.06 (d, J = 9.2 Hz, 3H), 4.23 (dd, J = 11.3, 6.9 Hz, 1H), 4.17 (dd, J = 11.3, 6.3 Hz, 1H), 4.08 (t, J = 6.6 Hz, 1H), 2.19 (s, 3H), 2.07 (d, J = 3.2 Hz, 3H), 2.06 (s, 3H), 2.02 (s, 3H). ^{13}C NMR (500 MHz, $CDCl_3$) δ 194.40, 170.33, 170.22, 170.10, 169.37, 165.78, 164.43, 156.98, 135.31, 130.57, 129.19, 117.18, 115.36, 108.90, 101.62, 99.59, 71.10, 70.81, 69.89, 68.66, 66.88, 61.35, 20.70, 20.62, 20.55. $C_{28}H_{30}O_{13}$: MS(ESI, m/z): $[M+Na]^+$ calcd for target, 597.15; found 597.13.

(7) Synthesis of Compound 10

9 (2.87 g, 5 mmol, 1.0 equiv), **7** (2.35 g, 5 mmol, 1.0 equiv), anhydrous K_2CO_3 (1.38 g, 10 mmol, 2.0 equiv), and catalytic amount of KI (83 mg, 0.5 mmol, 0.1 equiv) were

dissolved in anhydrous acetonitrile solution. The reaction mixture was refluxed at 85°C for 8 hours. The reaction mixture was then cooled to room temperature, the solvent was dried using a rotary evaporator, and petroleum ether:ethyl acetate = 3:1 (v/v) mixed solvent was used as the developing agent. Purification by silica gel column chromatography gave a white solid (3.32 g, 69.1% yield). ^{1}H NMR (500 MHz, $CDCl_3$) δ 10.34 (d, J = 11.6 Hz, 1H), 8.99 (s, 1H), 7.84 – 7.64 (m, 2H), 7.46 – 7.33 (m, 4H), 7.04 (d, J = 8.4 Hz, 2H), 6.63 – 6.48 (m, 2H), 5.46 (ddd, J = 46.3, 26.8, 7.6 Hz, 3H), 5.16 – 5.02 (m, 6H), 4.27 – 4.05 (m, 5H), 2.46 (dd, J = 14.1, 7.8 Hz, 2H), 2.19 (s, 3H), 2.07 (s, 3H), 2.06 (s, 3H), 2.02 (s, 3H), 1.94 – 1.75 (m, 2H), 1.51 (s, 2H), 1.49 (s, 2H), 1.46 (d, J = 4.2 Hz, 14H). ^{13}C NMR (500 MHz, $CDCl_3$) δ 194.39, 188.21, 171.23, 170.30, 170.19, 170.07, 169.35, 165.05, 164.43, 162.74, 156.97, 135.30, 130.80, 130.56, 130.47, 129.21, 129.18, 128.14, 119.87, 119.58, 117.18, 108.89, 106.95, 101.62, 100.11, 99.60, 83.30, 82.26, 80.50, 71.09, 70.80, 70.22, 69.86, 68.67, 66.88, 61.32, 60.36, 59.61, 31.13, 28.31, 27.97, 27.93, 27.92, 21.65, 21.01, 20.70, 20.62, 20.55, 14.18. $C_{49}H_{60}N_2O_{18}$: MS(ESI, m/z): $[M+Na]^+$ calcd for target, 987.37; found 987.31.

(8) Synthesis of Compound 11

At 0°C, sodium borohydride (98.8 mg, 2.6 mmol) was carefully added in portions to a methanol solution (150 mL) of compound **10** (1.93 g, 2 mmol). After stirring at room temperature for 4 hours, tetrahydrofuran was removed under reduced pressure. A mixture of saturated ammonium chloride solution (200 mL) and dichloromethane (250 mL) was added, the two phases were separated, and the aqueous phase was extracted with dichloromethane (3 × 50 mL). The combined organic phases were dried over anhydrous sodium sulfate and concentrated under reduced pressure. The crude product was purified by silica gel column chromatography (eluent: petroleum ether/ethyl acetate = 1:1) to give white solid product **11** (1.3 g, 80.2% yield). ^{1}H NMR (500 MHz, $CDCl_3$) δ 10.14 (d, J = 11.5 Hz, 1H), 8.97 (s, 1H), 7.85 – 7.63 (m, 2H), 7.56 – 7.34 (m, 4H), 7.05 (d, J = 8.4 Hz, 2H), 6.66 – 6.58 (m, 2H), 5.44 (ddd, J = 44.3, 26.9, 7.5 Hz, 5H), 5.13 – 5.00 (m, 6H), 4.26 – 4.03 (m, 5H), 2.47 (dd, J = 14.7, 7.7 Hz, 2H), 2.16 (s, 3H), 2.06 (s, 3H), 2.04 (s, 3H), 2.01 (s, 3H), 1.95 – 1.74 (m, 2H), 1.52 (s, 2H), 1.48 (s, 2H), 1.45 (d, J = 4.2 Hz, 14H). ^{13}C NMR (500 MHz, $CDCl_3$) δ 193.85, 189.61, 171.55, 170.48, 169.53, 169.01, 167.94, 165.03, 161.04, 160.07, 151.06, 139.06, 135.84, 134.82, 133.91, 128.21, 126.91, 125.92, 125.53, 119.38, 118.17, 113.20, 105.57, 103.39, 101.09, 98.92, 96.37, 83.95, 81.94, 74.03, 72.05, 70.54, 67.74, 65.42, 63.99, 60.33, 59.23, 36.38, 35.51, 33.53, 30.52, 30.10, 27.33, 24.79, 22.94, 20.38, 17.29. $C_{49}H_{62}N_2O_{18}$: HRMS(ESI, m/z): $[M+H]^+$ calcd for target, 811.2921; found 811.3018.

(9) Synthesis of Compound 12

Compound **Cy-OH** (125.0 mg, 0.2 mmol, 1.0 equiv) and triphosgene (19.8 mg, 0.66 mmol, 0.33 equiv) were dissolved in 15 mL anhydrous dichloromethane and stirred thoroughly to ensure proper mixing. Subsequently, N,N-diisopropylethylamine (84.1 mg, 0.652 mmol, 3.26 equiv) was slowly added dropwise, and the mixture was stirred at room temperature for 30 minutes. After formation of the acyl chloride intermediate of Cy-OH, compound **11** (162.5 mg, 0.2 mmol, 1.0 equiv) was added, followed by

addition of a few drops of N,N-diisopropylethylamine. The mixture was then stirred at room temperature for 6 hours. After the reaction was essentially complete, the reaction mixture was directly transferred to a silica gel column by wet loading, then purified by column chromatography using DCM:MeOH = 20:1 (v/v) as the developing agent to give the final product **Cy-GGT-β-gal**, bright purple solid (130.4 mg, 43.7% yield). ^{1}H NMR (400 MHz, DMSO) δ 9.89 (s, 1H), 8.91 – 8.77 (m, 1H), 8.58 (d, J = 31.5 Hz, 1H), 8.16 (s, 1H), 7.88 (d, J = 11.6 Hz, 3H), 7.73 – 7.61 (m, 6H), 7.53 – 7.34 (m, 6H), 7.33 – 7.09 (m, 6H), 7.04 – 6.82 (m, 4H), 6.59 (t, J = 13.9 Hz, 4H), 6.13 (d, J = 13.7 Hz, 1H), 5.27 (d, J = 22.3 Hz, 4H), 5.11 (d, J = 10.8 Hz, 2H), 4.96 – 4.82 (m, 2H), 4.59 (s, 1H), 4.39 (s, 2H), 2.82 (d, J = 9.5 Hz, 4H), 2.30 (d, J = 6.7 Hz, 2H), 2.08 (s, 12H), 1.47 (d, J = 26.5 Hz, 29H). ^{13}C NMR (400 MHz, $CDCl_3$) δ 179.65, 173.04, 167.40, 161.26, 154.85, 151.11, 146.17, 137.27, 132.25, 131.53, 130.67, 129.98, 129.19, 128.96, 127.58, 127.09, 126.40, 125.44, 122.84, 121.47, 117.42, 111.60, 105.45, 100.00, 85.20, 81.67, 80.27, 70.16, 67.73, 65.86, 60.41, 55.07, 45.60, 31.96, 29.38, 27.01, 24.43, 23.75, 20.91, 13.59. $C_{77}H_{88}N_3O_{21}$: HRMS(ESI, m/z): $[M]^+$ calcd for target, 1390.5905; found 1390.5940.

(10) Synthesis of Compound Cy-GGT-β-gal

Compound **12** (151.7 mg, 0.1 mmol) was dissolved in 2 mL dry dichloromethane (CH_2Cl_2) and stirred at room temperature for 10 minutes. Subsequently, 2 mL CH_2Cl_2-TFA solution (1:1, v/v) was added dropwise to the above mixture. After the addition was complete, the reaction mixture was stirred overnight at room temperature. The crude product was purified by silica gel column chromatography (eluent: dichloromethane/methanol = 10:1) to give orange-red solid product **Cy-GGT-β-gal** (99.4 mg, 73.2% yield). ^{1}H NMR (400 MHz, DMSO) δ 12.54 (s, 1H), 10.66 – 10.52 (m, 1H), 8.95 – 8.81 (m, 3H), 8.58 (d, J = 15.1 Hz, 3H), 8.16 (s, 3H), 7.87 (t, J = 23.8 Hz, 2H), 7.76 – 7.53 (m, 2H), 7.50 – 7.32 (m, 3H), 7.33 – 7.08 (m, 4H), 7.04 – 6.83 (m, 4H), 6.63 (t, J = 9.7 Hz, 1H), 5.99 – 5.80 (m, 1H), 5.38 – 5.25 (m, 2H), 5.17 – 5.05 (m, 6H), 4.61 (s, 2H), 4.42 (s, 1H), 3.48 (d, J = 33.7 Hz, 1H), 2.76 (s, 4H), 2.16 – 1.96 (m, 16H), 1.51 (d, J = 34.9 Hz, 11H). ^{13}C NMR (400 MHz, $CDCl_3$) δ 192.60, 183.14, 179.17, 173.53, 167.40, 163.86, 160.96, 154.66, 149.92, 143.12, 137.94, 131.35, 130.86, 130.14, 129.19, 127.78, 126.15, 122.66, 121.18, 117.42, 111.60, 105.17, 99.78, 74.56, 74.34, 70.16, 67.73, 66.11, 60.72, 55.07, 45.16, 29.88, 28.41, 26.81, 19.92, 12.41. $C_{68}H_{72}N_3O_{19}$: HRMS(ESI, m/z): $[M]^+$ calcd for target, 1234.4755; found 1234.4736.

(11) Synthesis of Compound 13

2,4-Dihydroxybenzaldehyde (1.38 g, 10 mmol, 1.0 equiv), benzyl bromide (1.7 g, 10 mmol, 1.0 equiv), anhydrous K_2CO_3 (2.76 g, 20 mmol, 2.0 equiv), and catalytic amount of KI (166 mg, 1 mmol, 0.1 equiv) were dissolved in anhydrous acetonitrile solution. The reaction mixture was refluxed at 85°C for 8 hours. The reaction mixture was then cooled to room temperature, the solvent was dried using a rotary evaporator, and petroleum ether:ethyl acetate = 3:1 (v/v) mixed solvent was used as the developing agent. Purification by silica gel column chromatography gave a yellow oily liquid (1.71 g, 74.9% yield). ^{1}H NMR (400 MHz, $CDCl_3$) δ 10.53 (s, 1H), 10.02 (s, 1H), 8.37 (d, J

= 8.7 Hz, 2H), 7.82 (d, J = 8.7 Hz, 3H), 7.05 (d, J = 8.7 Hz, 1H), 6.67 (dd, J = 8.7, 2.2 Hz, 2H), 6.28 (d, J = 2.2 Hz, 1H), 5.36 (s, 2H). ^{13}C NMR (400 MHz, $CDCl_3$) δ 189.69, 165.71, 160.23, 144.50, 139.16, 135.19, 126.41, 124.28, 113.30, 108.45, 102.10, 70.34. $C_{14}H_{12}O_3$: HRMS(ESI, m/z): $[M+H]^+$ calcd for target, 229.0860; found 229.0850.

(12) Synthesis of Compound 14

13 (2.28 g, 10 mmol, 1.0 equiv), **4** (5.16 g, 10 mmol, 1.0 equiv), anhydrous K_2CO_3 (2.76 g, 20 mmol, 2.0 equiv), and catalytic amount of KI (166 mg, 1 mmol, 0.1 equiv) were dissolved in anhydrous acetonitrile solution. The reaction mixture was refluxed at 85°C for 8 hours. The reaction mixture was then cooled to room temperature, the solvent was dried using a rotary evaporator, and petroleum ether:ethyl acetate = 3:1 (v/v) mixed solvent was used as the developing agent. Purification by silica gel column chromatography gave a yellow oily liquid (4.06 g, 65.6% yield). ^{1}H NMR (500 MHz, $CDCl_3$) δ 11.42 (s, 1H), δ 9.87 (s, 1H), 7.72 (d, J = 8.2 Hz, 2H), 7.56 (d, J = 8.4 Hz, 1H), 7.52 (d, J = 8.2 Hz, 1H), 7.42 (d, J = 8.6 Hz, 2H), 6.97 (dd, J = 45.6, 19.6 Hz, 2H), 6.73 (d, J = 8.2 Hz, 2H), 6.51 (d, J = 8.2 Hz, 2H), 5.72 (t, J = 5.6 Hz, 2H), 5.06 (t, J = 5.6 Hz, 1H), 4.43 (d, J = 5.5 Hz, 2H), 4.03 (q, J = 7.1 Hz, 1H), 2.24 (t, J = 7.4 Hz, 2H), 1.86 (d, J = 11.5 Hz, 2H), 1.38 (t, J = 14.0 Hz, 18H). ^{13}C NMR (500 MHz, $CDCl_3$) δ 196.48, 186.19, 177.29, 166.43, 164.75, 149.71, 142.90, 134.61, 129.69, 122.66, 117.17, 104.96, 97.88, 80.96, 65.85, 60.71, 57.17, 46.35, 39.49, 37.87, 31.47, 20.68. $C_{35}H_{42}N_2O_8$: HRMS(ESI, m/z): $[M+H]^+$ calcd for target, 619.3014; found 619.3084.

(13) Synthesis of Compound 15

Compound **2-14** (2.47 g, 4.0 mmol, 1.0 equiv) was dissolved in a mixed solution of 15 mL dichloromethane and 15 mL methanol with stirring. After stirring uniformly, $NaBH_4$ solid (303 mg, 8.0 mmol, 2.0 equiv) was slowly added to the reaction in batches, paying attention to controlling the reaction exotherm. The reaction was stirred at room temperature for 45 minutes to 1 hour, and TLC showed that the reaction was essentially complete. Then an appropriate amount of water was slowly added to the reaction mixture to quench the remaining $NaBH_4$, followed by extraction of the organic phase with ethyl acetate three times. The organic phase was washed with saturated sodium chloride water and dried over anhydrous Na_2SO_4. Purification by silica gel column chromatography using petroleum ether:ethyl acetate = 2:1 (v/v) mixed solution as eluent gave a colorless viscous oily liquid compound **2-15** (1.79 g, 72.3% yield). ^{1}H NMR (500 MHz, $CDCl_3$) δ 9.87 (s, 1H), δ 7.87 (d, J = 8.5 Hz, 3H), 7.56 (d, J = 8.4 Hz, 2H), 7.52 (d, J = 8.2 Hz, 2H), 7.42 (d, J = 8.6 Hz, 3H), 6.95 (dd, J = 45.6, 19.6 Hz, 4H), 6.72 (d, J = 8.3 Hz, 2H), 5.76 (t, J = 5.6 Hz, 2H), 5.08 (t, J = 5.6 Hz, 2H), 4.45 (d, J = 5.6 Hz, 1H), 4.03 (q, J = 7.4 Hz, 2H), 2.24 (t, J = 7.7 Hz, 2H), 1.86 (d, J = 12.5 Hz, 2H), 1.33 (t, J = 14.5 Hz, 18H). ^{13}C NMR (500 MHz, $CDCl_3$) δ 177.01, 166.43, 164.56, 149.92, 137.27, 135.60, 133.71, 130.66, 129.47, 127.59, 118.12, 116.55, 110.39, 104.49, 97.46, 75.31, 74.88, 70.80, 65.85, 60.71, 57.17, 46.58, 38.07, 37.60, 31.26, 26.54. $C_{35}H_{44}N_2O_8$: HRMS(ESI, m/z): $[M+H]^+$ calcd for target, 621.3171; found 621.3142.

(14) Synthesis of Compound 16

Compound Cy-OH (125.0 mg, 0.2 mmol, 1.0 equiv) and triphosgene (19.8 mg, 0.66 mmol, 0.33 equiv) were dissolved in 15 mL anhydrous dichloromethane and stirred thoroughly to ensure proper mixing. Subsequently, N,N-diisopropylethylamine (84.1 mg, 0.652 mmol, 3.26 equiv) was slowly added dropwise, and the mixture was stirred at room temperature for 30 minutes. After formation of the acyl chloride intermediate of Cy-OH, compound **11** (124.5 mg, 0.2 mmol, 1.0 equiv) was added, followed by addition of a few drops of N,N-diisopropylethylamine. The mixture was then stirred at room temperature for 6 hours. After the reaction was essentially complete, the reaction mixture was directly transferred to a silica gel column by wet loading, then purified by column chromatography using DCM:MeOH = 20:1 (v/v) as the developing agent to give the final product **16**, bright purple solid (101.4 mg, 43.5% yield). ^{1}H NMR (400 MHz, DMSO) δ 10.14 – 10.03 (m, 1H), 9.11 – 9.01 (m, 1H), 8.16 (d, 1H), 7.91 (d, J = 8.4 Hz, 1H), 7.75 – 7.54 (m, 4H), 7.48 – 7.37 (m, 2H), 7.30 – 7.08 (m, 3H), 7.06 – 6.95 (m, 4H), 6.88 (d, J = 15.2 Hz, 2H), 6.63 (t, J = 9.7 Hz, 4H), 5.31 (dd, J = 15.3, 10.6 Hz, 2H), 5.24 (s, 3H), 5.14 (d, J = 17.5 Hz, 2H), 4.42 (s, 1H), 4.02 (s, 2H), 2.74 (s, 4H), 2.08 (s, 2H), 2.03 – 1.99 (m, 2H), 1.46 (d, J = 5.5 Hz, 29H). ^{13}C NMR (400 MHz, $CDCl_3$) δ 178.87, 173.24, 166.20, 160.09, 155.35, 149.01, 142.63, 139.84, 134.20, 133.71, 129.69, 128.07, 127.10, 125.92, 124.26, 118.39, 112.48, 111.12, 84.03, 70.83, 63.99, 61.21, 53.90, 47.30, 40.06, 34.05, 33.35, 26.36, 25.89, 24.68, 18.34. $C_{63}H_{70}N_3O_{11}$: HRMS(ESI, m/z): $[M]^+$ calcd for target, 1044.5005; found 1044.5029.

(15) Synthesis of Compound Cy-GGT

Compound **16** (117.1 mg, 0.1 mmol) was dissolved in 2 mL dry dichloromethane (CH_2Cl_2) and stirred at room temperature for 10 minutes. Subsequently, 2 mL CH_2Cl_2-TFA solution (1:1, v/v) was added dropwise to the above mixture. After the addition was complete, the reaction mixture was stirred overnight at room temperature. The crude product was purified by silica gel column chromatography (eluent: dichloromethane/methanol = 10:1) to give orange-red solid product **Cy-GGT** (47.2 mg, 53.2% yield). ^{1}H NMR (400 MHz, DMSO) δ 12.49 – 12.30 (m, 1H), 10.09 – 9.97 (m, 1H), 9.02 – 8.86 (m, 1H), 8.16 (s, 2H), 7.91 (d, J = 8.4 Hz, 2H), 7.74 – 7.57 (m, 4H), 7.53 – 7.39 (m, 2H), 7.33 – 7.13 (m, 4H), 7.05 – 6.97 (m, 4H), 6.86 (s, 2H), 6.63 (t, J = 9.7 Hz, 2H), 5.33 (t, J = 4.7 Hz, 2H), 5.28 – 5.18 (m, 3H), 5.09 (d, J = 23.7 Hz, 2H), 4.02 (s, 2H), 3.52 (s, 1H), 2.71 (d, J = 24.2 Hz, 4H), 2.07 – 1.90 (m, 4H), 1.46 (d, J = 5.5 Hz, 11H). ^{13}C NMR (400 MHz, $CDCl_3$) δ 181.73, 173.24, 168.78, 161.26, 155.15, 149.23, 143.62, 139.84, 134.90, 133.22, 129.47, 128.29, 127.31, 125.71, 123.55, 119.32, 113.68, 111.12, 69.41, 64.54, 53.90, 41.65, 28.03, 26.84, 26.09, 24.68, 17.87. $C_{54}H_{54}N_3O_9$: HRMS(ESI, m/z): $[M]^+$ calcd for target, 888.3855; found 888.3914.

(16) Synthesis of Compound 17

9 (5.74 g, 10 mmol, 1.0 equiv), **4** (5.17 g, 10 mmol, 1.0 equiv), anhydrous K_2CO_3 (2.76 g, 20 mmol, 2.0 equiv), and catalytic amount of KI (166 mg, 1 mmol, 0.1 equiv) were dissolved in anhydrous acetonitrile solution. The reaction mixture was refluxed at 85°C for 8 hours. The reaction mixture was then cooled to room temperature, the solvent was dried using a rotary evaporator, and petroleum ether:ethyl acetate = 3:1 (v/v) mixed solvent was used as the developing agent. Purification by silica gel column

chromatography gave a yellow oily liquid (4.8 g, 72.5% yield). ^{1}H NMR (500 MHz, DMSO) δ 11.53 (s, 1H), 8.14 (s, 1H), 7.44 (m, J = 8.7 Hz, 4H), 7.37 (d, J = 8.5 Hz, 2H), 7.03 (d, J = 8.6 Hz, 2H), 6.59 (dd, J = 8.5, 2.2 Hz, 2H), 6.53 (d, J = 2.1 Hz, 1H), 5.51 – 5.37 (m, 3H), 5.13 (dt, J = 10.1, 5.0 Hz, 3H), 5.06 (d, J = 9.1 Hz, 2H), 4.24 (dd, J = 11.5, 6.9 Hz, 1H), 4.16 (dd, J = 11.4, 6.3 Hz, 1H), 4.08 (t, J = 6.6 Hz, 1H), 2.02 (s, 6H), 1.97 (d, J = 3.2 Hz, 6H). ^{13}C NMR (400 MHz, $CDCl_3$) δ 188.48, 169.84, 160.14, 155.17, 140.06, 135.31, 133.87, 129.92, 125.57, 120.80, 111.34, 104.06, 72.64, 70.10, 67.03, 64.59, 61.76, 25.90, 24.42. $C_{35}H_{36}O_{13}$: HRMS(ESI, m/z): $[M+H]^+$ calcd for target, 665.2229; found 665.2212.

(17) Synthesis of Compound 18

Compound **17** (2.66 g, 4.0 mmol, 1.0 equiv) was dissolved in a mixed solution of 15 mL dichloromethane and 15 mL methanol with stirring. After stirring uniformly, $NaBH_4$ solid (303 mg, 8.0 mmol, 2.0 equiv) was slowly added to the reaction in batches, paying attention to controlling the reaction exotherm. The reaction was stirred at room temperature for 45 minutes to 1 hour, and TLC showed that the reaction was essentially complete. Then an appropriate amount of water was slowly added to the reaction mixture to quench the remaining $NaBH_4$, followed by extraction of the organic phase with ethyl acetate three times. The organic phase was washed with saturated sodium chloride water and dried over anhydrous Na_2SO_4. Purification by silica gel column chromatography using petroleum ether:ethyl acetate = 2:1 (v/v) mixed solution as eluent gave a colorless viscous oily liquid compound **18** (2.10 g, 79.0% yield). ^{1}H NMR (500 MHz, $CDCl_3$) δ 8.14 (s, 1H), 7.74 (s, 1H), 7.57 (m, J = 8.7 Hz, 5H), 7.47 (d, J = 8.5 Hz, 2H), 6.93 (d, J = 8.6 Hz, 2H), 6.60 (dd, J = 8.5, 2.2 Hz, 2H), 6.58 (d, J = 2.1 Hz, 1H), 5.51 – 5.37 (m, 2H), 5.13 (dt, J = 10.1, 5.0 Hz, 3H), 5.06 (d, J = 9.1 Hz, 3H), 4.58 (m, 1H), 4.24 (dd, J = 11.5, 6.9 Hz, 1H), 4.16 (dd, J = 11.4, 6.3 Hz, 1H), 4.08 (t, J = 6.6 Hz, 1H), 2.28 (s, 6H), 2.12 (d, J = 3.2 Hz, 6H). ^{13}C NMR (500 MHz, $CDCl_3$) δ 171.92, 162.63, 160.73, 157.25, 155.42, 147.90, 140.69, 135.19, 133.87, 129.47, 126.42, 119.78, 111.54, 104.31, 72.82, 69.71, 65.02, 62.07, 26.92, 24.91. $C_{35}H_{38}O_{13}$: HRMS(ESI, m/z): $[M+H]^+$ calcd for target, 667.2386; found 667.2309.

(18) Synthesis of Compound Cy-β-gal

Compound Cy-OH (65.1 mg, 0.1 mmol, 1.0 equiv) and triphosgene (9.9 mg, 0.33 mmol, 0.33 equiv) were dissolved in 15 mL anhydrous dichloromethane and stirred thoroughly to ensure proper mixing. Subsequently, N,N-diisopropylethylamine (42 mg, 0.326 mmol, 3.26 equiv) was slowly added dropwise, and the mixture was stirred at room temperature for 30 minutes. After formation of the acyl chloride intermediate of CyI-OH, compound **18** (66.5 mg, 0.1 mmol, 1.0 equiv) was added, followed by addition of a few drops of N,N-diisopropylethylamine. The mixture was then stirred at room temperature for 6 hours. After the reaction was essentially complete, the reaction mixture was directly transferred to a silica gel column by wet loading, then purified by column chromatography using DCM:MeOH = 20:1 (v/v) as the developing agent to give the final product **Cy-β-gal**, bright purple solid (67.3 mg, 55.7% yield). ^{1}H NMR (400 MHz, DMSO) δ 9.06 – 8.90 (s, 1H), 8.58 (d, J = 15.1 Hz, 2H), 8.16 (s, 2H), 7.91 (d, J = 8.4 Hz, 3H), 7.73 – 7.55 (m, J = 12.2 Hz, 4H), 7.49 – 7.37 (m, J = 11.7 Hz, 3H),

7.27 – 7.09 (m, J = 9.1 Hz, 3H), 7.08 – 6.83 (m, J = 9.7 Hz, 3H), 6.63 (t, J = 9.7 Hz, 3H), 6.01 – 5.86 (m, 2H), 5.42 – 5.26 (m, 1H), 5.24 – 5.07 (m, 6H), 4.87 – 4.70 (m, J = 9.7 Hz, 1H), 4.35 – 4.24 (m, J = 9.5 Hz, 2H), 4.07 (d, J = 42.2 Hz, 2H), 2.79 (s, 4H), 2.00 (ddd, J = 30.2, 24.1, 17.0 Hz, 12H), 1.46 (d, J = 5.5 Hz, 11H). ^{13}C NMR (400 MHz, $CDCl_3$) δ 174.77, 170.64, 160.23, 156.71, 153.44, 152.40, 148.52, 144.64, 140.93, 138.28, 135.59, 134.58, 133.73, 129.23, 126.57, 125.71, 124.91, 117.34, 112.80, 108.74, 106.44, 105.39, 101.94, 74.41, 72.78, 68.72, 67.70, 66.24, 63.57, 55.78, 45.31, 33.43, 30.74, 26.22, 25.59, 24.58, 21.11, 13.90. $C_{63}H_{64}NO_{16}$: HRMS(ESI, m/z): $[M]^+$ calcd for target, 1090.4220; found 1090.4241.

3. Spectroscopic Property

Table R1. Summary of GGT and β-Gal probes

Probe structure	Target enzyme	Absorption/Emission (nm)	References
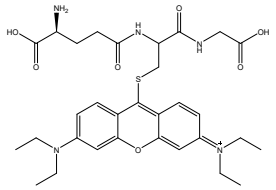	GGT	593/620	1
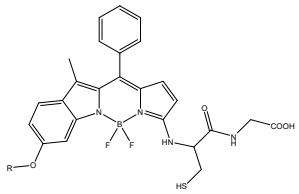	GGT	510/582	2
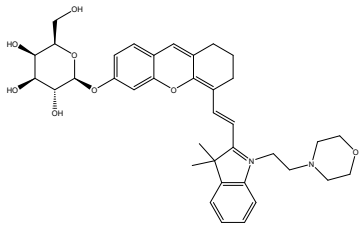	β-Gal	685/710	3
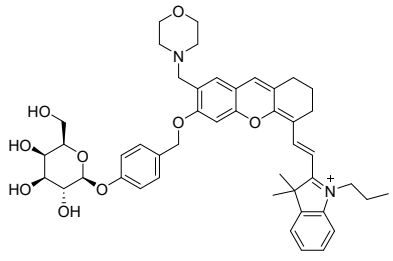	β-Gal	685/710	4
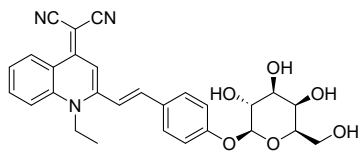	β-Gal	435/560	5

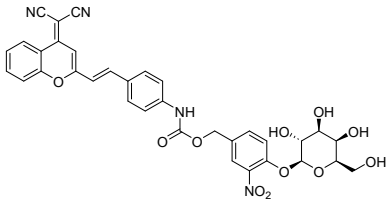	β-Gal	526/676	6
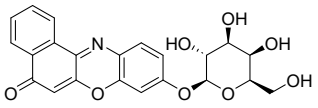	β-Gal	575/642	7
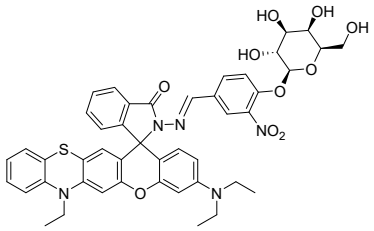	β-Gal	596/738	8
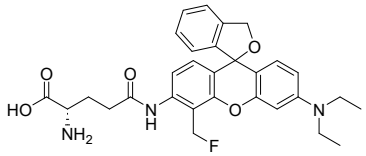	GGT	533/576	9
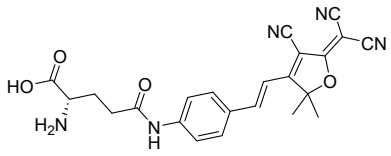	GGT	510/610	10
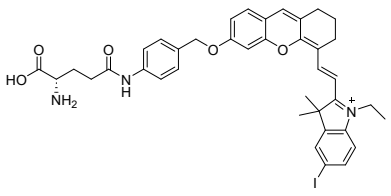	GGT	670/710	11
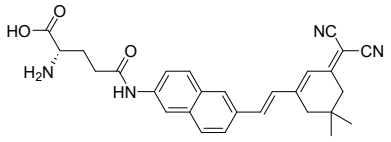	GGT	500/700	12
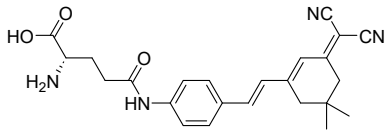	GGT	445/658	13

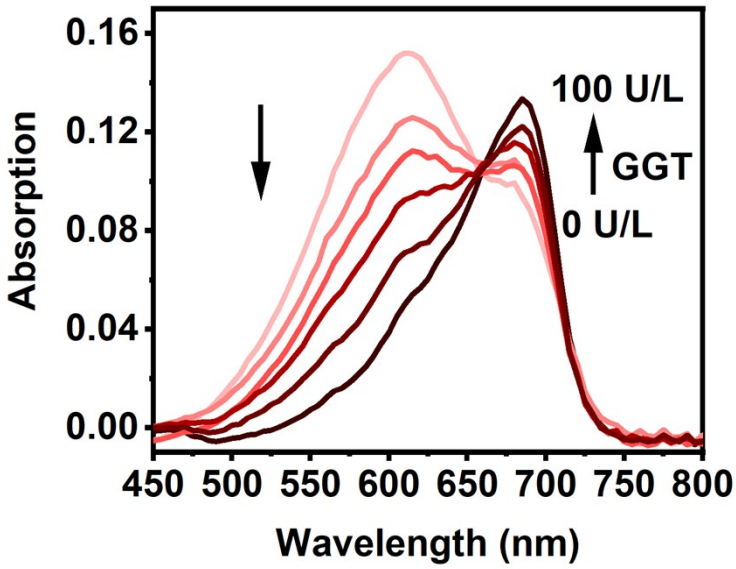

Fig. S1 UV–vis spectra absorbance changes of **Cy-GGT-β-gal** (5 μm) in PBS buffer (10.0 mm, pH 7.4, containing 20% DMSO), after introduction of GGT (0.0–100.0 U/L).

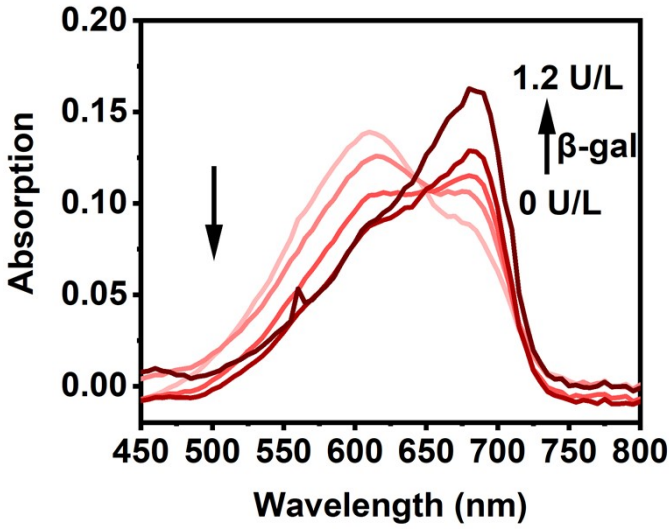

Fig. S2 UV–vis spectra absorbance changes of **Cy-GGT-β-gal** (5 μm) in PBS buffer (10.0 mm, pH 7.4, containing 20% DMSO), after introduction of β-gal (0.0–1.2 U/L).

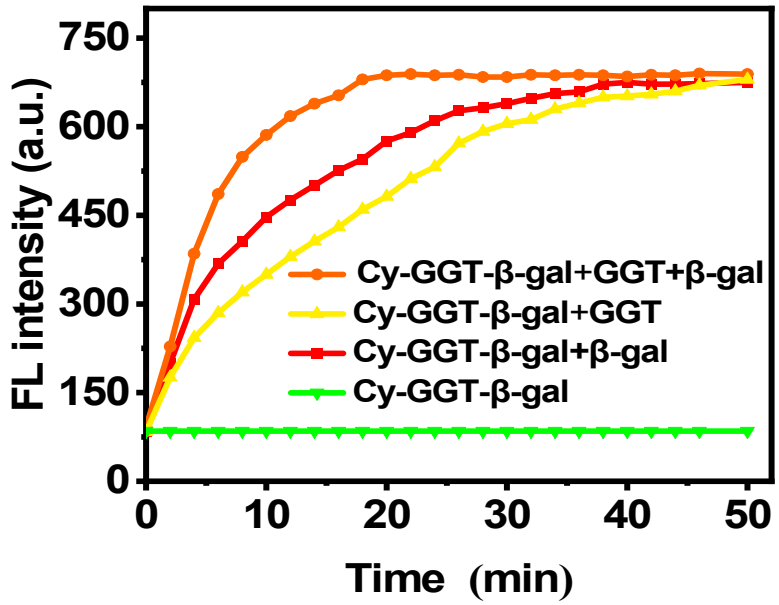

Fig. S3 Time-dependent fluorescence of **Cy-GGT-β-gal** with the addition of GGT (0.0–100.0 U/L) or β-gal (0.0–1.2 U/L) in PBS buffer.

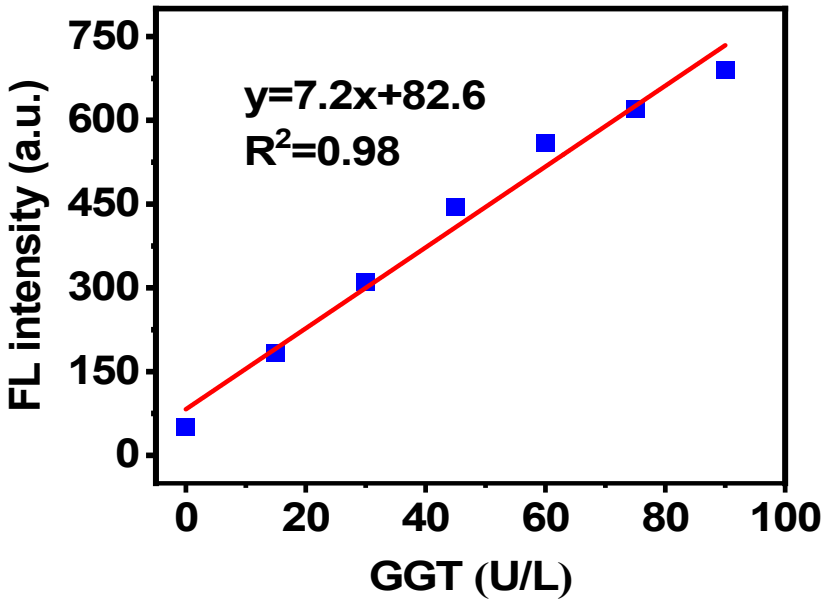

Fig. S4 The linear relationship between $I_{720\,nm}$ and the concentration of GGT (0.0–90.0 U/L).

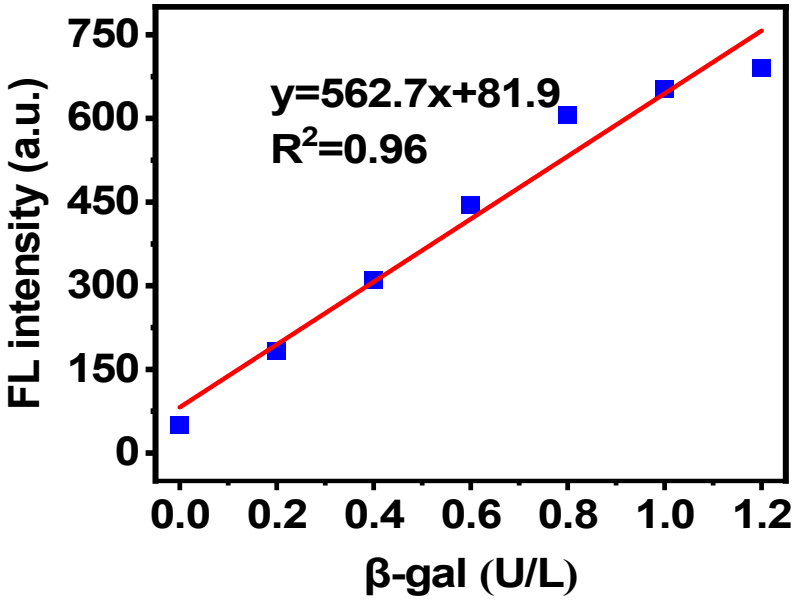

Fig. S5 The linear relationship between $I_{720\ nm}$ and the concentration of β-gal (0.0–1.2 U/L).

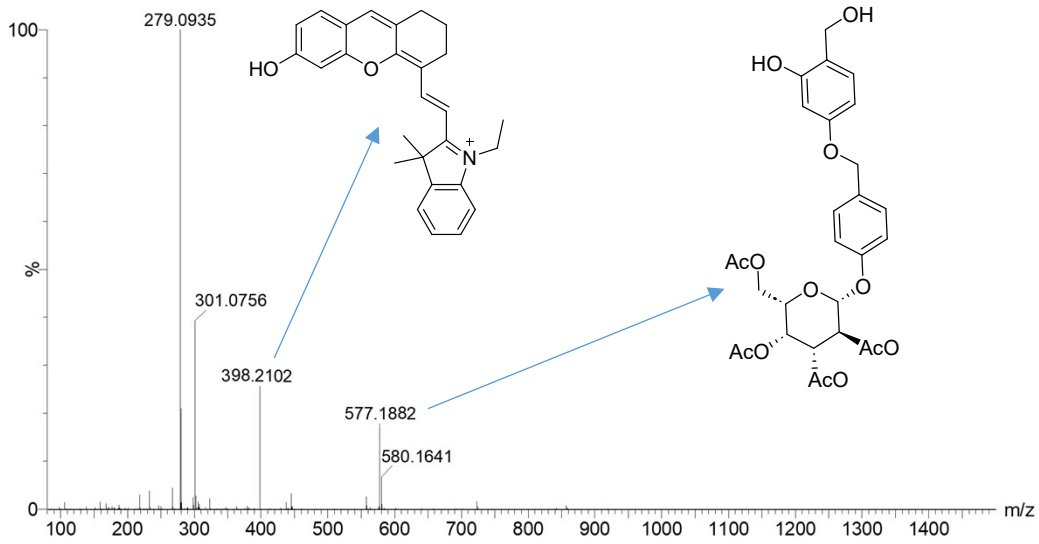

Fig. S6 MS (ESI) spectrum of the reaction mixture of probe **Cy-GGT-β-gal** with GGT.

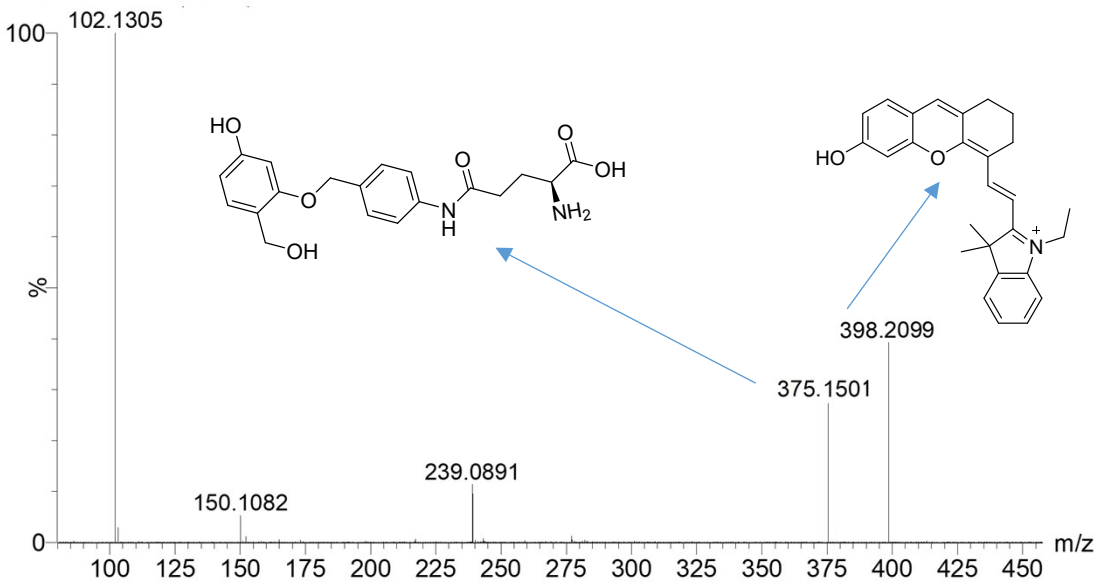

Fig. S7. MS (ESI) spectrum of the reaction mixture of probe **Cy-GGT-β-gal** with β-gal.

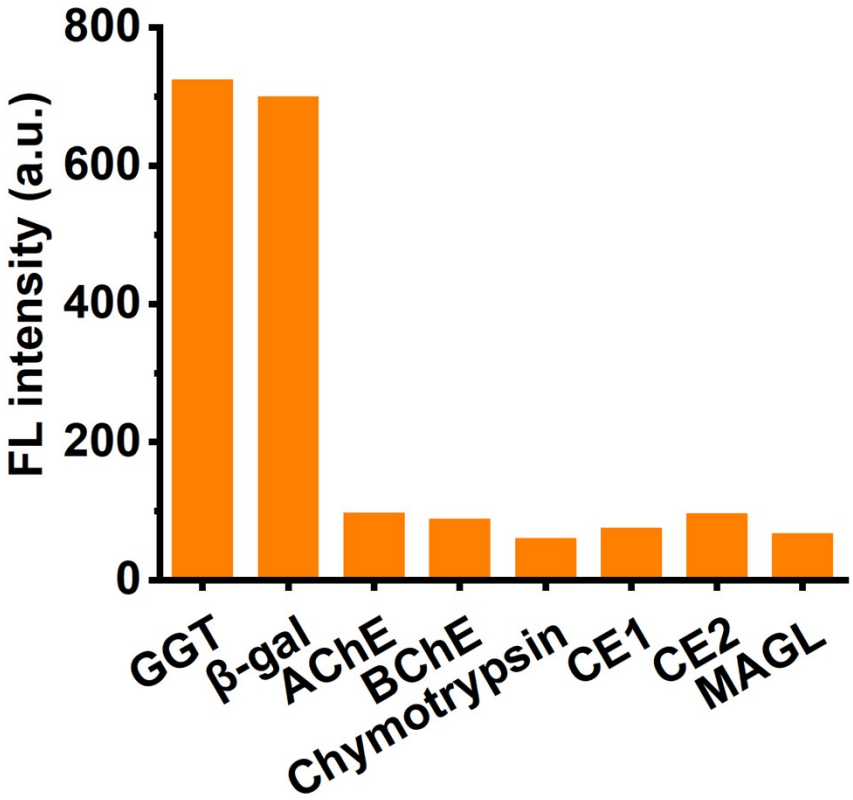

Fig. S8. The column analysis of the fluorescence response for 5 μM Cy-GGT-β-gal to various analytes in PBS (10 mM, pH 7.4, 30 °C, 20% DMSO). The concentrations of analytes are thus GGT (100.0 U/L), β-gal (1.2 U/L), AChE (10 μg/mL), BChE (10 μg/mL), chymotrypsin (10 μg/mL), CE1 (10 μg/mL), CE2 (10 μg/mL), and MAGL (10 μg/mL).

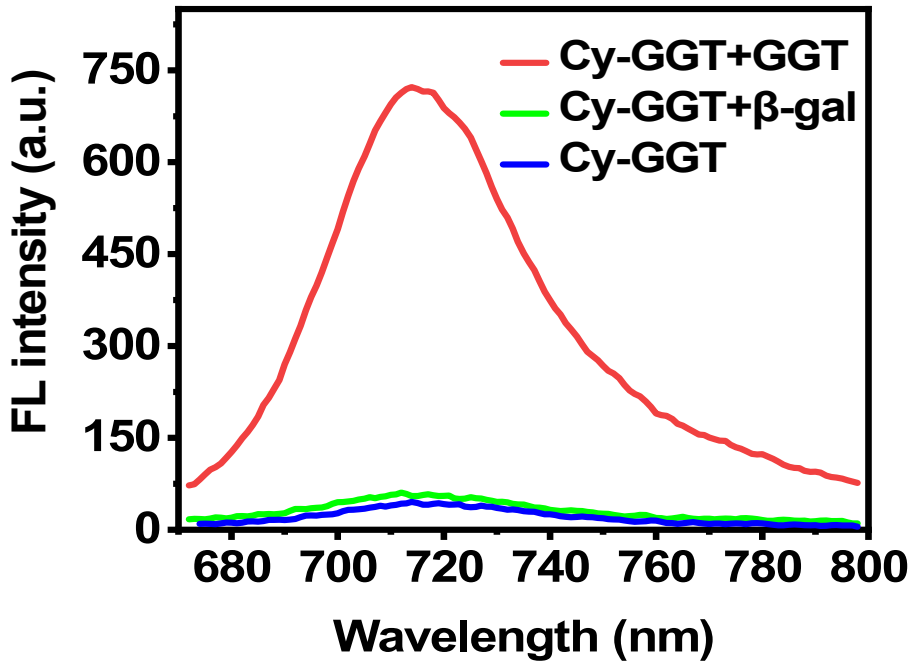

Fig. S9 Fluorescence spectra absorbance changes of **Cy-GGT** (5 μM) in PBS buffer (10.0 mM, pH 7.4, containing 20% DMSO), after introduction of GGT or β-gal.

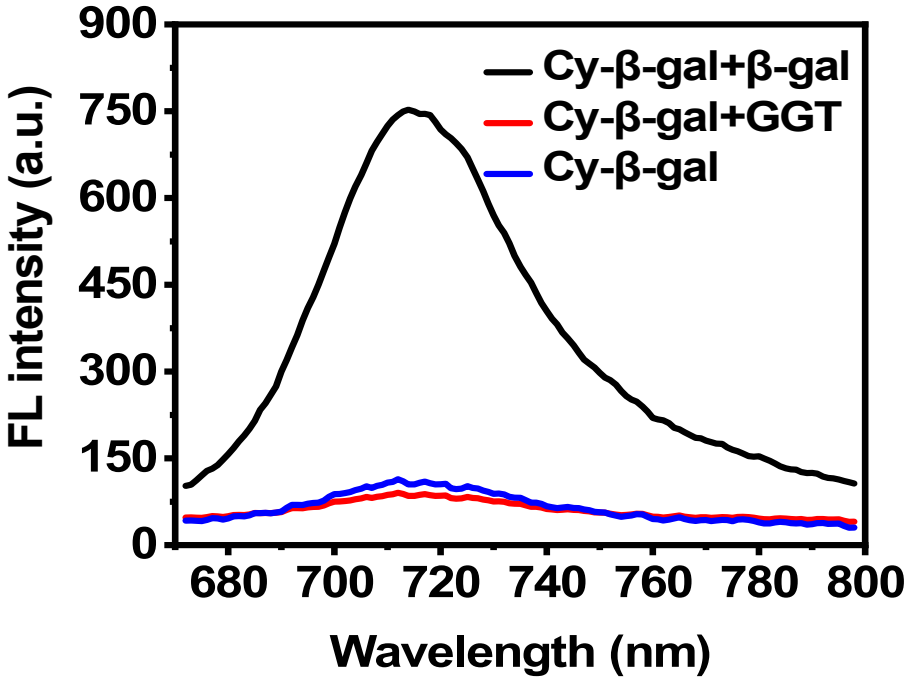

Fig. S10 Fluorescence spectra absorbance changes of **Cy-β-gal** (5 μM) in PBS buffer (10.0 mM, pH 7.4, containing 20% DMSO), after introduction of GGT or β-gal.

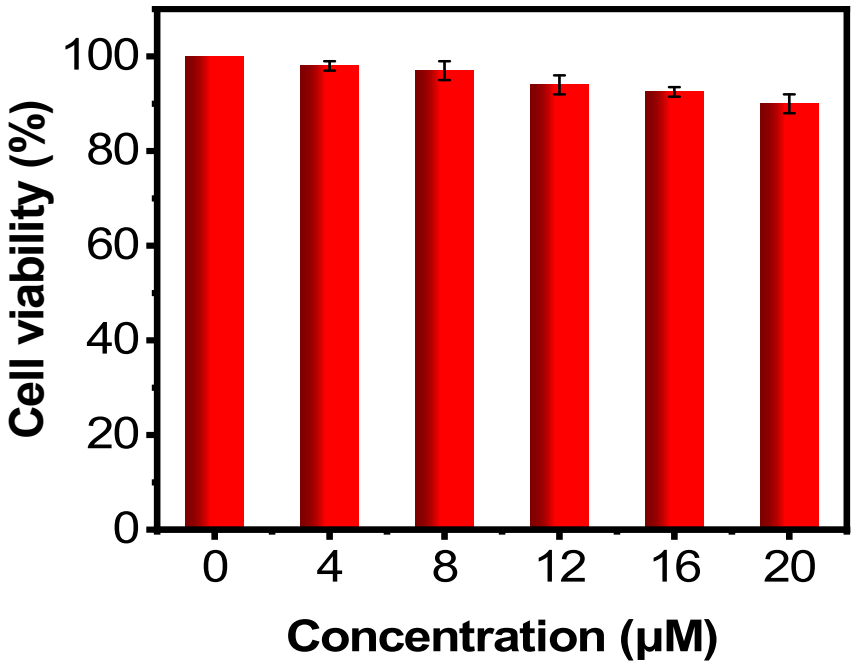

Fig. S11 The cytotoxicity of **Cy-GGT-β-gal** on IOSE80 cells.

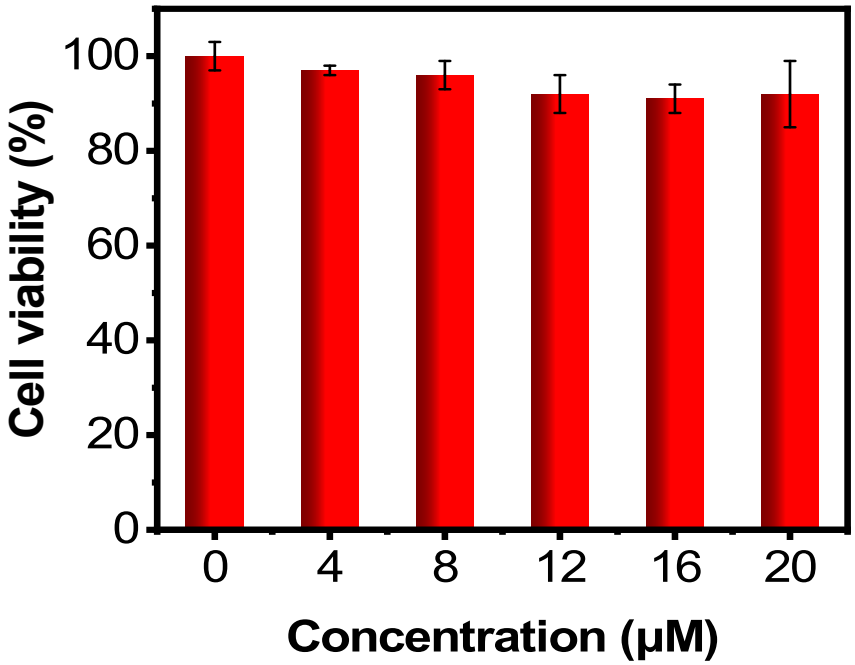

Fig. S12 The cytotoxicity of **Cy-GGT-β-gal** on OVCAR3 cells.

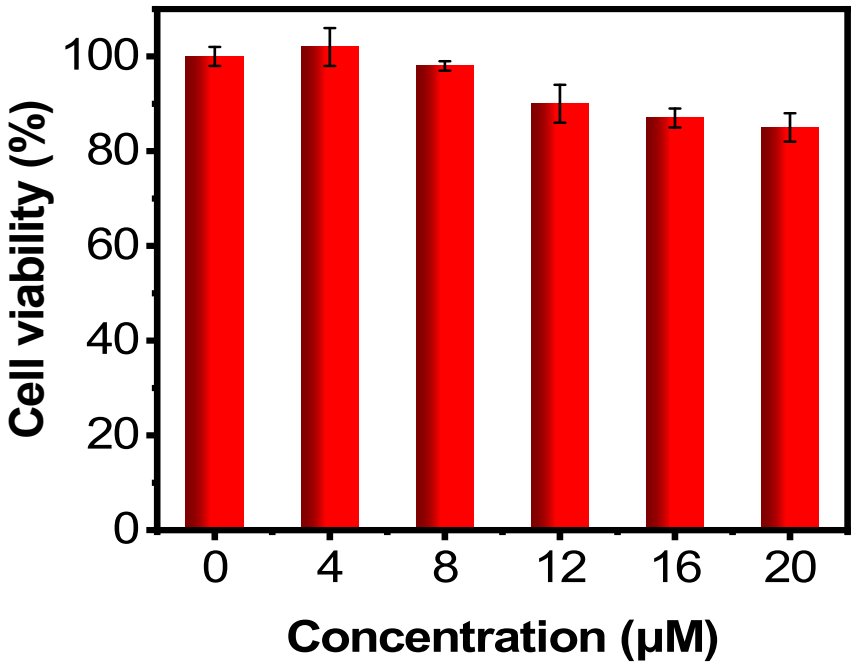

Fig. S13 The cytotoxicity of **Cy-GGT-β-gal** on SKOV3 cells.

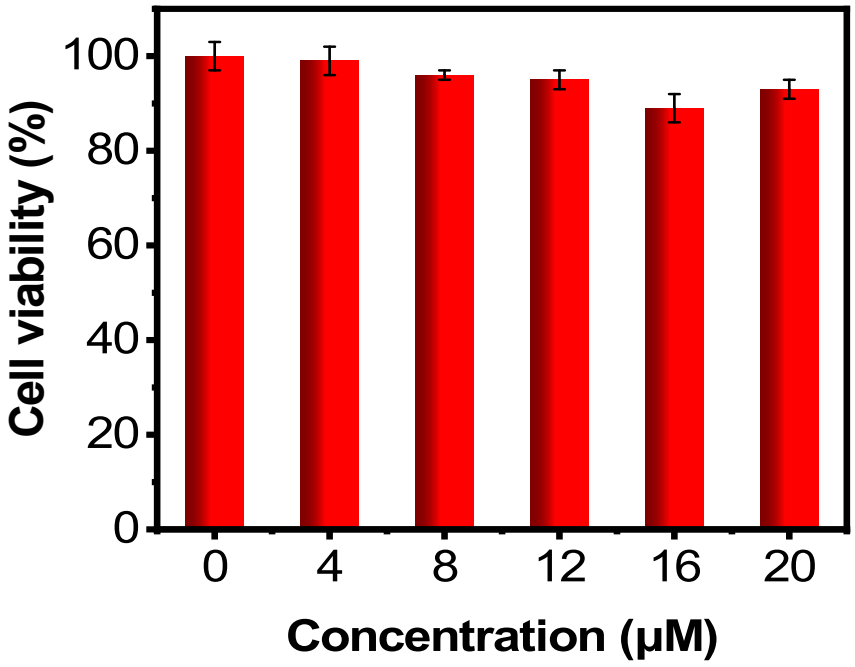

Fig. S14 The cytotoxicity of **Cy-GGT-β-gal** on SHIN3 cells.

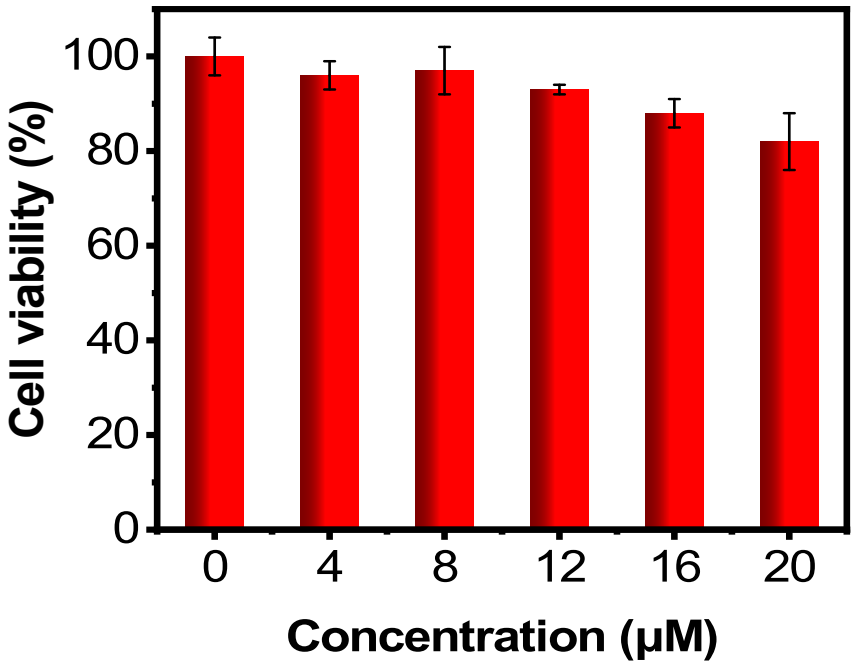

Fig. S15 The cytotoxicity of **Cy-GGT-β-gal** on A2780 cells.

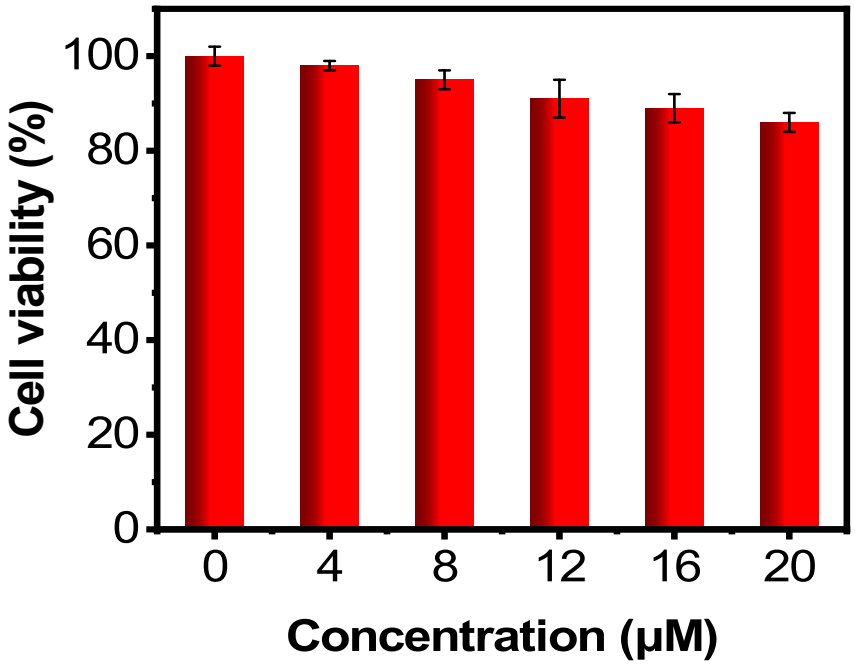

Fig. S16 The cytotoxicity of **Cy-GGT-β-gal** on OVCAR5 cells.

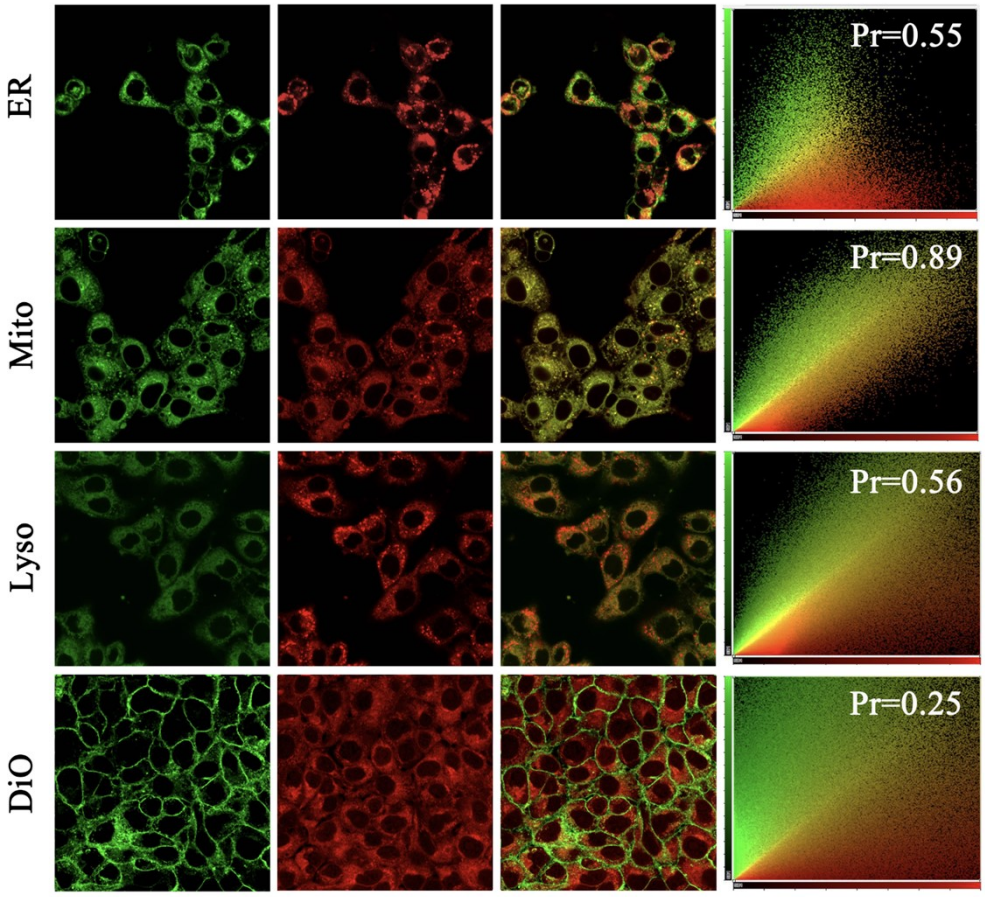

Fig. S17 Subcellular colocalization assays of **Cy-GGT-β-gal** in SHIN3 cells. The green channel of ER-Tracker Green, Lyso-Tracker Green, Mito-Tracker Green and DiO was excited at 488 nm and collected at 500-550 nm. The red channel represents the fluorescent signal of **Cy-GGT-β-gal** (λ_{ex}: 640 nm and λ_{em}: 670-750 nm). Scale bars: 10 μm.

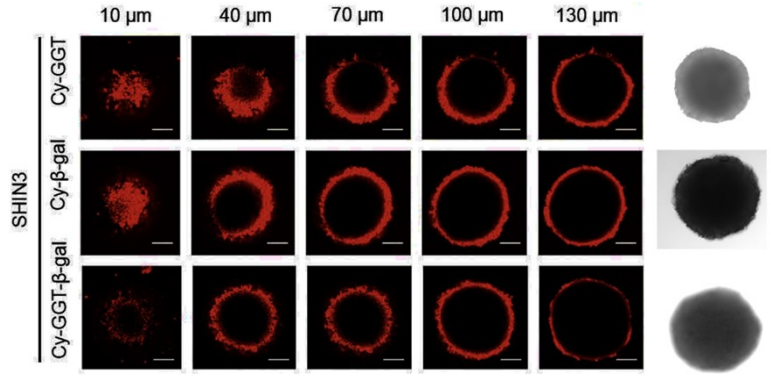

Fig. S18 Fluorescence imaging in the SHIN3-derived multicellular spheroids after treatments with **Cy-GGT, Cy-β-gal, and Cy-GGT-β-gal (5 μM)**. Scale bar: 100 μm.

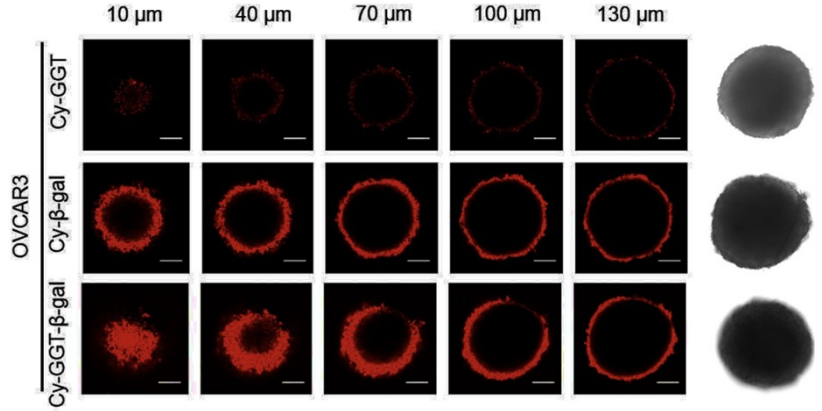

Fig. S19 Fluorescence imaging in the OVCAR3-derived multicellular spheroids after treatments with **Cy-GGT, Cy-β-gal, and Cy-GGT-β-gal (5 μM)**. Scale bar: 100 μm.

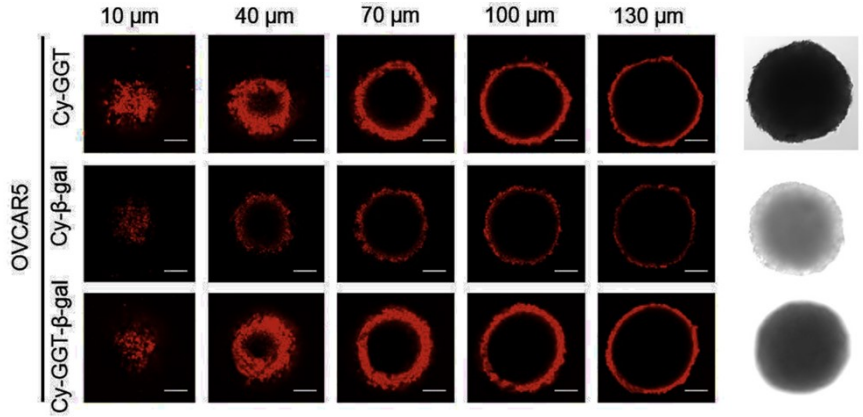

Fig. S20 Fluorescence imaging in the OVCAR5-derived multicellular spheroids after treatments with **Cy-GGT, Cy-β-gal, and Cy-GGT-β-gal (5 μM)**. Scale bar: 100 μm.

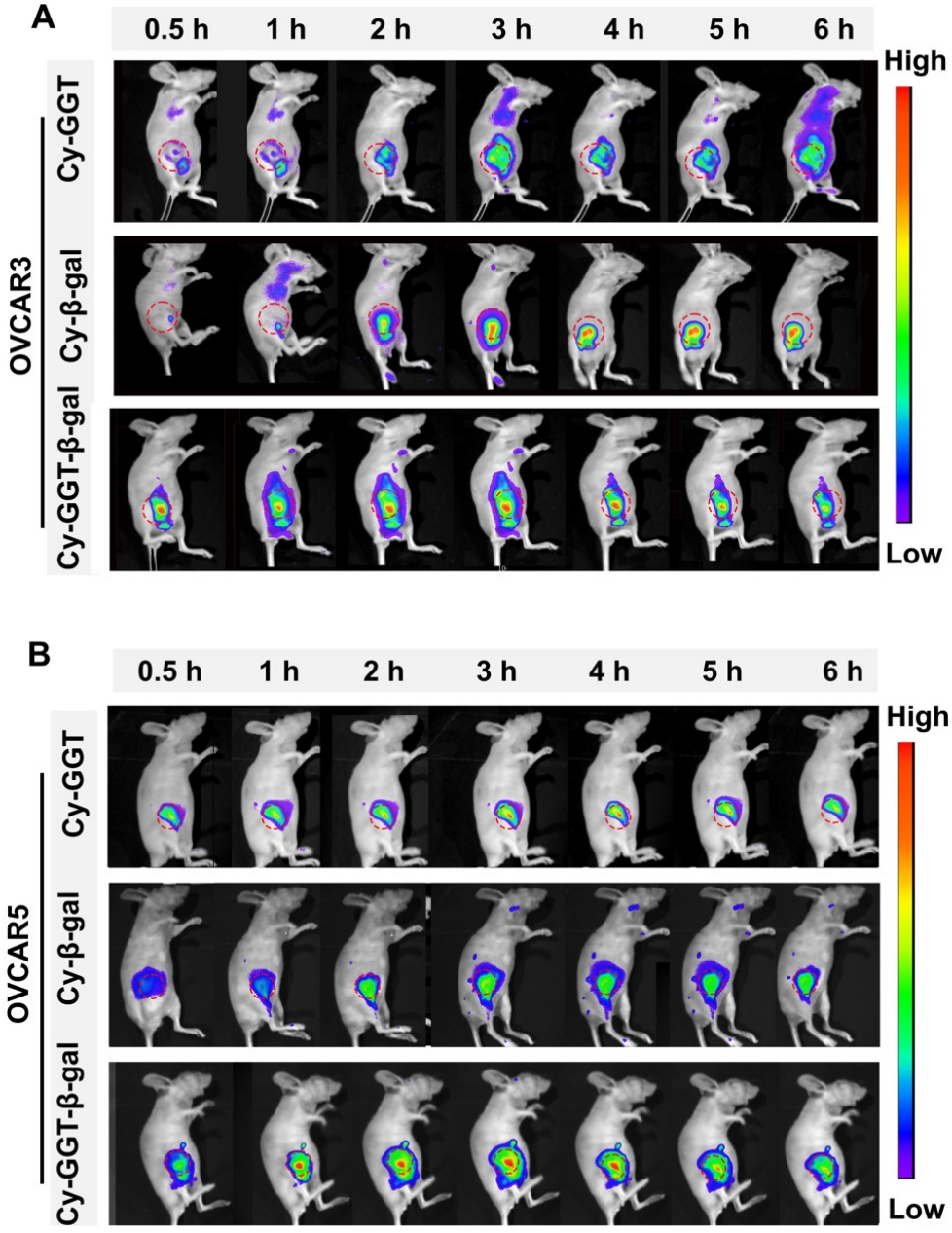

Fig. S21 Imaging of GGT or β-gal activity in bare BABL/c mice bearing (A) OVCAR3 and (B) OVCAR5 tumors.

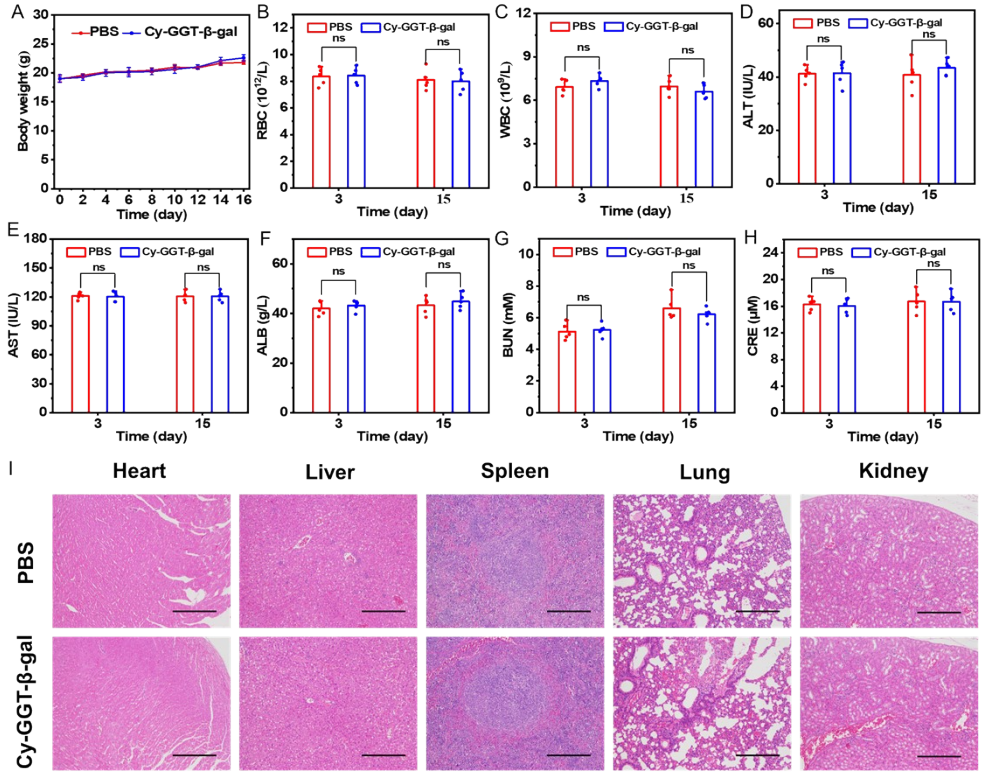

Fig. S22 H&E staining of organs from the PBS group and **Cy-GGT-β-gal** group after 15 days of treatment. Scale bar: 200 μm.

4. ^{1}H NMR, ^{13}C NMR and HRMS spectra

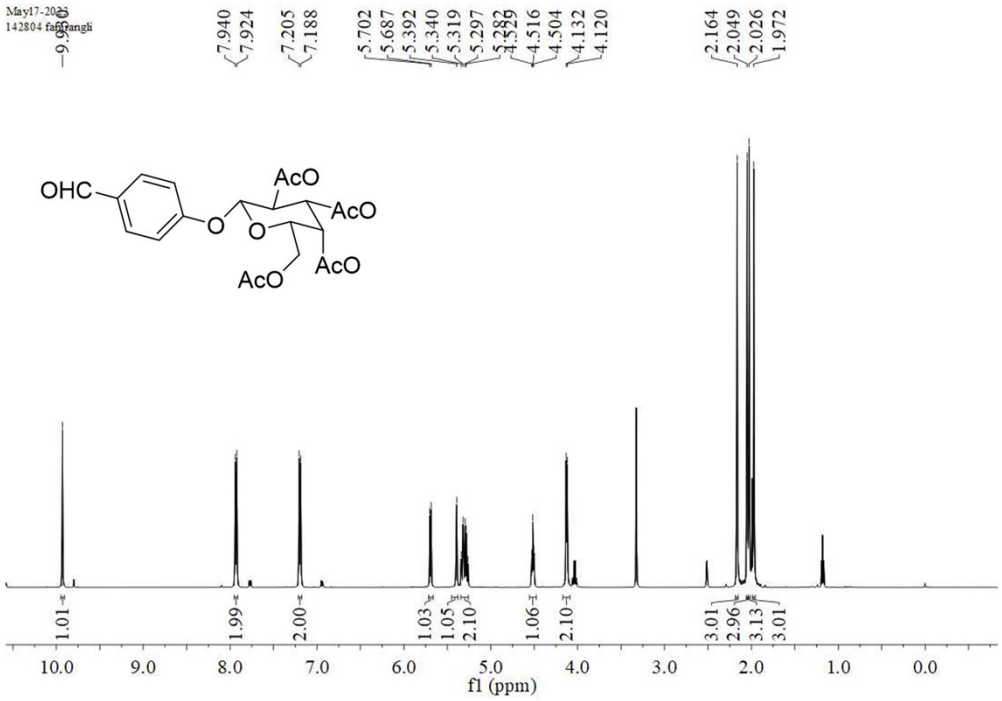

Fig. S 23 ^{1}H NMR spectrum of Compound 2-2.

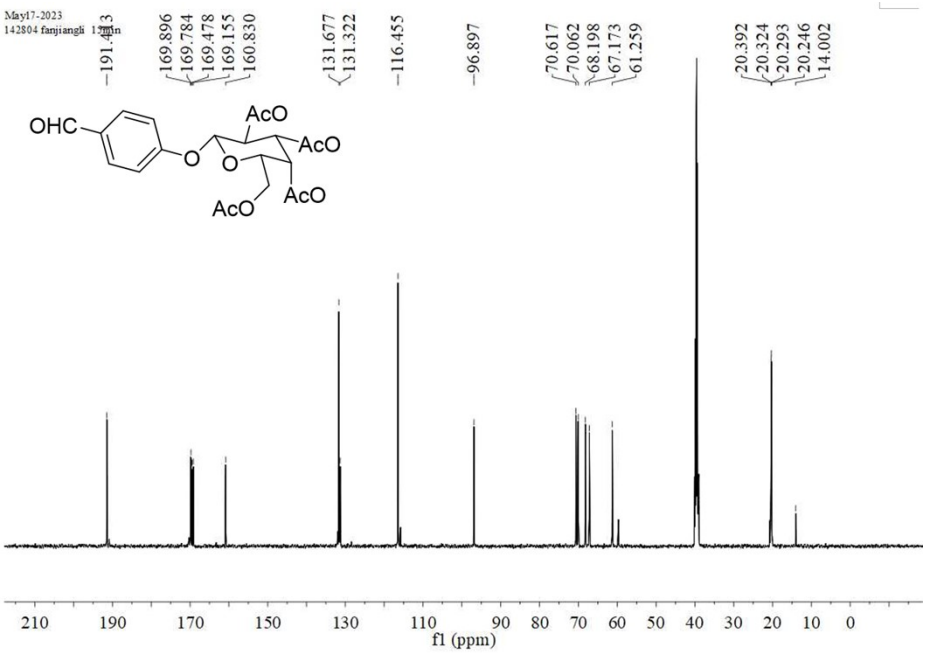

Fig. S 24 ^{13}C NMR spectrum of Compound 2-2.

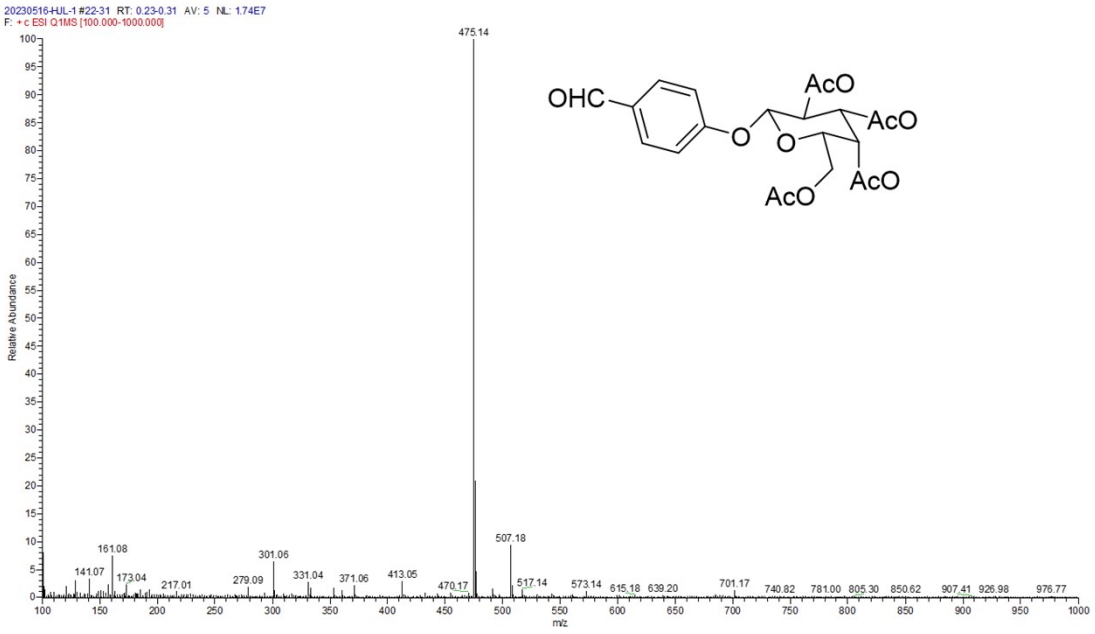

Fig. S 25 MS spectrum of Compound **2-2**.

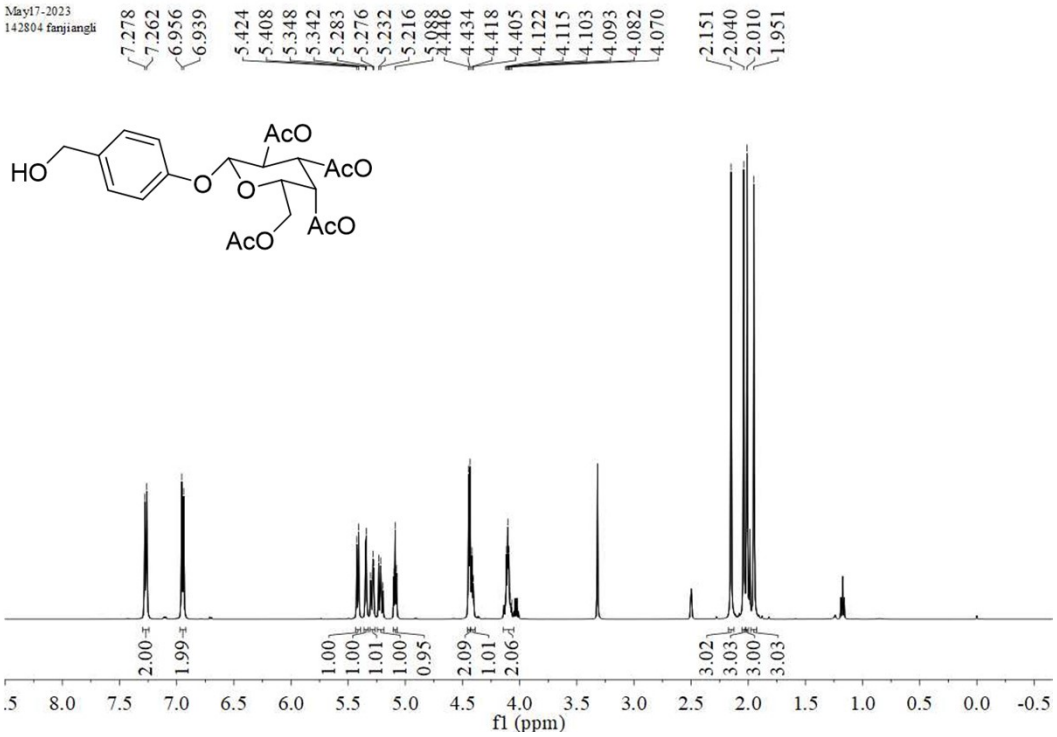

Fig. S 26 ^{1}H NMR spectrum of Compound **2-3**.

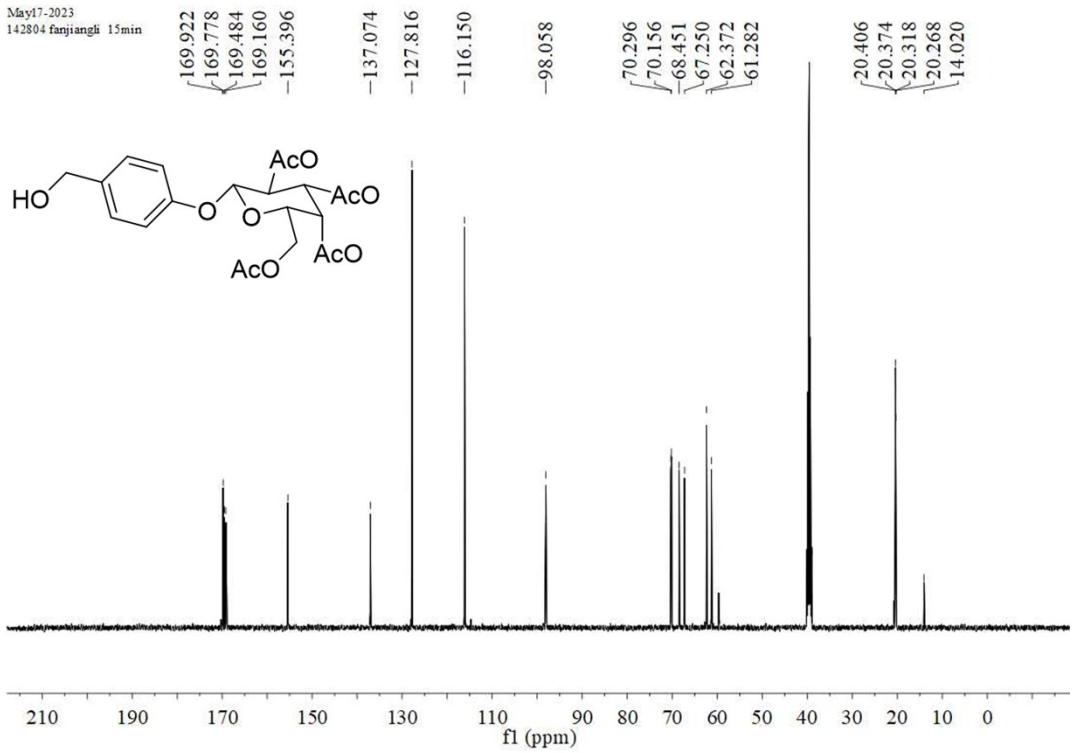

Fig. S 27 ^{13}C NMR spectrum of Compound **2-3**.

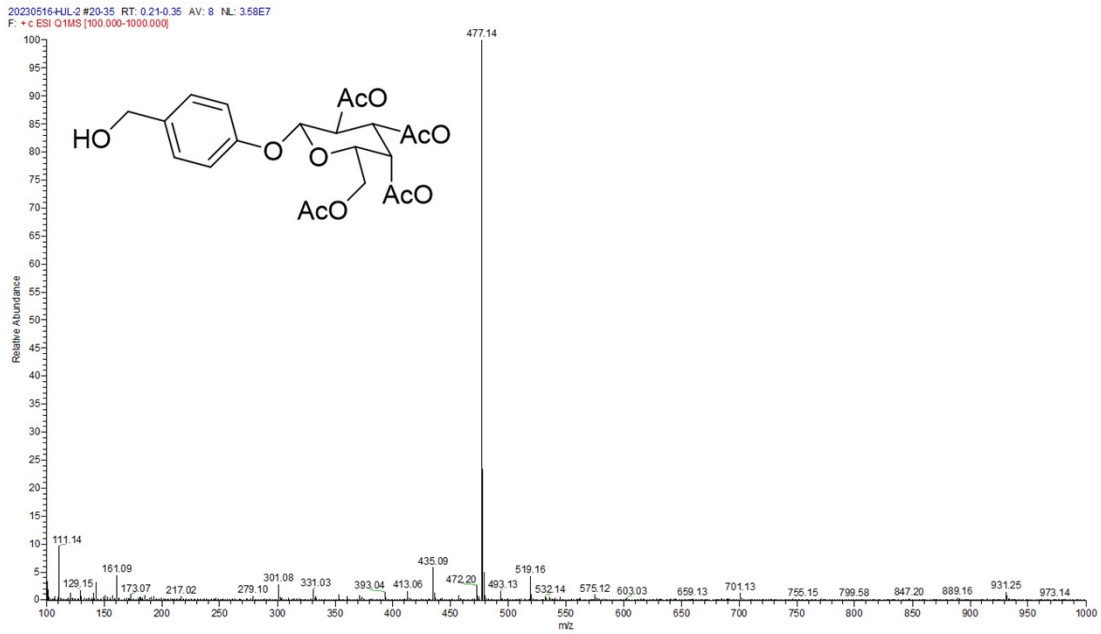

Fig. S 28 MS spectrum of Compound **2-3**.

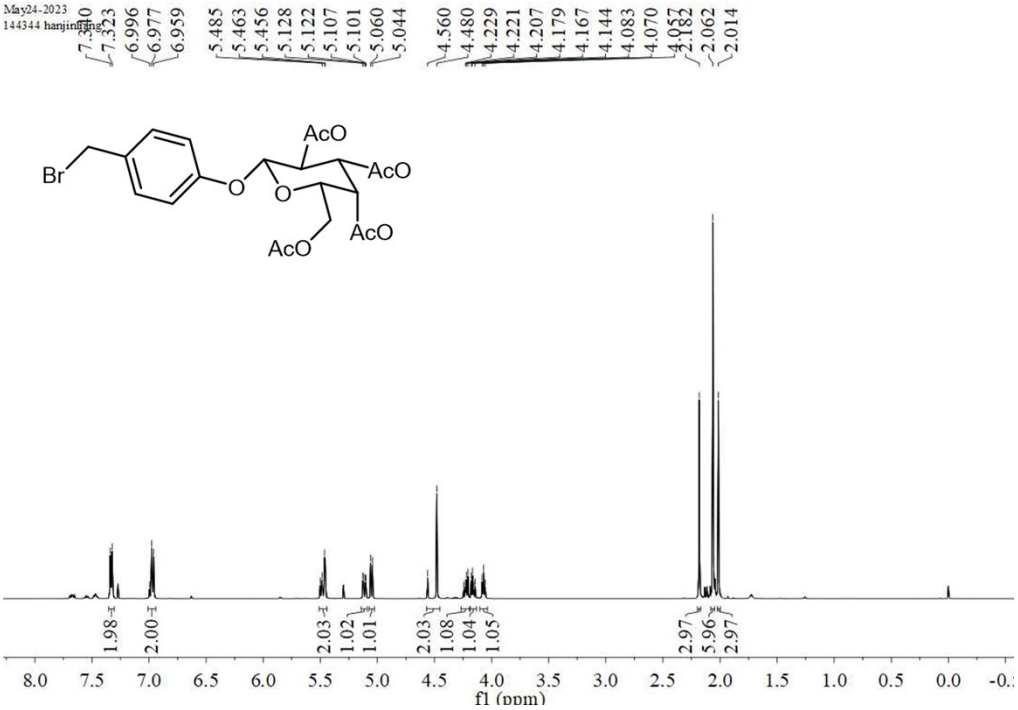

Fig. S 29 ^{1}H NMR spectrum of Compound **2-4**.

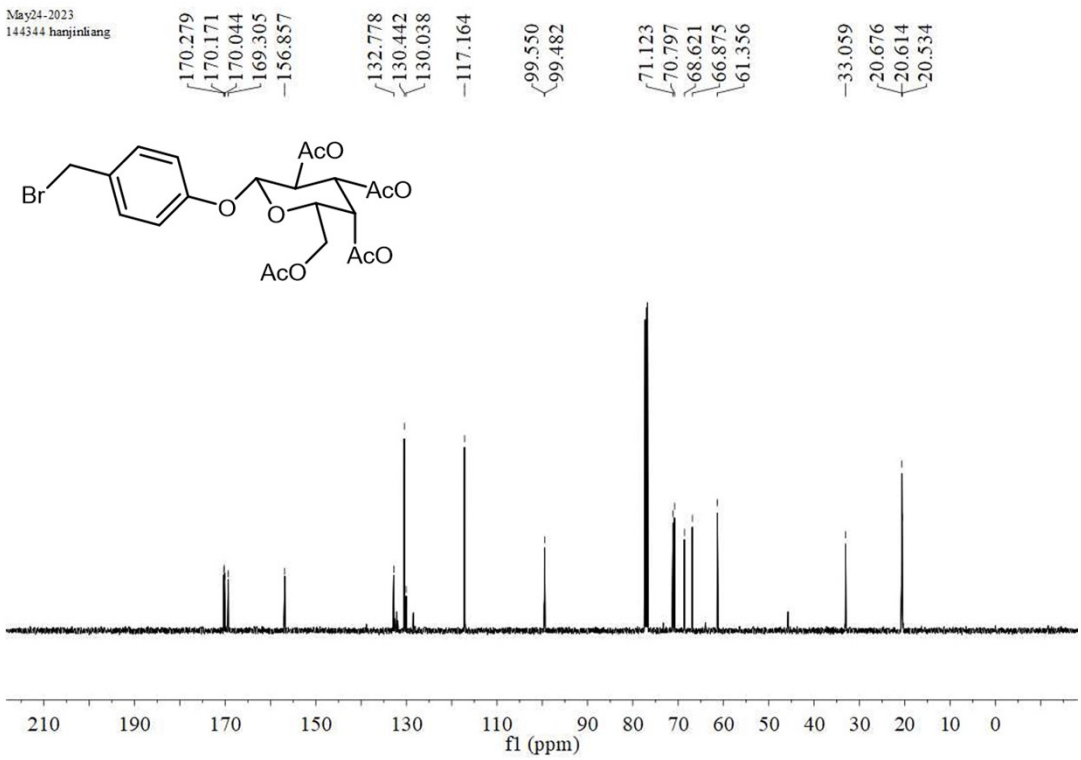

Fig. S 30 ^{13}C NMR spectrum of Compound **2-4**.

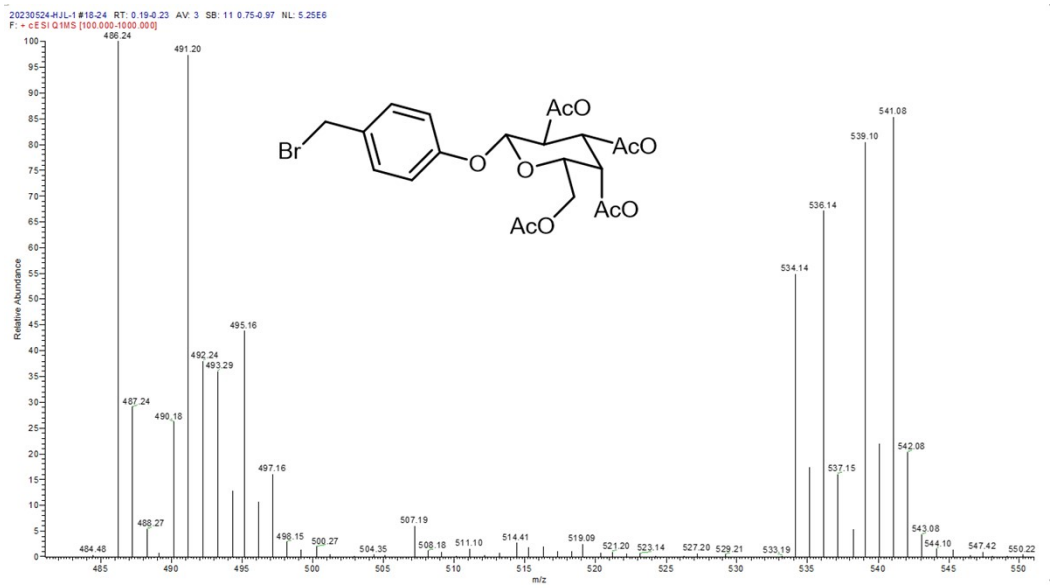

Fig. S 31 MS spectrum of Compound **2-4**.

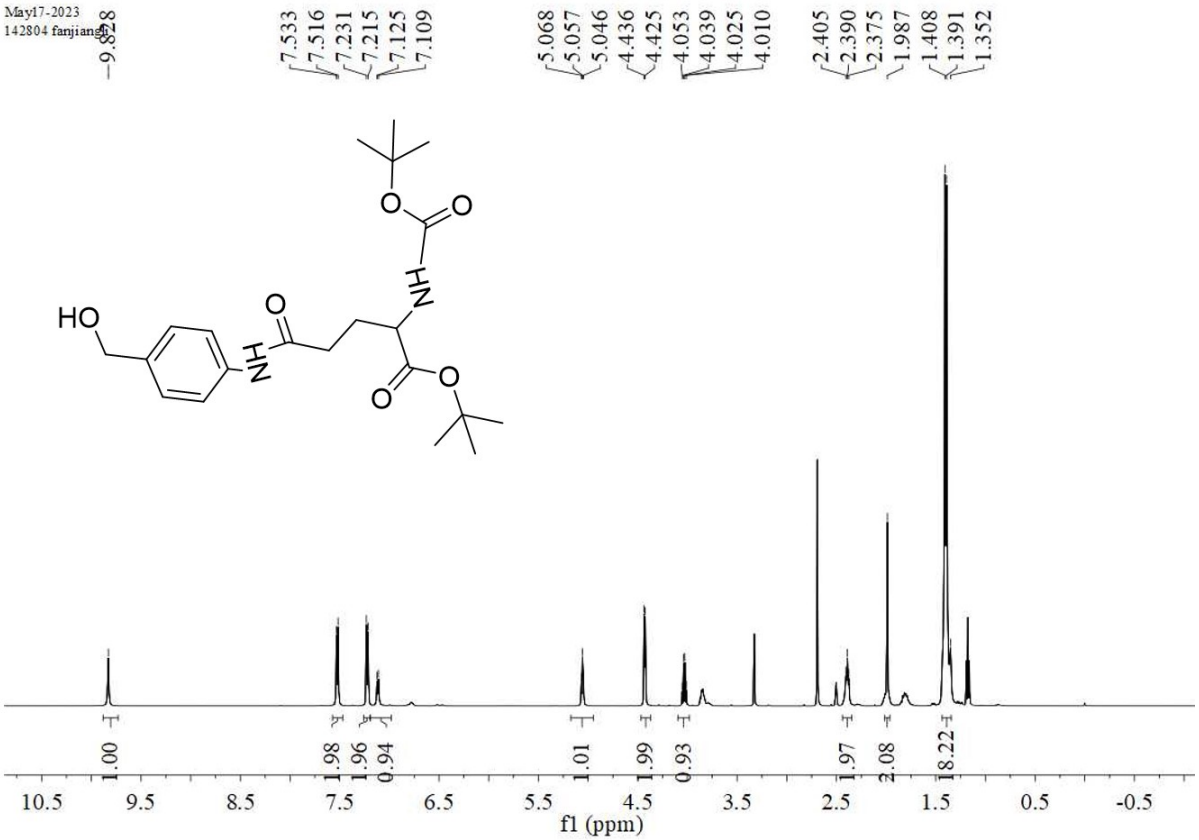

Fig. S 32 ^{1}H NMR spectrum of Compound **2-6**.

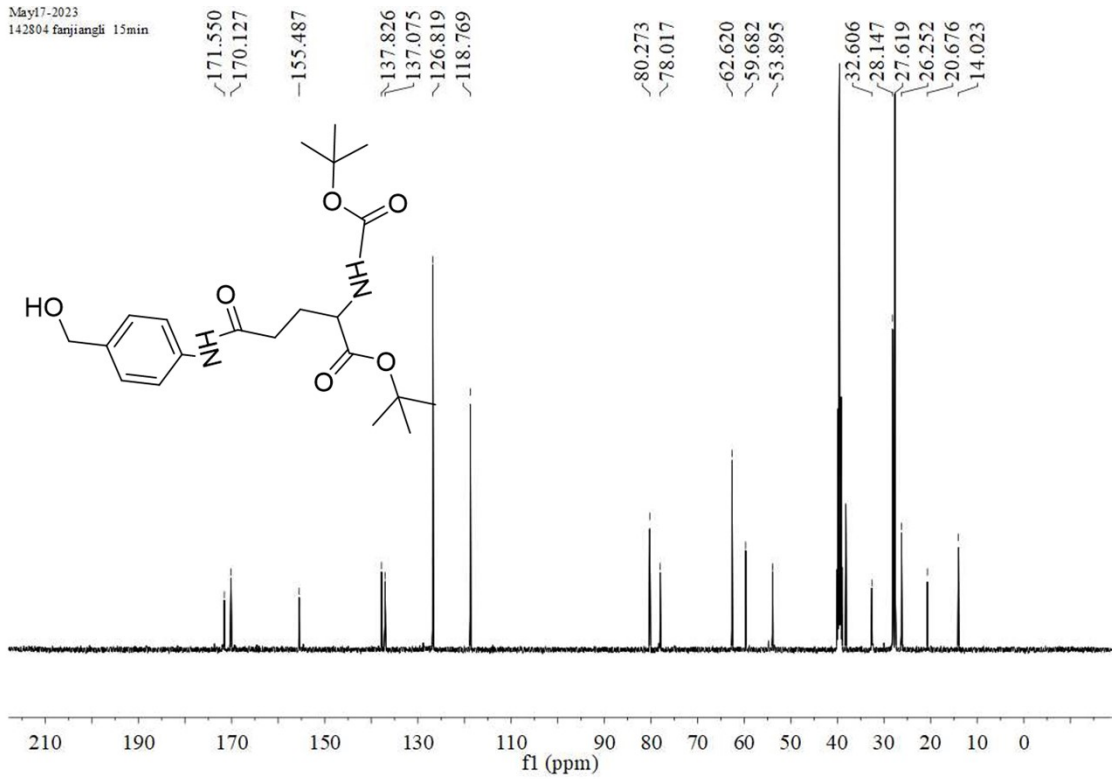

Fig. S 33 ^{13}C NMR spectrum of Compound **2-6**.

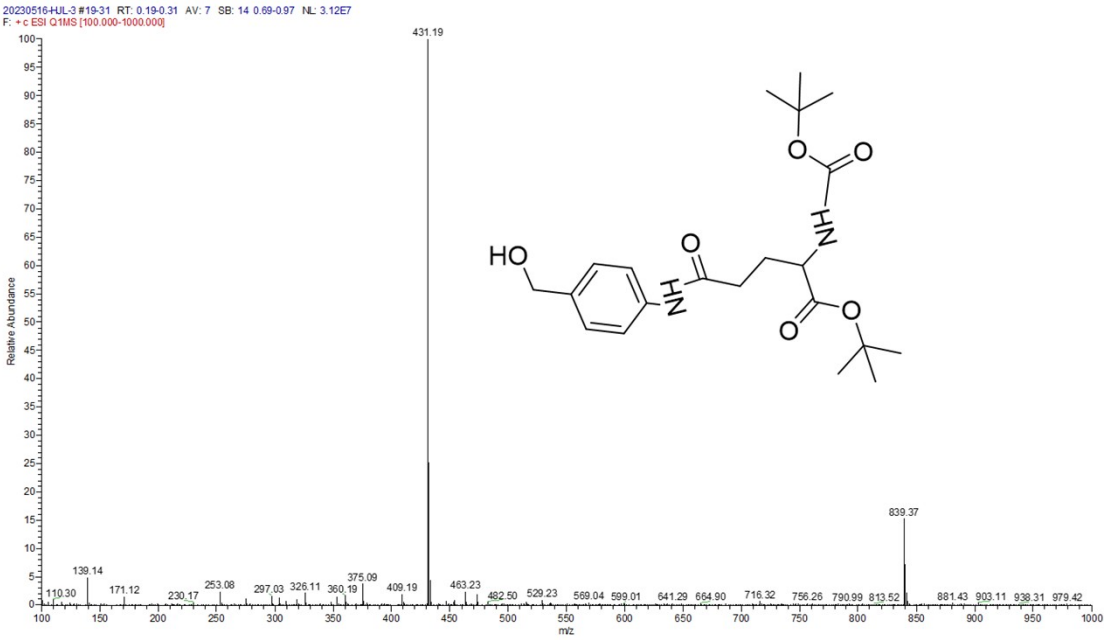

Fig. S 34 MS spectrum of Compound **2-6**.

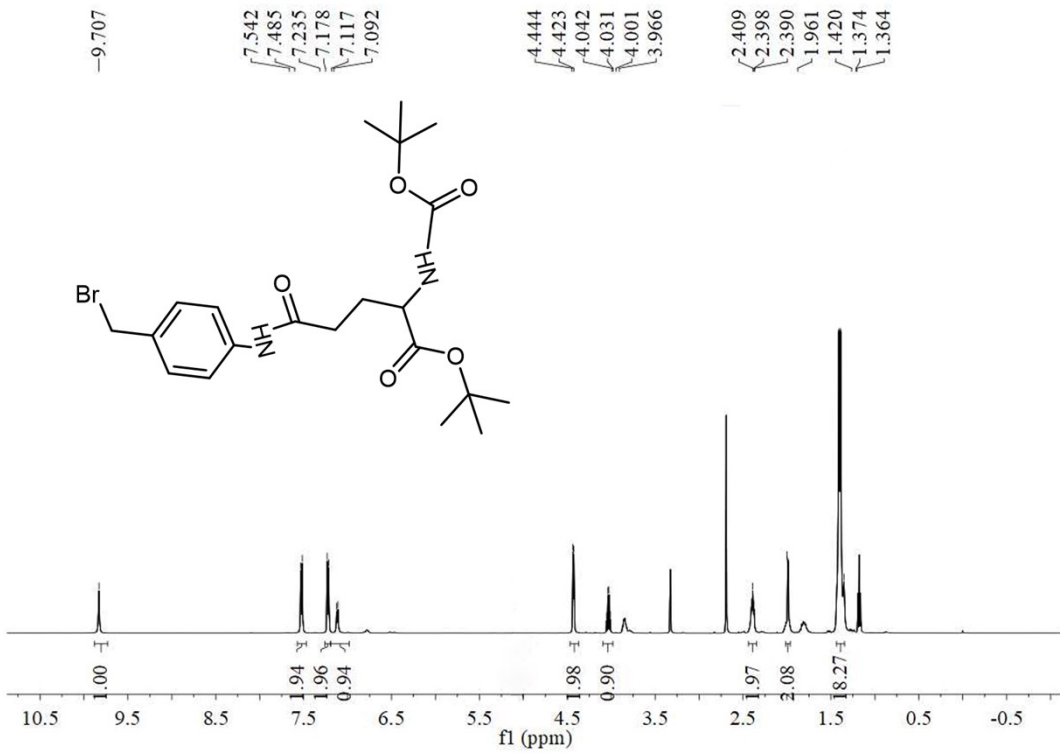

Fig. S 35 ^{1}H NMR spectrum of Compound **2-7**.

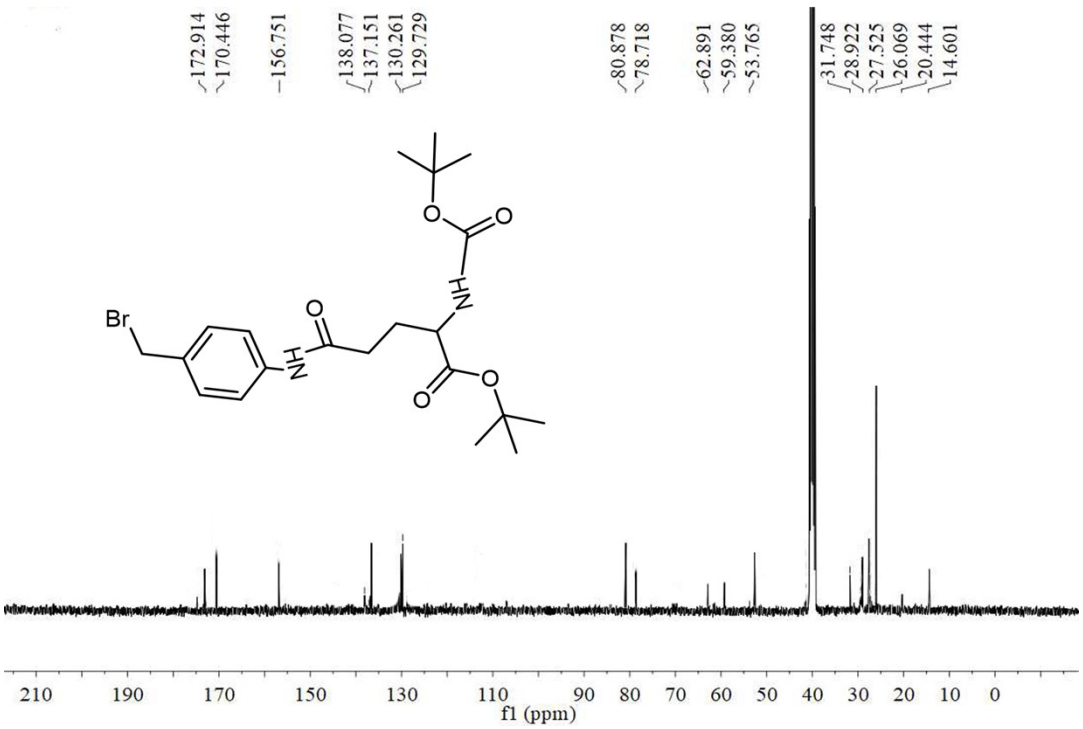

Fig. S 36 ^{13}C NMR spectrum of Compound **2-7**.

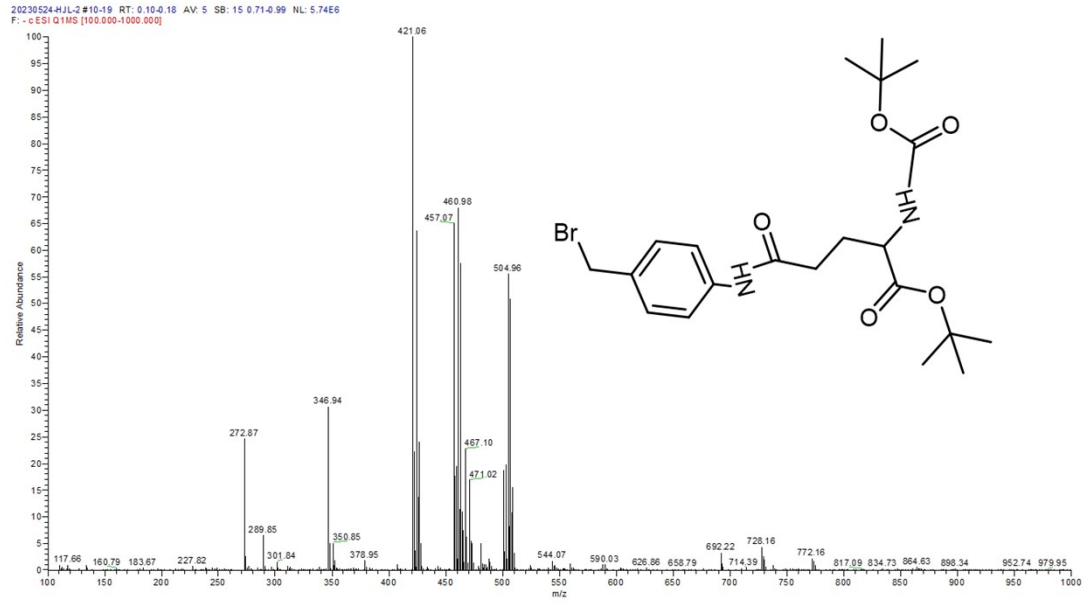

Fig. S 37 MS spectrum of Compound **2-7**.

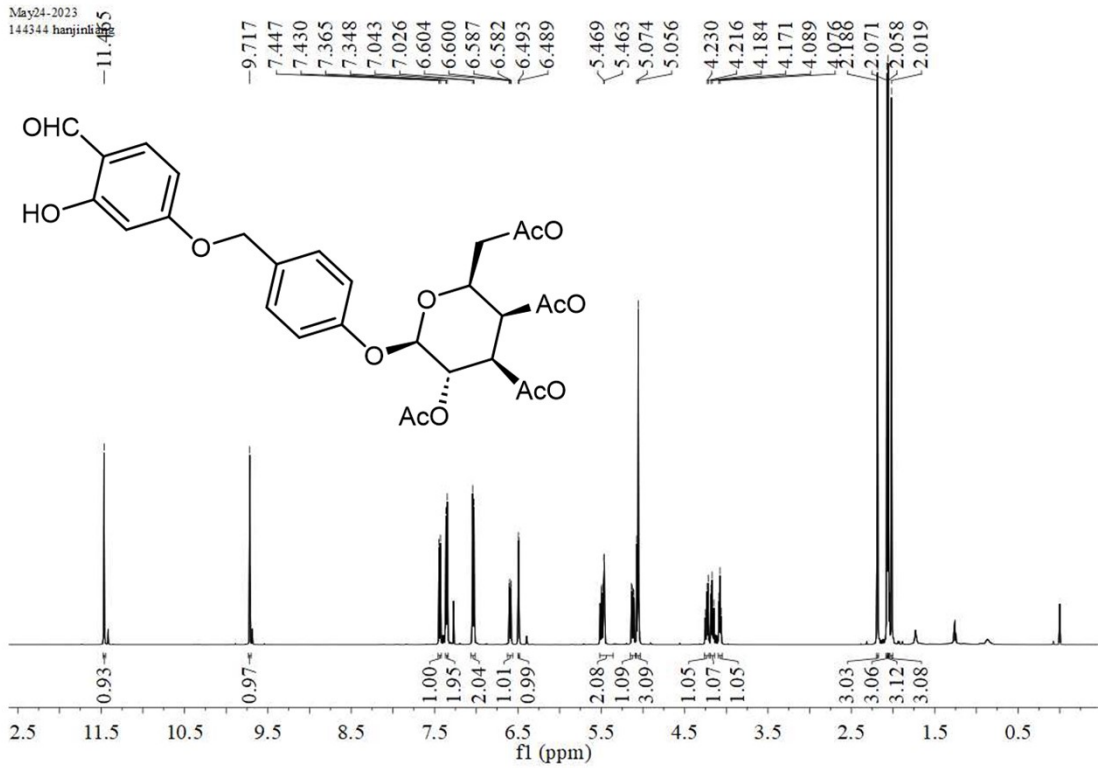

Fig. S 38 ^{1}H NMR spectrum of Compound **2-9**.

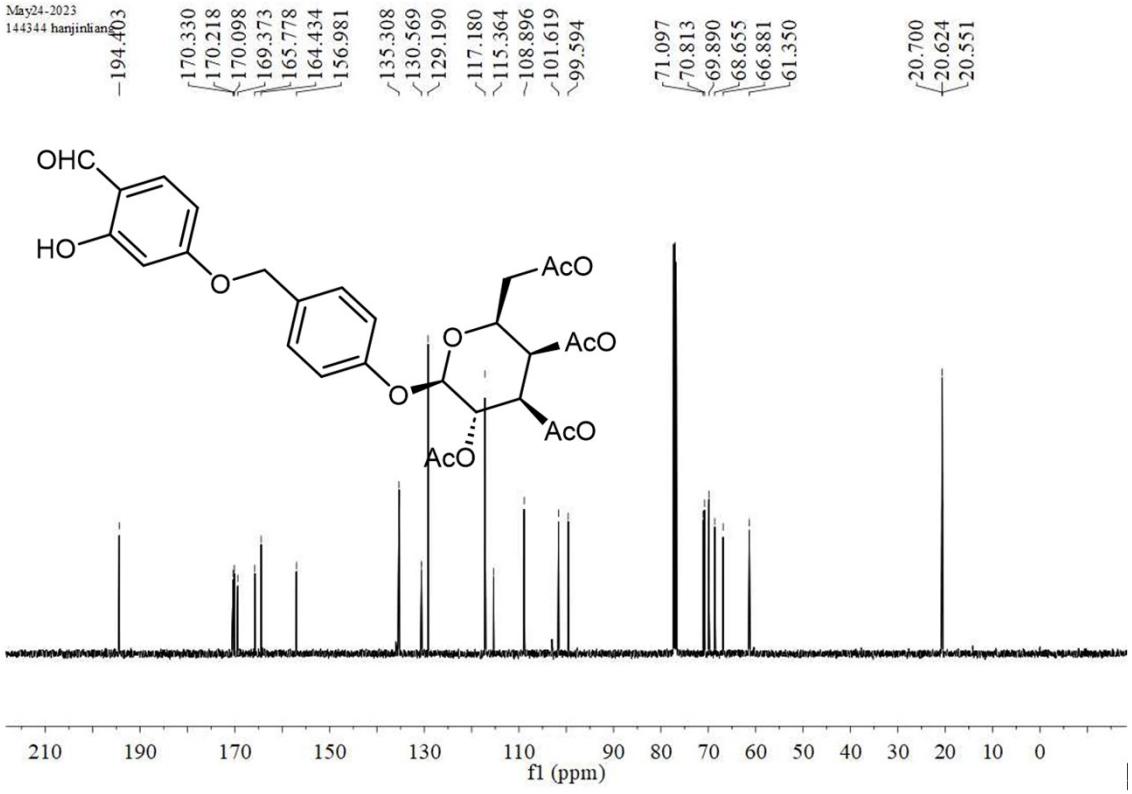

Fig. S 39 ^{13}C NMR spectrum of Compound **2-9**.

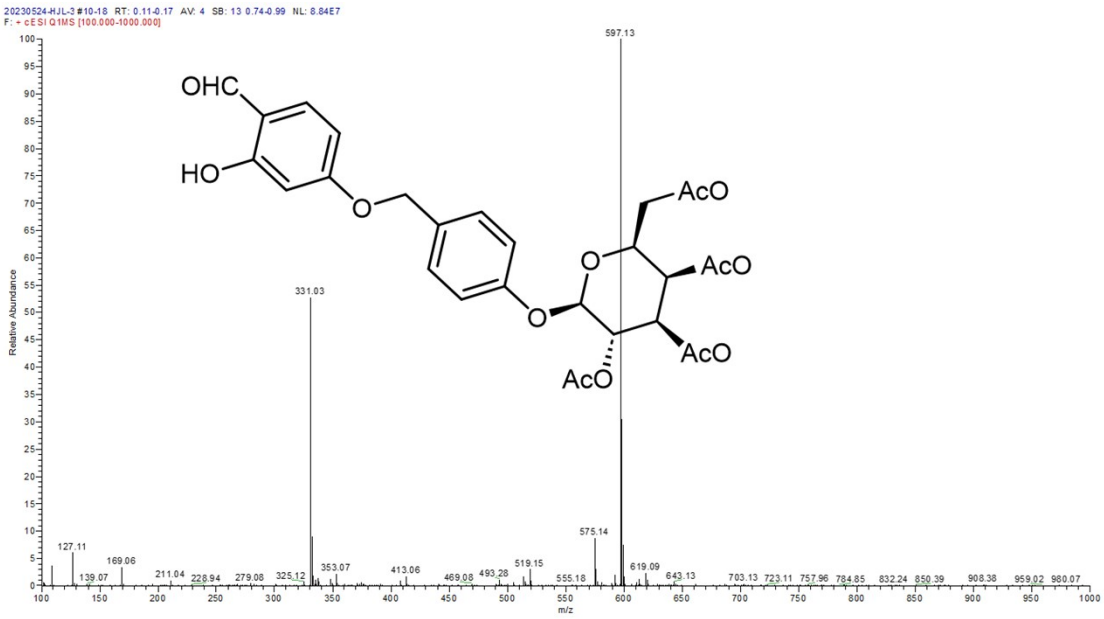

Fig. S 40 MS spectrum of Compound **2-9**.

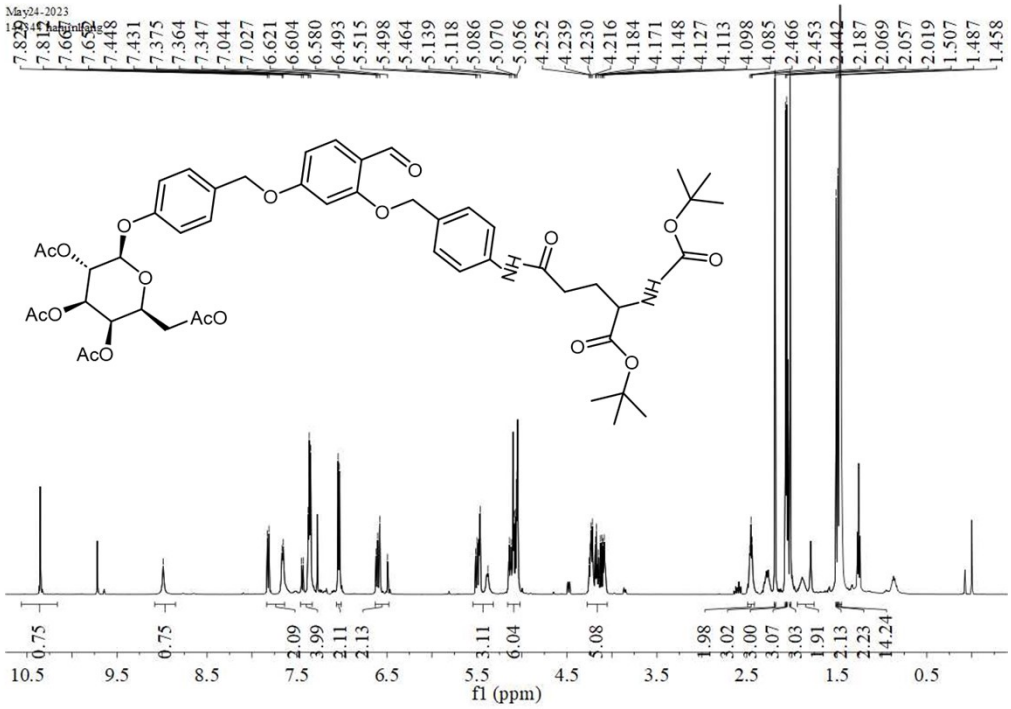

Fig. S 41 ^{1}H NMR spectrum of Compound **2-10**.

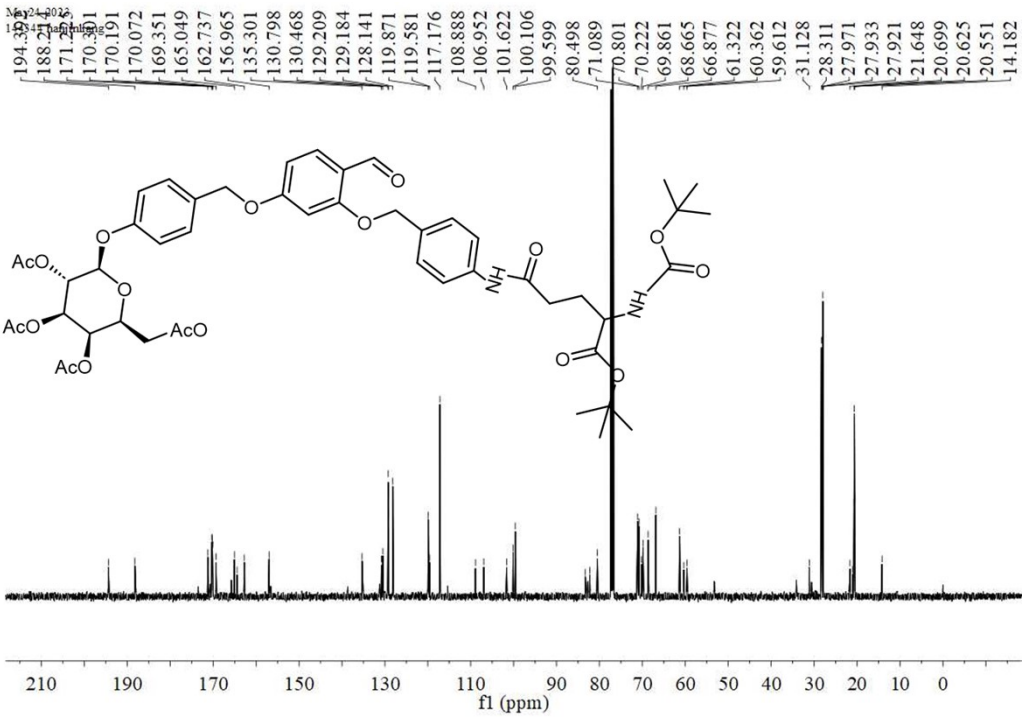

Fig. S 42 ^{13}C NMR spectrum of Compound **2-10**.

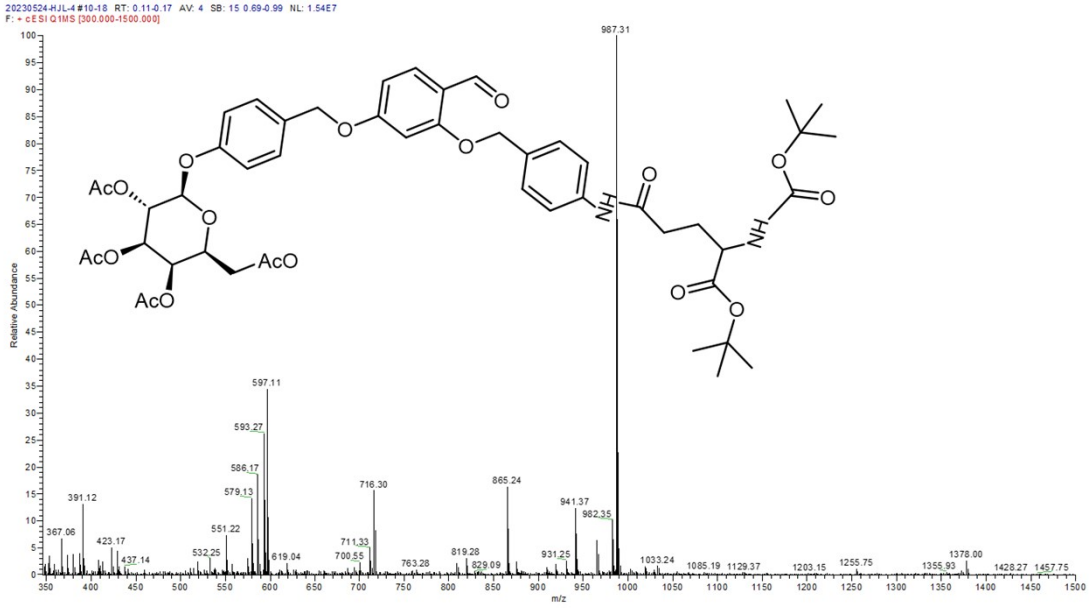

Fig. S 43 MS spectrum of Compound **2-10**.

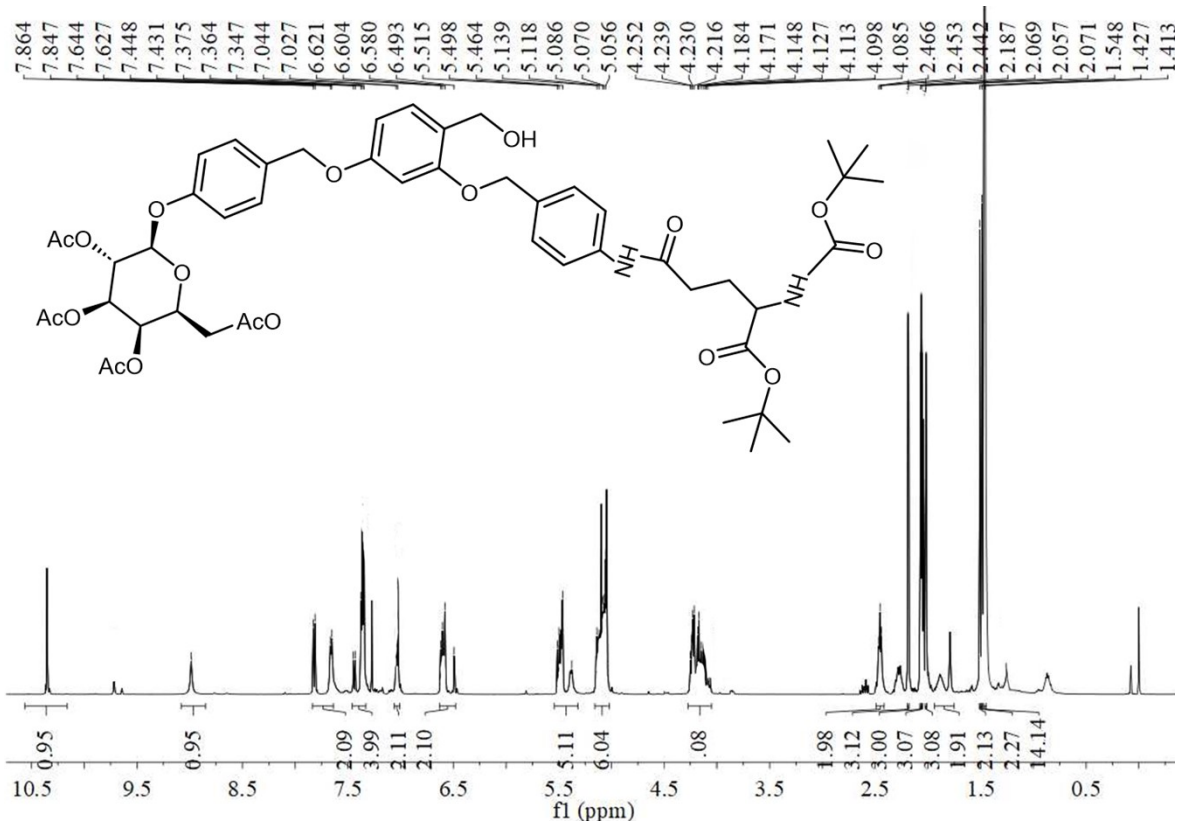

Fig. S 44 ^{1}H NMR spectrum of Compound **2-11**.

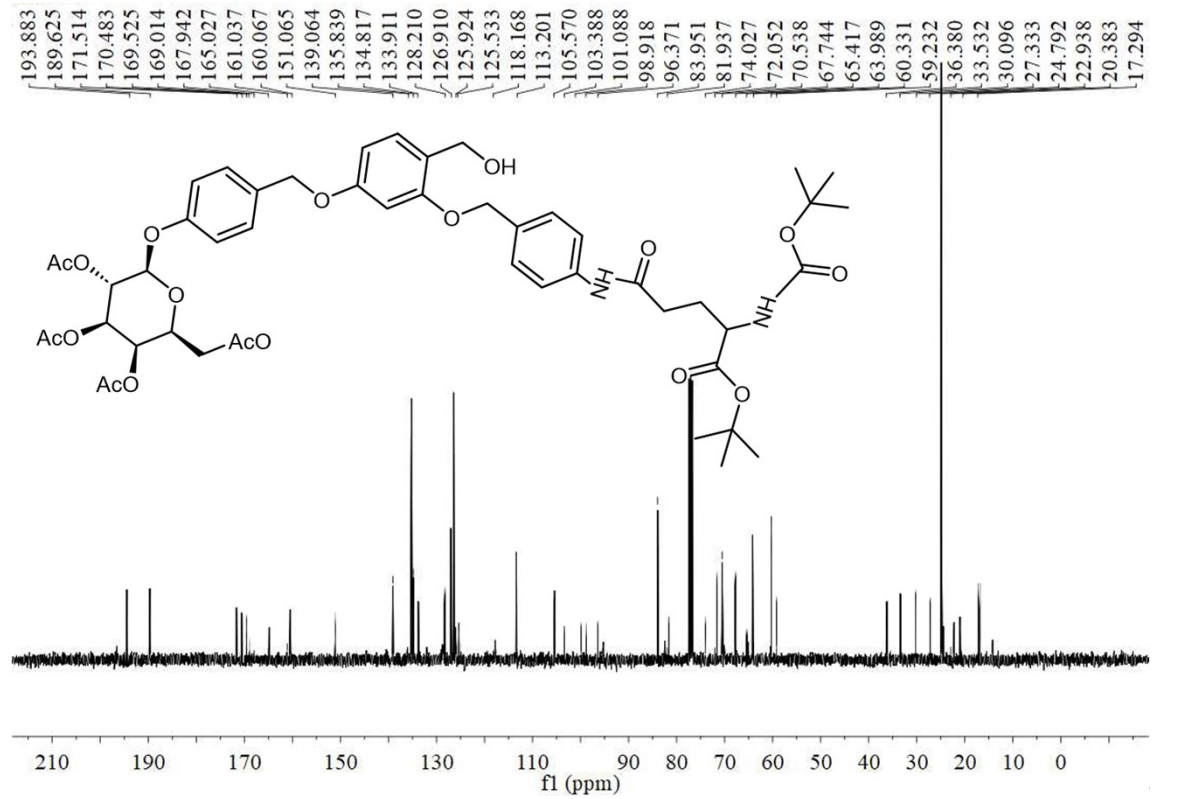

Fig. S 45 ^{13}C NMR spectrum of Compound **2-11**.

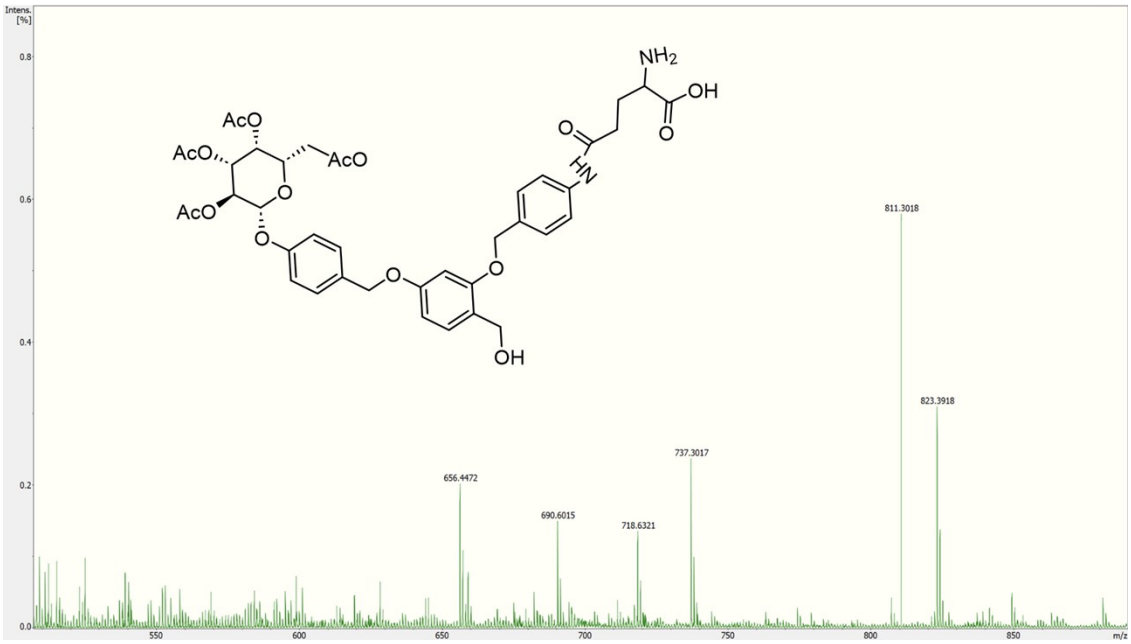

Fig. S 46 HRMS spectrum of Compound **2-11**.

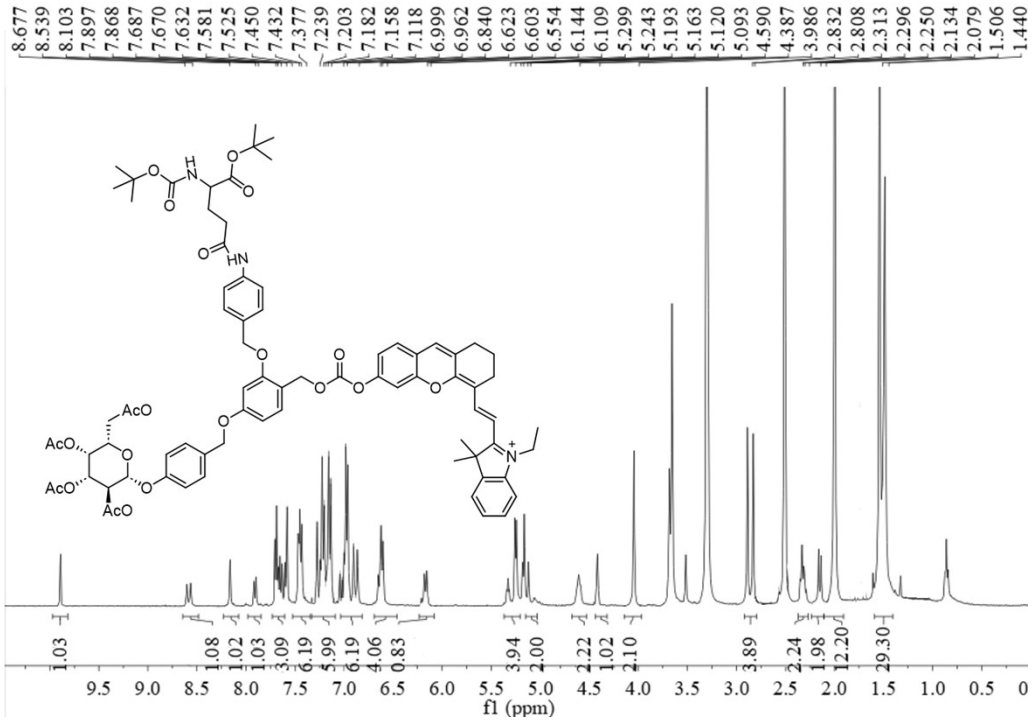

Fig. S 47 ^{1}H NMR spectrum of Compound **2-12**.

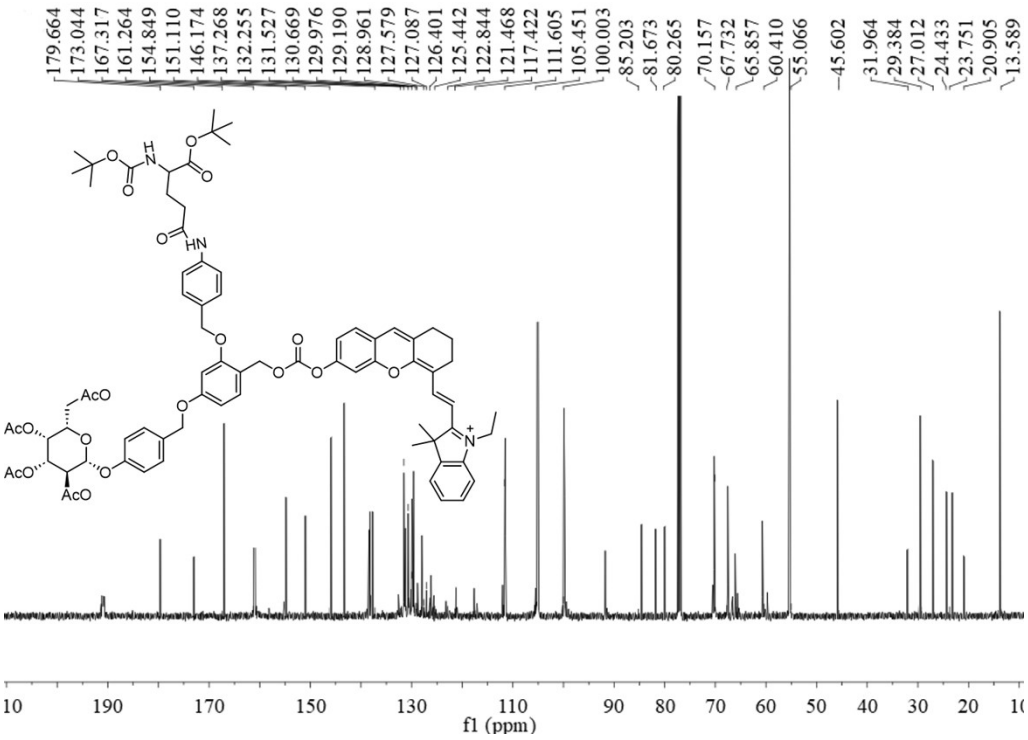

Fig. S 48 ^{13}C NMR spectrum of Compound **2-12**.

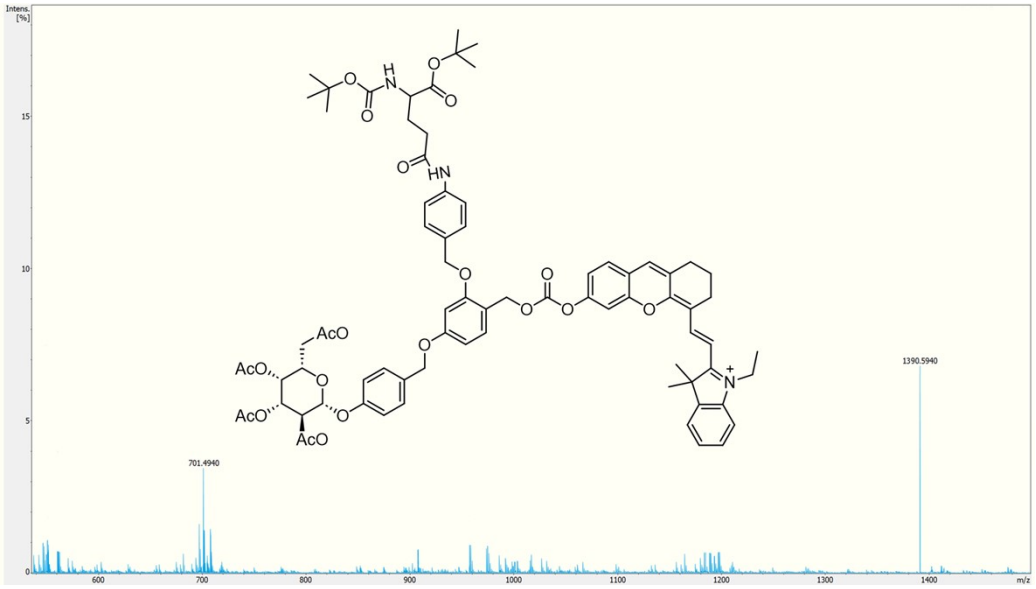

Fig. S 49 HRMS spectrum of Compound **2-12**.

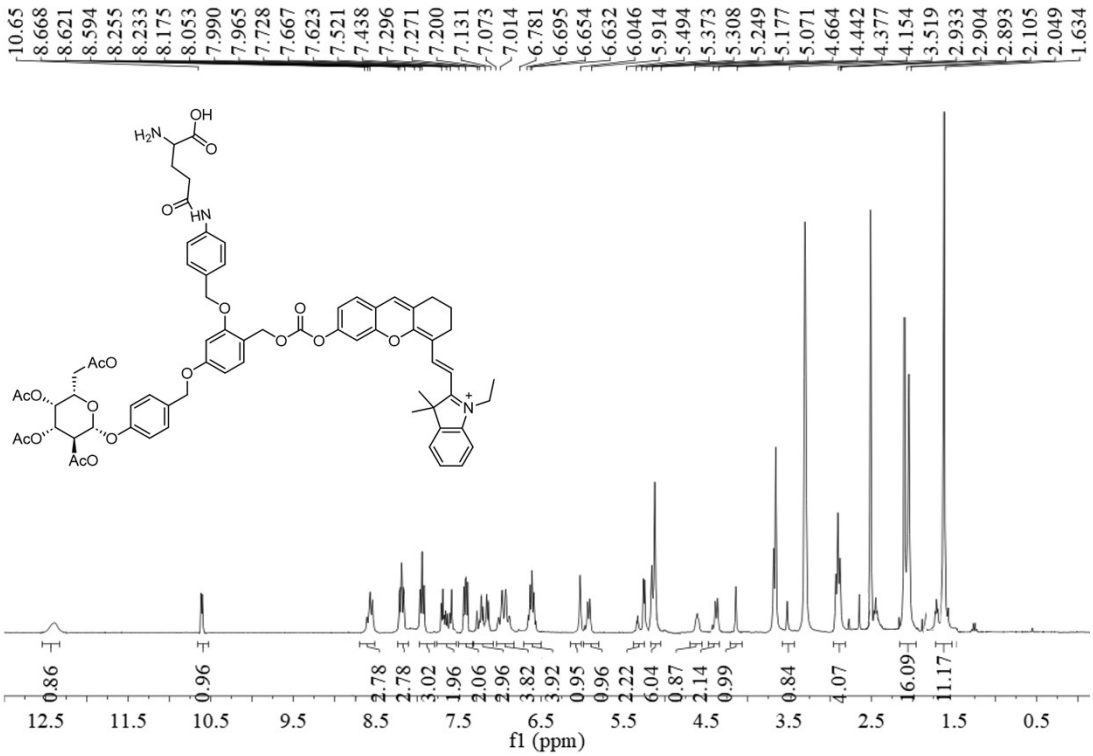

Fig. S 50 ^{1}H NMR spectrum of Compound **Cy-GGT-β-gal**.

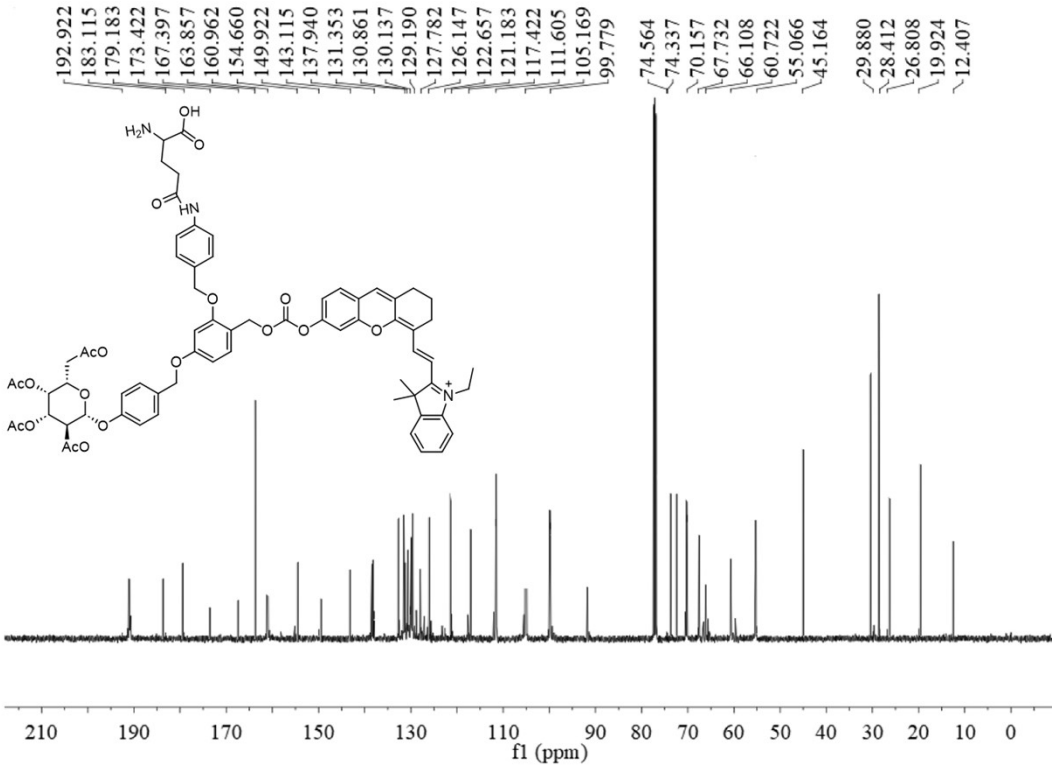

Fig. S 51 ^{13}C NMR spectrum of Compound **Cy-GGT-β-gal**.

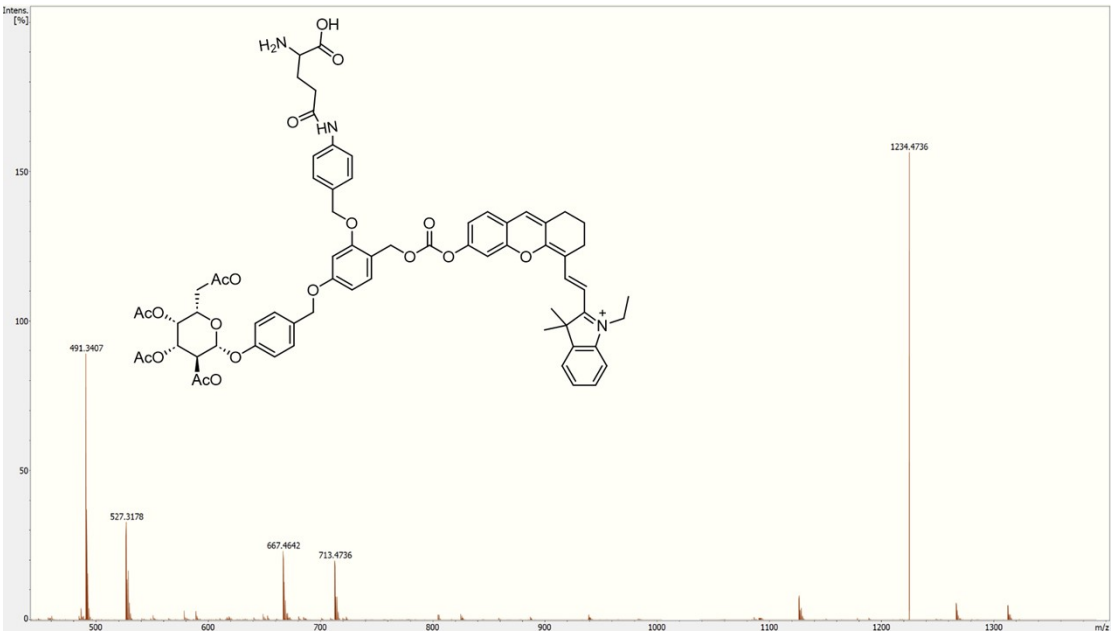

Fig. S 52 HRMS spectrum of Compound **Cy-GGT-β-gal**.

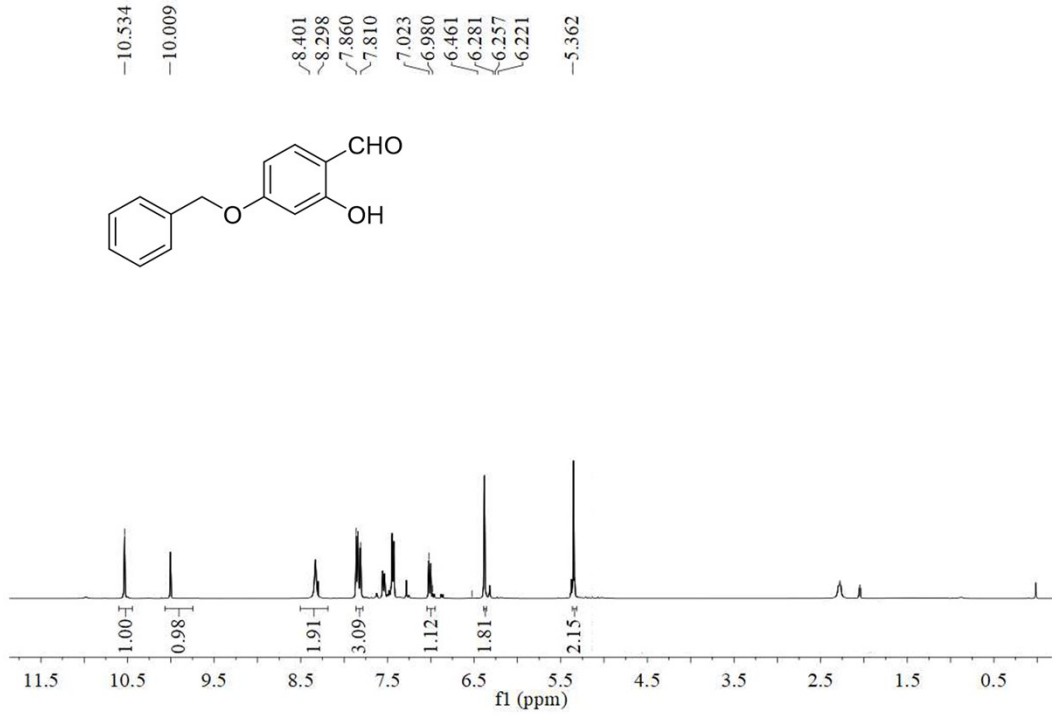

Fig. S 53 ^{1}H NMR spectrum of Compound **2-13**.

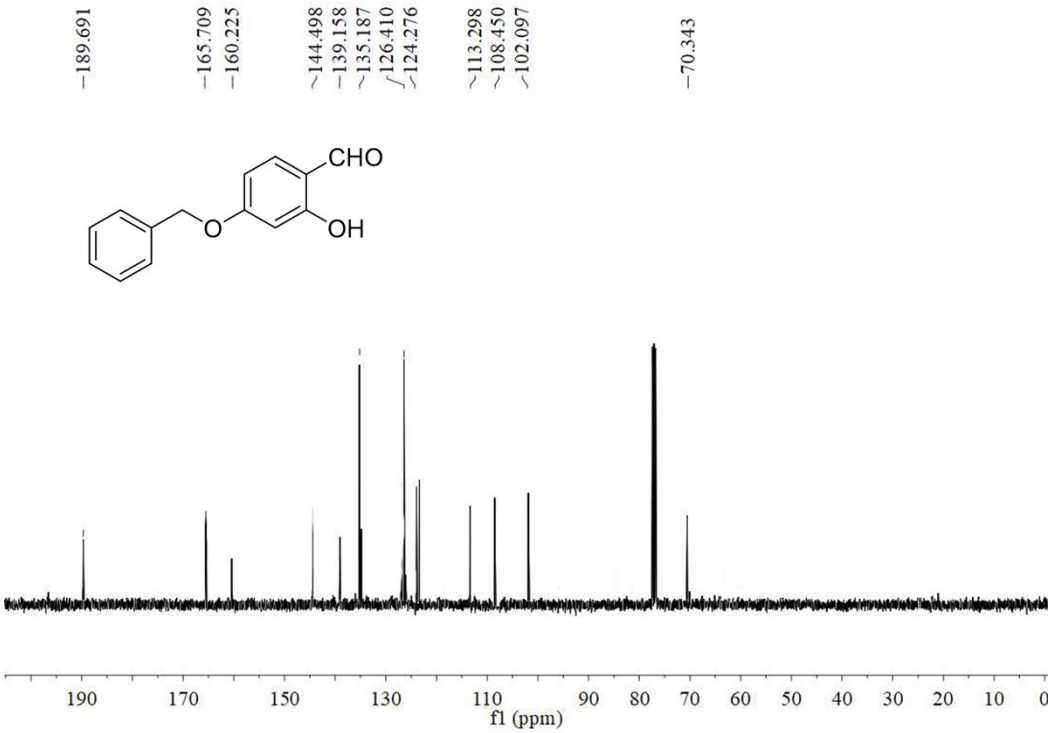

Fig. S 54 ^{13}C NMR spectrum of Compound **2-13**.

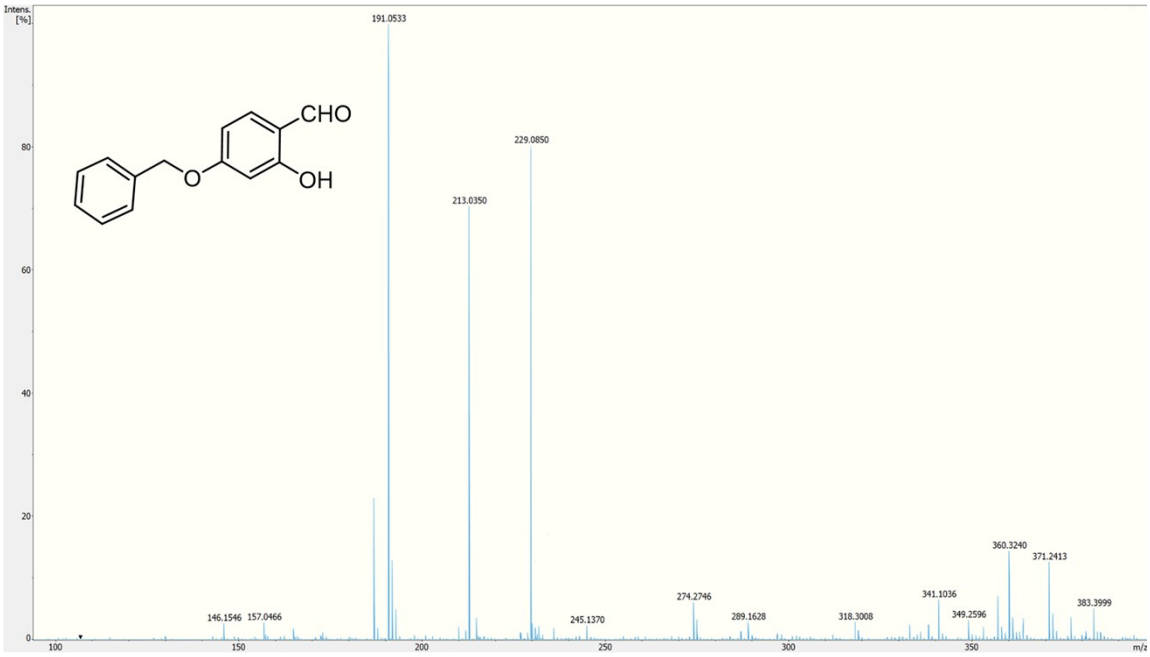

Fig. S 55 HRMS spectrum of Compound **2-13**

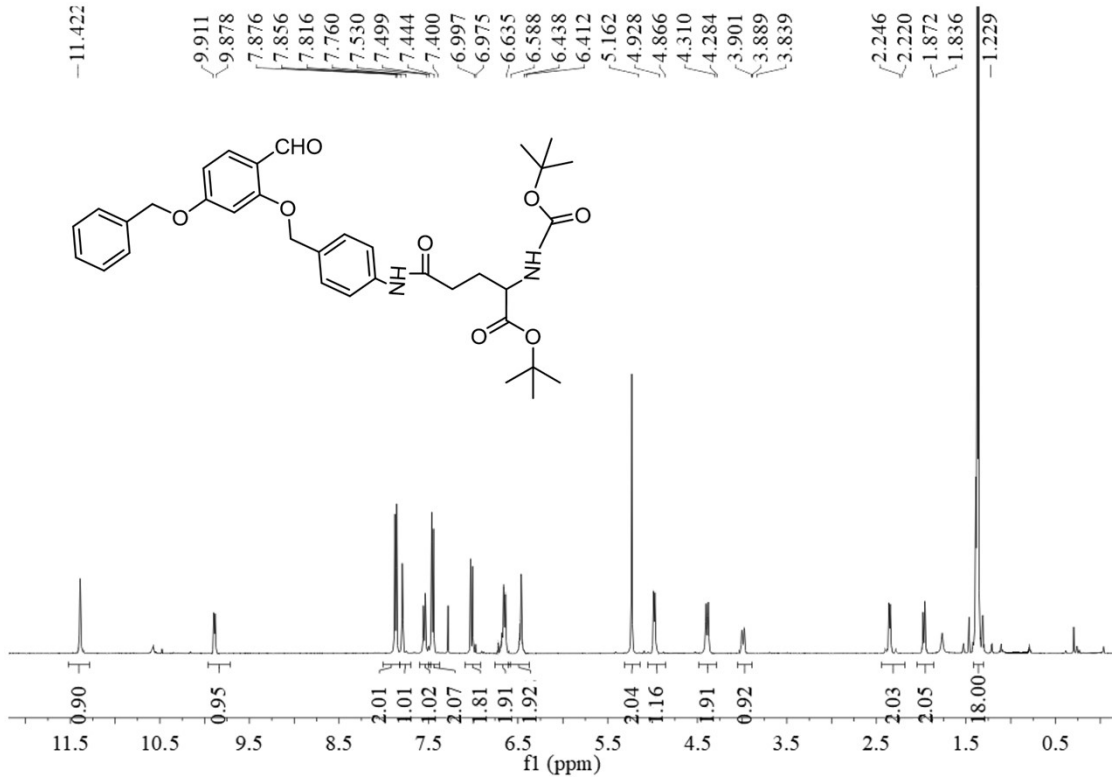

Fig. S 56 ^{1}H NMR spectrum of Compound **2-14**.

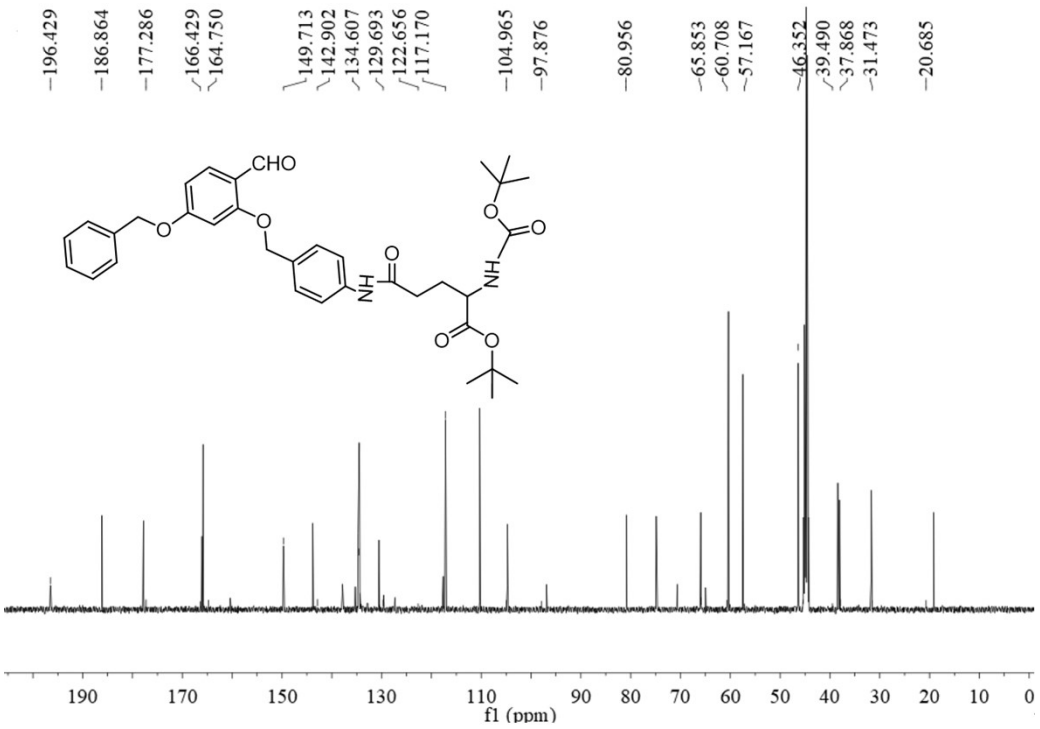

Fig. S 57 ^{13}C NMR spectrum of Compound **2-14**.

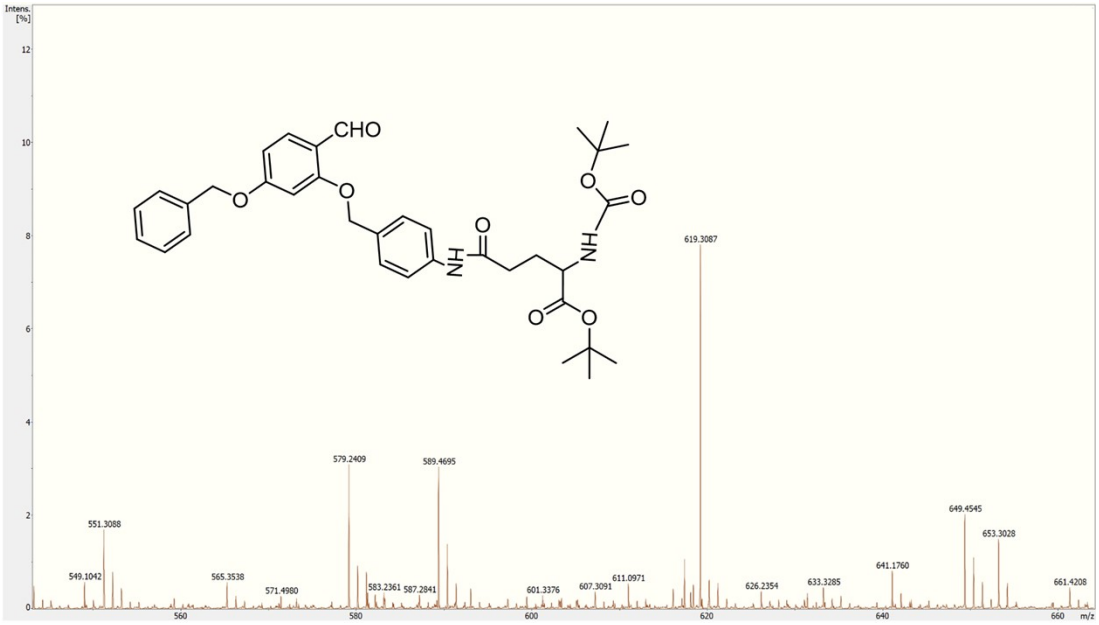

Fig. S 58 HRMS spectrum of Compound **2-14**.

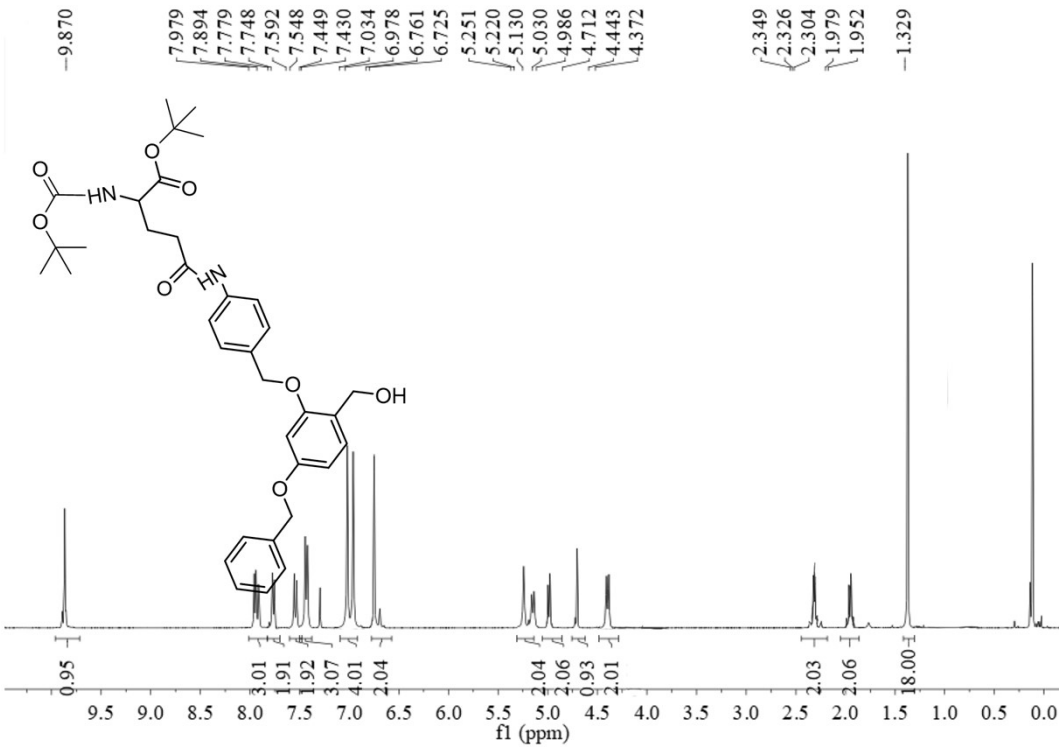

Fig. S 59 ^{1}H NMR spectrum of Compound **2-15**.

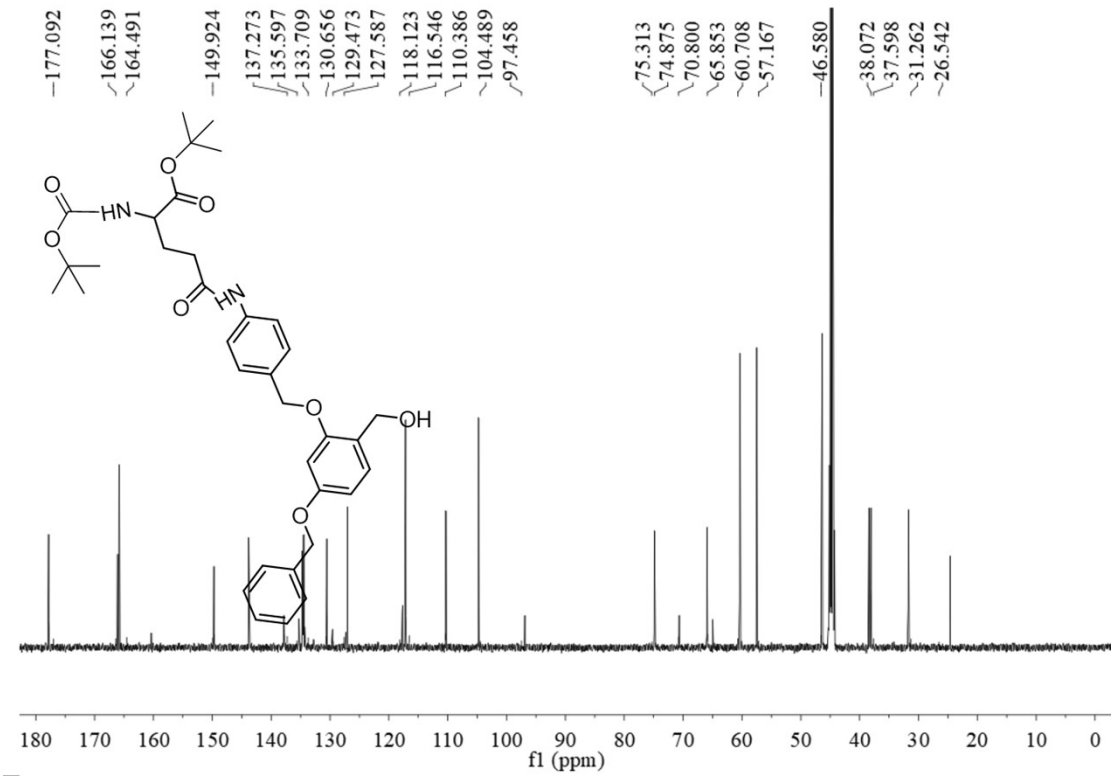

Fig. S 60 ^{13}C NMR spectrum of Compound **2-15**.

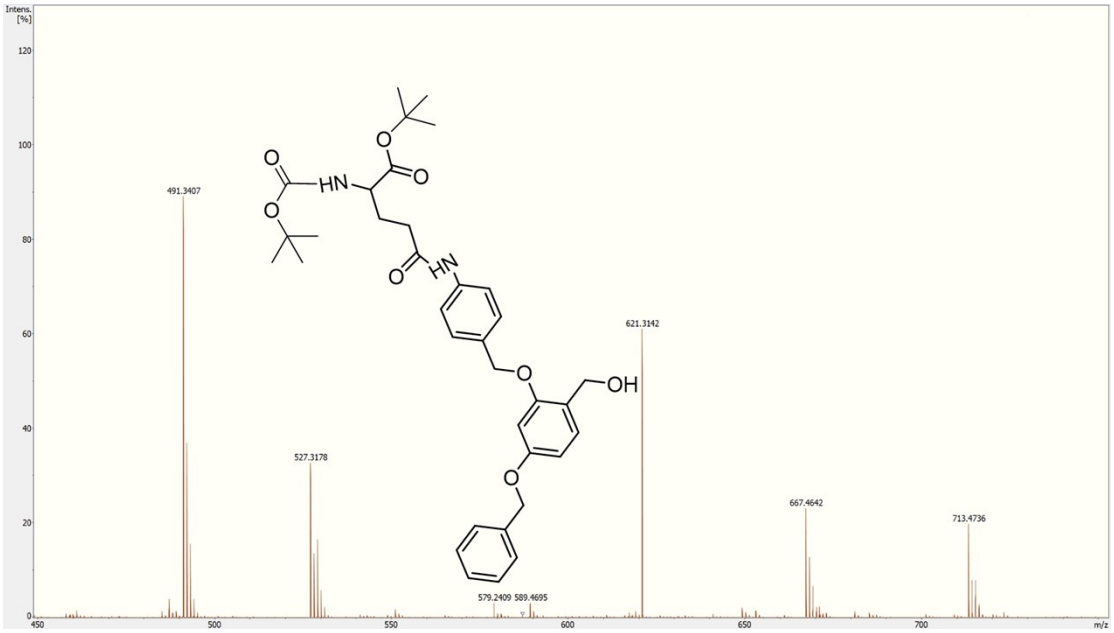

Fig. S 61 HRMS spectrum of Compound **2-15**.

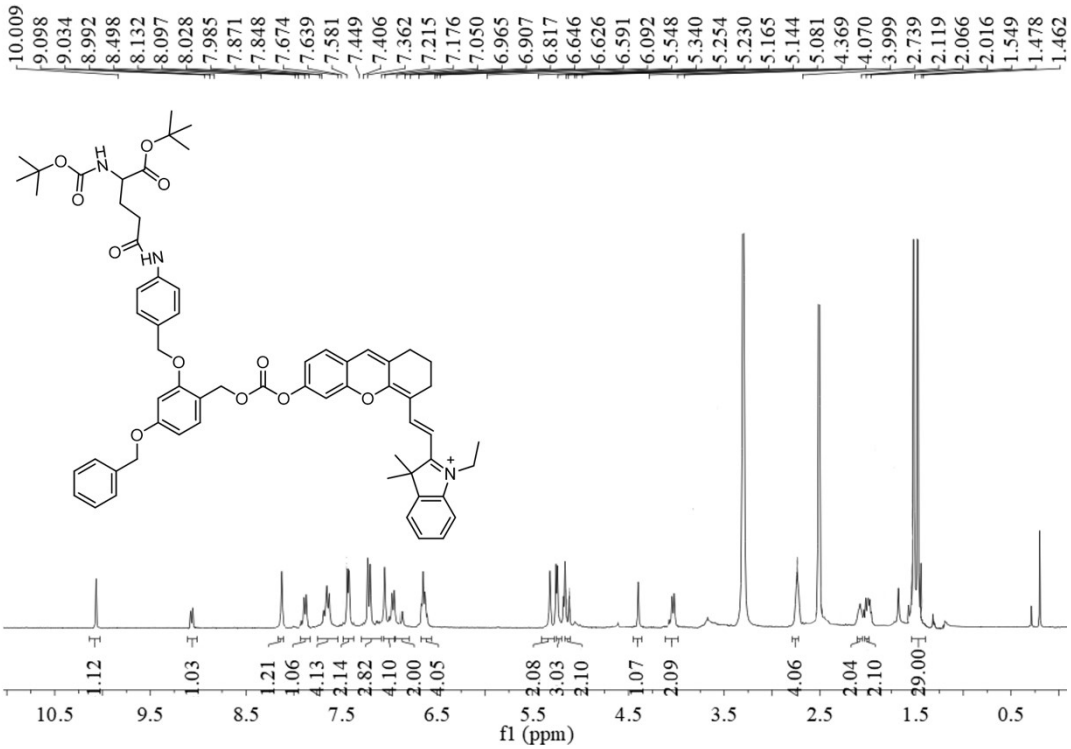

Fig. S 62 ^{1}H NMR spectrum of Compound **2-16**.

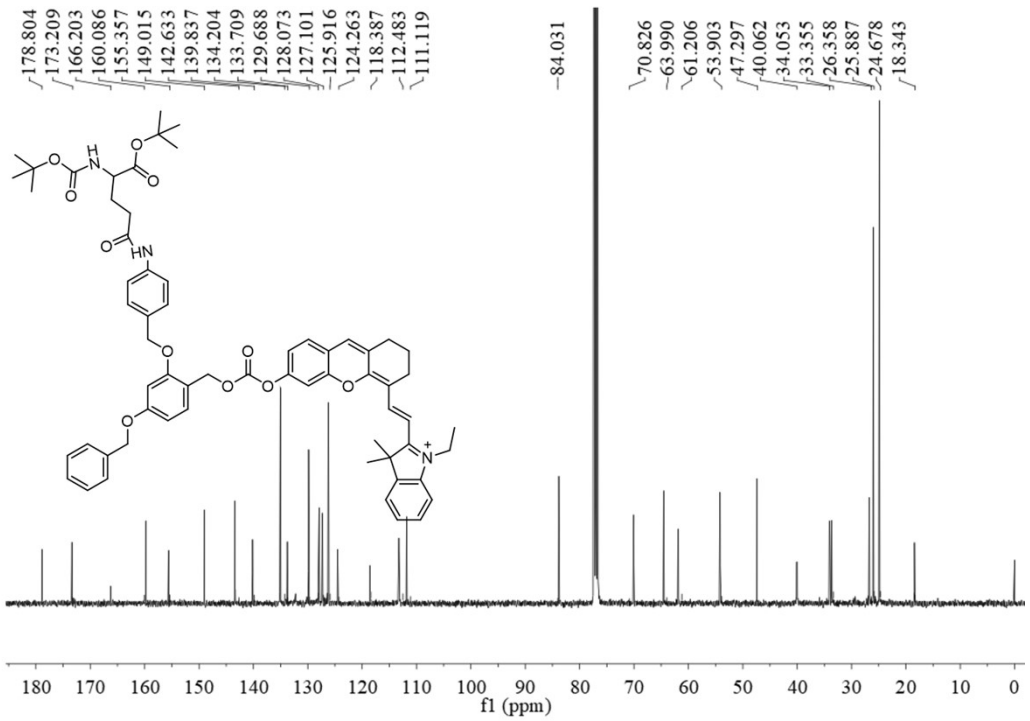

Fig. S 63 ^{13}C NMR spectrum of Compound **2-16**.

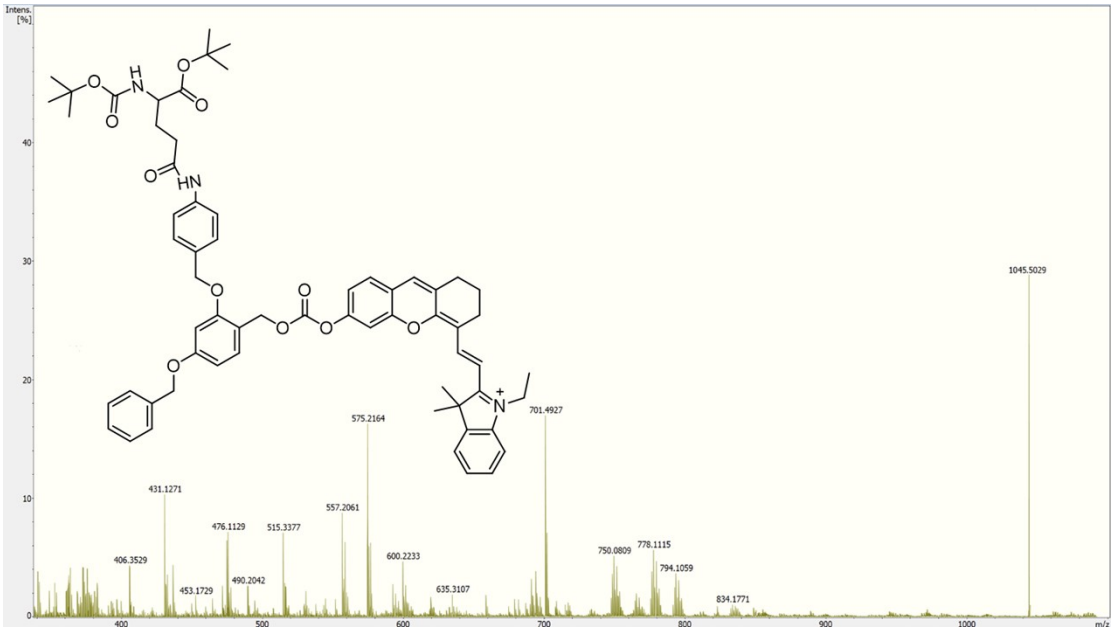

Fig. S 64 HRMS spectrum of Compound **2-16**.

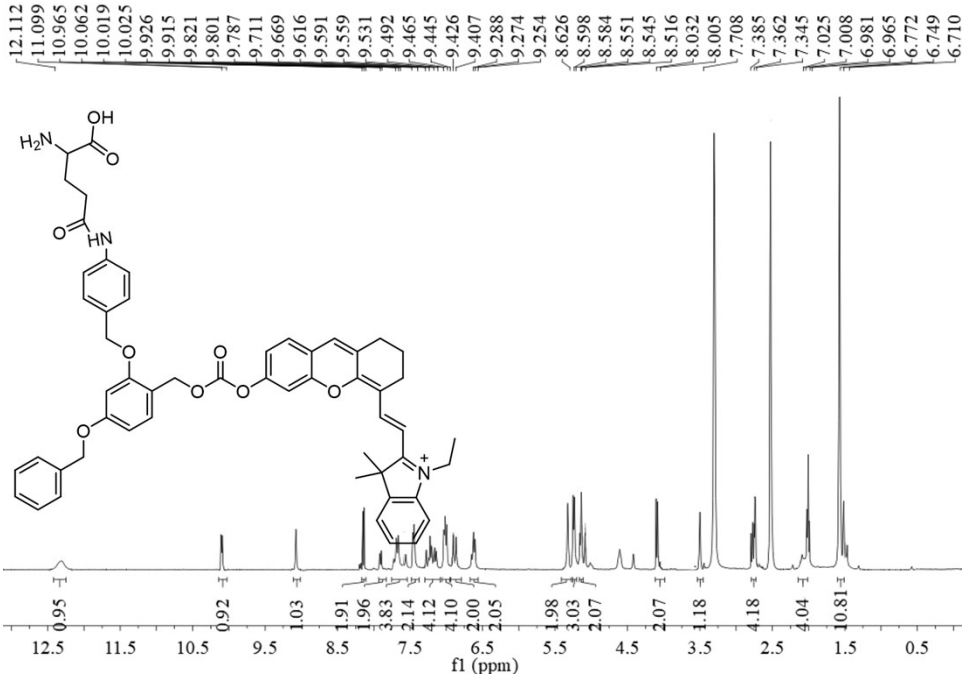

Fig. S 65 ^{1}H NMR spectrum of Compound **Cy-GGT**.

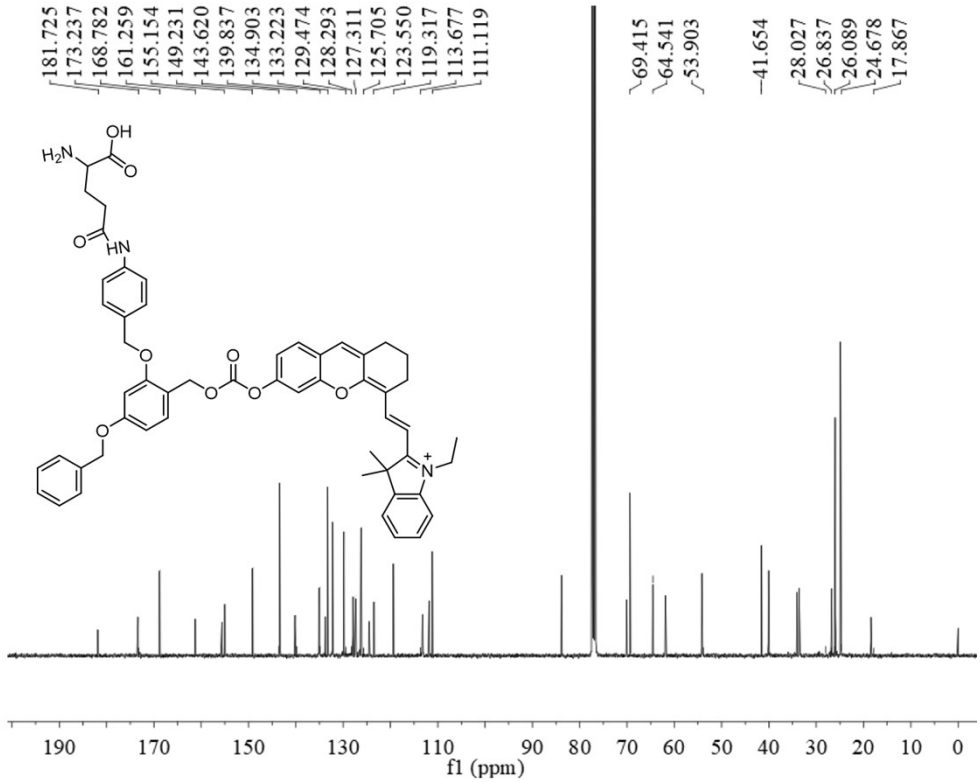

Fig. S 66 ^{13}C NMR spectrum of Compound **Cy-GGT**.

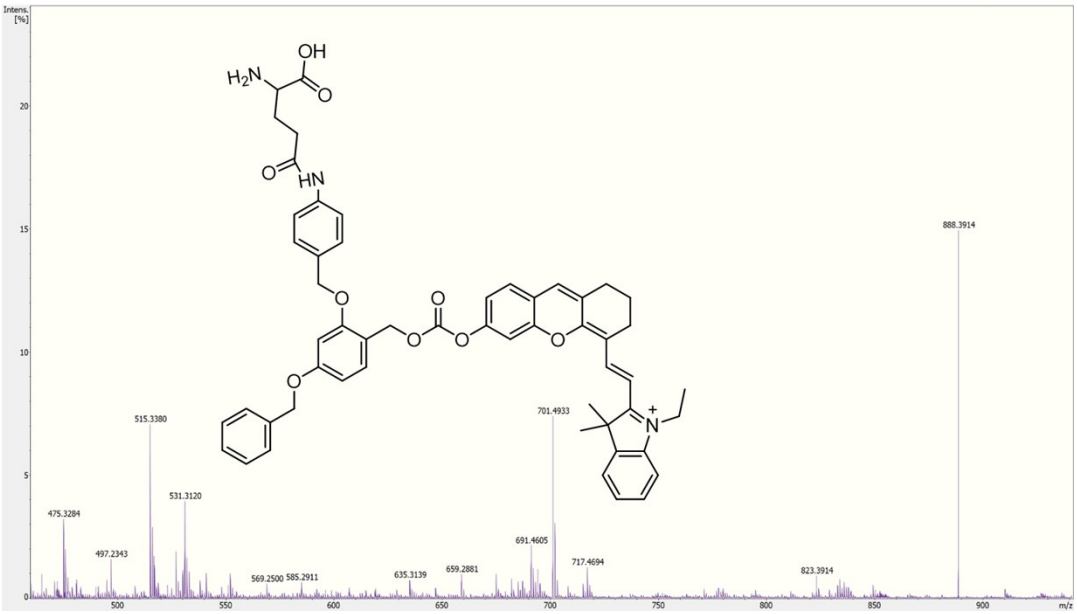

Fig. S 67 HRMS spectrum of Compound **Cy-GGT**.

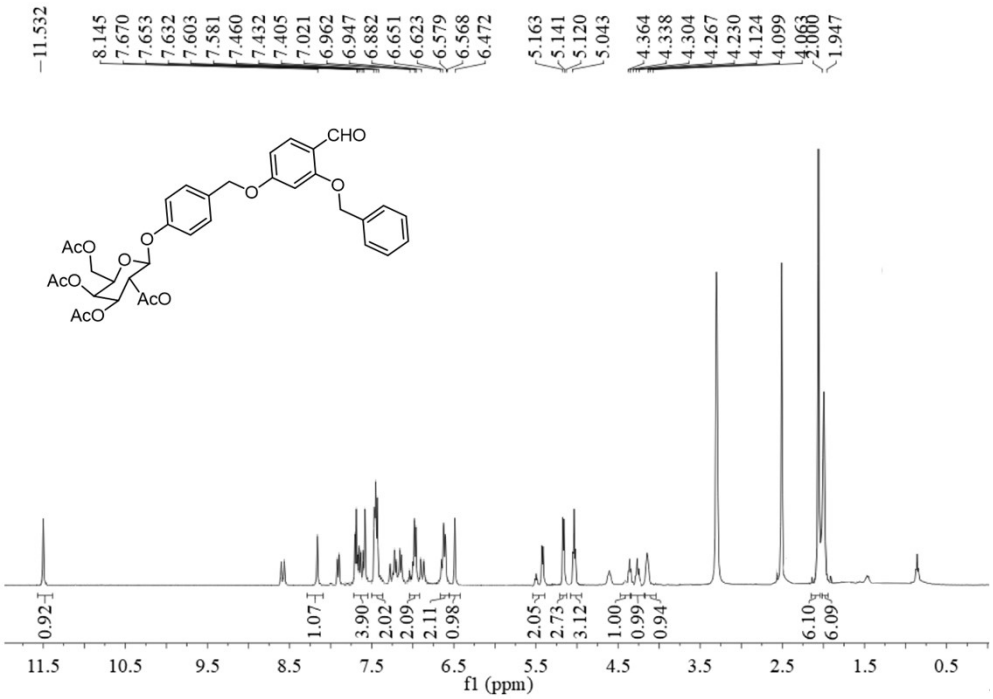

Fig. S 68 ^{1}H NMR spectrum of Compound **2-17**.

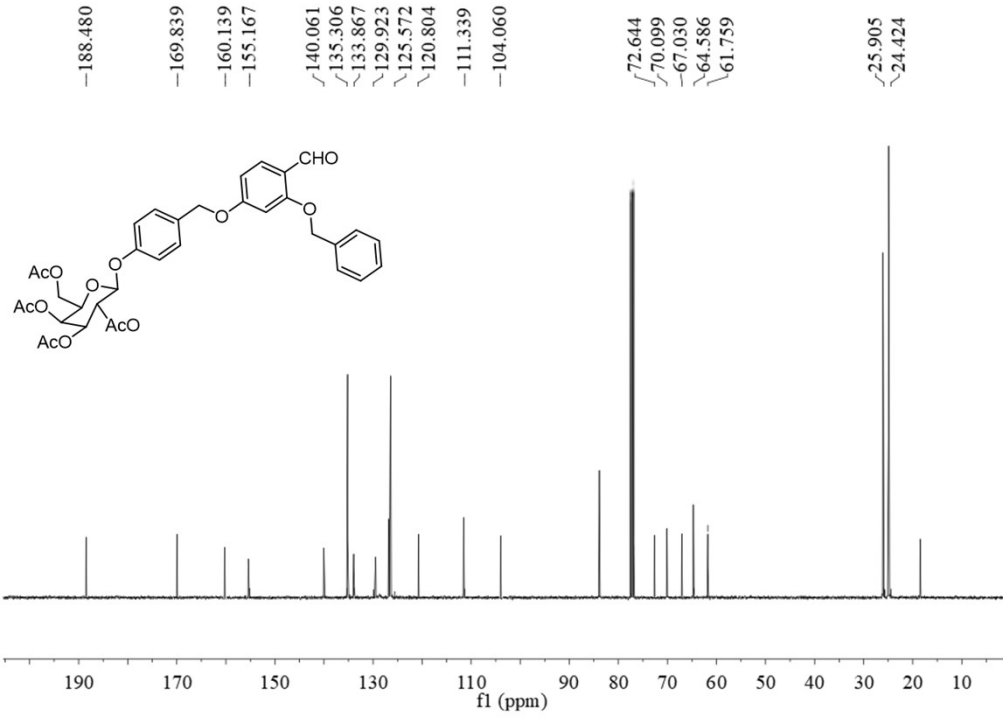

Fig. S 69 HRMS spectrum of Compound **2-17**.

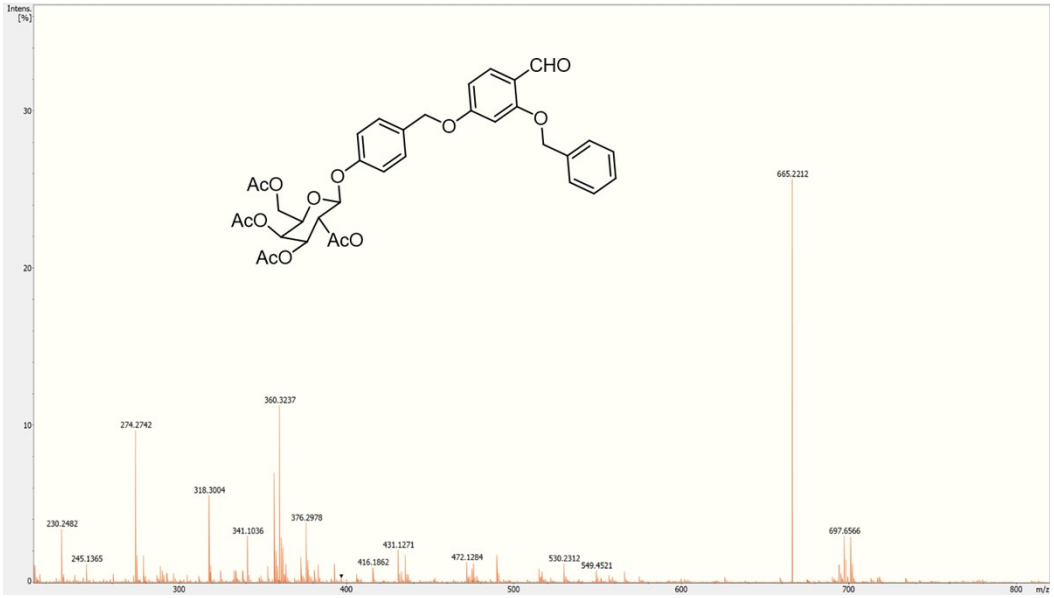

Fig. S 70 HRMS spectrum of Compound **2-17**.

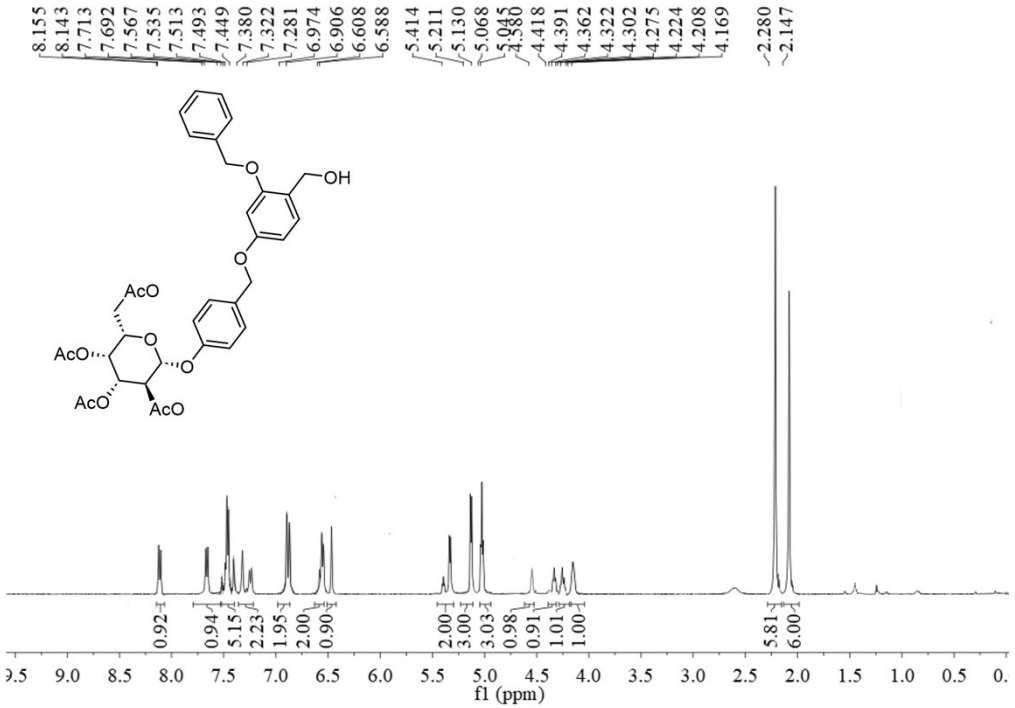

Fig. S 71 ^{1}H NMR spectrum of Compound **2-18**.

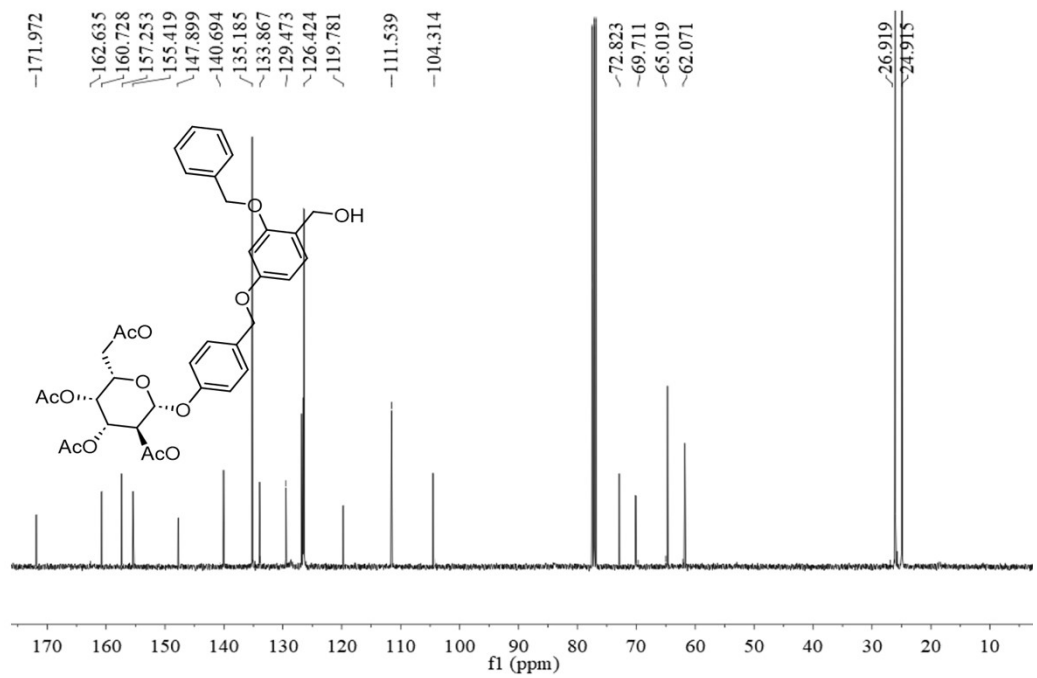

Fig. S 72 ^{13}C NMR spectrum of Compound **2-18**.

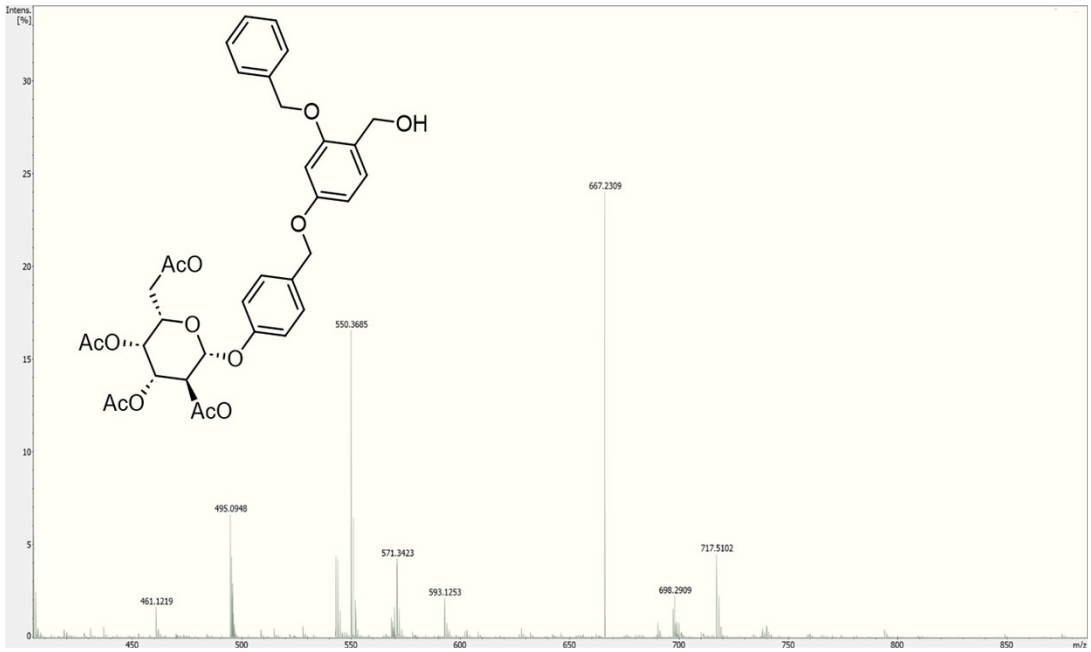

Fig. S 73 HRMS spectrum of Compound **2-18**.

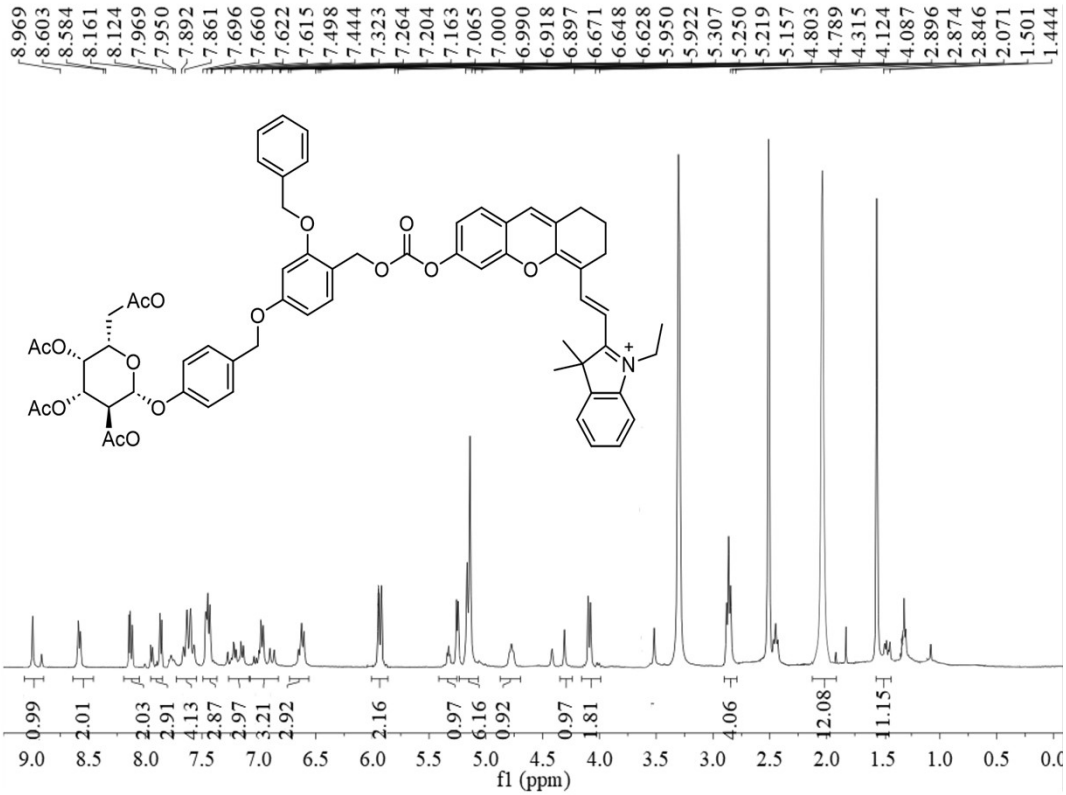

Fig. S 74 ^{13}C NMR spectrum of Compound **Cy-β-gal**

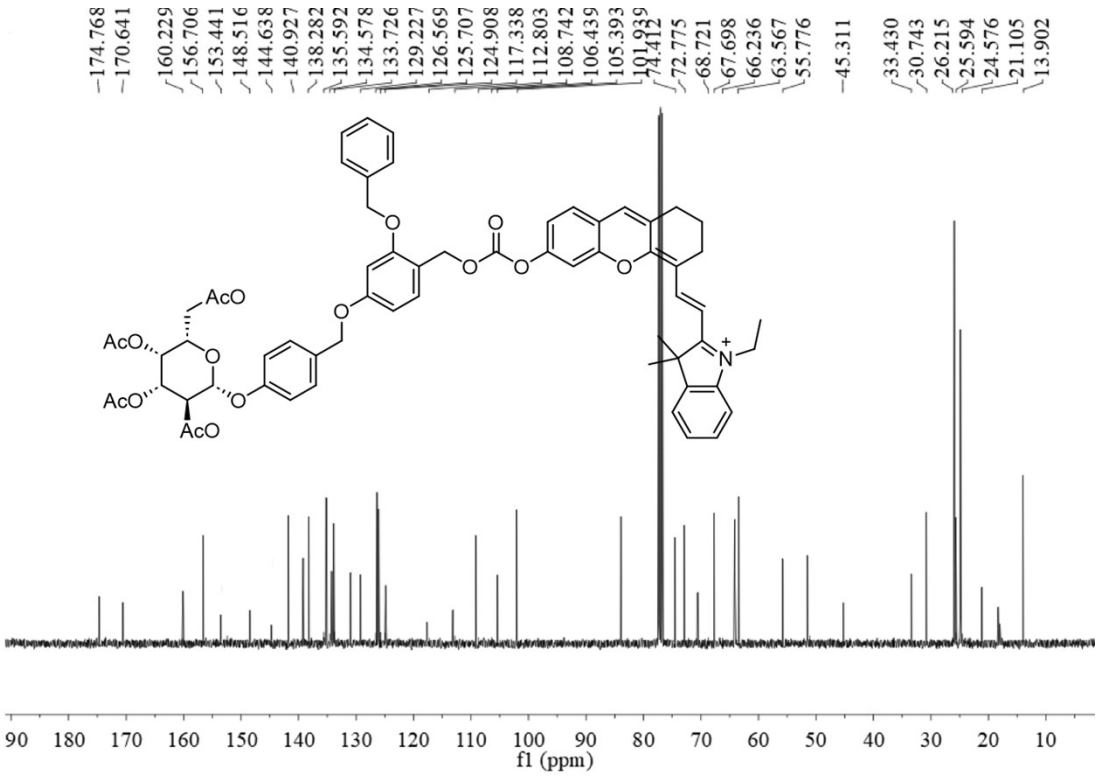

Fig. S 75 ^{13}C NMR spectrum of Compound **Cy-β-gal**.

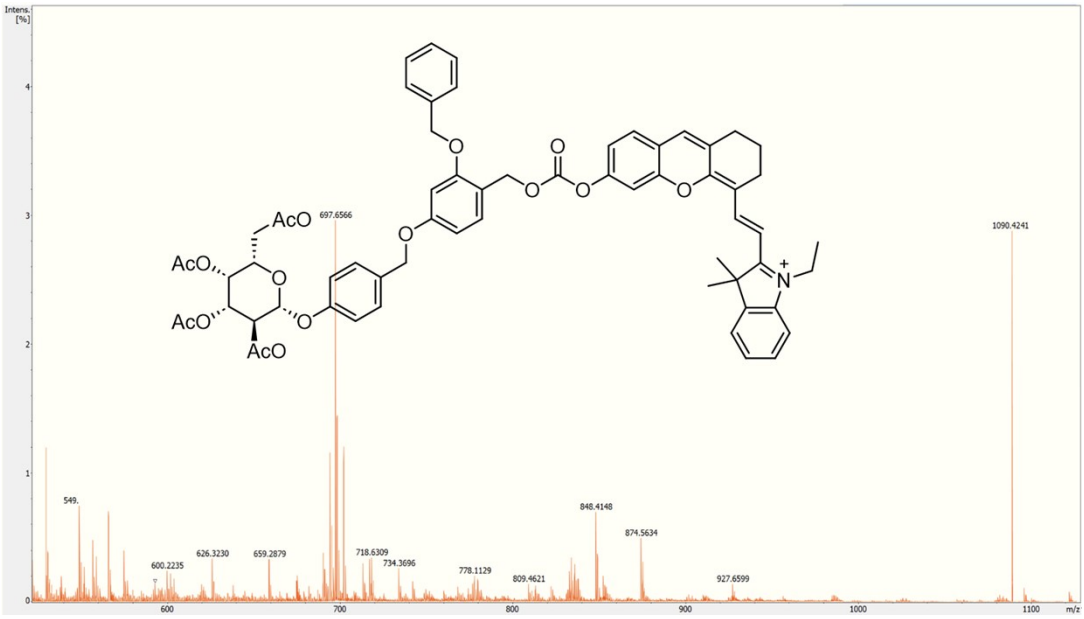

Fig. S 76 HRMS spectrum of Compound **Cy-β-gal**.

Refence：

1 F. Wang, Y. Zhu, L. Zhou, L. Pan, Z. Cui, Q. Fei, S. Luo, D. Pan, Q. Huang, R. Wang, C. Zhao, H. Tian and C. Fan, *Angew. Chem. Int. Ed.,* 2015, **54**, 7349.

2 X. Zhou, Y. Liu, Q. Liu, L. Yan, M. Xue, W. Yuan, M. Shi, W. Feng, C. Xu and F. Li, *Theranostics,* 2019, **9**, 4597.

3 H. Pan, X. Chai and J. Zhang, *Chin. Chem. Lett.,* 2023, **34**, 108321.

4 X. Li, Y. Pan, H. Chen, Y. Duan, S. Zhou, W. Wu, S. Wang and B. Liu, *Anal. Chem.,* 2020, **92**, 5772.

5 K. Gu, W. Qiu, Z. Guo, C. Yan, S. Zhu, D. Yao, P. Shi, H. Tian and W.-H. Zhu, *Chem. Sci.,* 2019, **10**, 398.

6 F. Fan, L. Zhang, X. Zhou, F. Mu and G. Shi, *J. Mater. Chem. B,* 2021, **9**, 170.

7 L. Xu, H. Chu, D. Gao, Q. Wu, Y. Sun, Z. Wang, P. Ma and D. Song, *Anal. Chem.,* 2023, **95**, 2949.

8 S. Chen, X. Ma and C. A. Wang, *Anal. Chim. Acta*, 2023, **1272**: 341482.

9 R. Obara, M. Kamiya, Y. Tanaka, A. Abe, R. Kojima, T. Kawaguchi, M. Sugawara, A. Takahashi, T. Noda and Y. Urano, *Angew. Chem. Int. Ed.,* 2021, **60**, 2125.

10 L. Haidong, Y. Qichao, X. Feng, X. Ning, D. Ran, L. Saran, F. Jiangli, D. Jianjun, W. Jingyun and P. Xiaojun, *Biomaterials*, 2018, **179**: 1-14.

11 L. Kong, F. Liu, D. Zhu, Y. Li, M. Y. Kong, Y. L. Li and J. J. S. E. J. Luo, *Sens. Actuators, B*, 2022, **363**: 131838.

12 C. Jin, Z. Cao, H. L. Zhu, Z. J. B. Li. *Biosens. Bioelectron.*, 2024, **261**: 116484.

13 Liu, F., Wang, Z., Zhu, T., Wang, W., Nie, B., Li, J., and Kong, L. *Talanta*, 2019, **191**: 126-132.